DP - 532

Criticality Studies

AEC Research and Development Report

HANDBOOK OF NUCLEAR SAFETY

by

H. K. Clark

Theoretical Physics Division

January 1961

E. I. du Pont de Nemours & Co.
Savannah River Laboratory
Aiken, South Carolina

Printed in USA. Price $2.75
Available from the Office of Technical Services
U. S. Department of Commerce
Washington 25, D. C.

USAEC Division of Technical Information Extension, Oak Ridge, Tennessee

DISCLAIMER

DP - 532

CRITICALITY STUDIES
(TID-4500, 15th Ed.)

HANDBOOK OF NUCLEAR SAFETY

by

Hugh K. Clark

January 1961

E. I. du Pont de Nemours & Co.
Explosives Department - Atomic Energy Division
Technical Division - Savannah River Laboratory

Printed for
The United States Atomic Energy Commission
Contract AT(07-2)-1

Approved by
D. S. St. John, Research Manager
Theoretical Physics Division

PREFACE

Operations with fissionable material outside of nuclear reactors involve the danger that a sufficient amount of material will be accumulated in one place to constitute a critical mass, that is, to sustain a nuclear chain reaction. Safety can easily be ensured by keeping amounts and sizes well below those estimated to be critical; but in many cases the critical masses and sizes are small and there is economic pressure to approach them closely in large-scale operations. It is necessary, therefore, to determine accurately the critical conditions for fissionable materials.

During the last several years, numerous experiments have been performed from which was obtained a large amount of data on critical conditions for fissionable material. These data are assembled in a readily usable form in this Handbook.

The critical experiments have generally been performed for idealized situations. Hence they may readily be compared with calculations, and theoretical procedures for extending the data may be developed with a high degree of confidence. These procedures may be as elaborate as one wishes; but since the departure from experimental conditions will generally be small, it appears desirable to use the simplest method that will give reasonably accurate results. Simple calculations can be performed quickly without recourse to high speed computing machines, allow a wide range of variations in parameters to be studied easily, and do not require a large amount of specialized knowledge on the part of those performing them. This Handbook presents these simple methods of calculation in such a form that they may readily be used.

In practical applications of critical mass data or calculated extensions thereof, it is necessary to know how closely actual conditions may safely be permitted to approach critical conditions. The margin of safety must include reasonable estimates of the uncertainty in the data and in the methods of calculation, and perhaps should also include an additional margin thrown in "for good luck". Even if the critical conditions were known accurately enough that actual conditions could be set so that neutron multiplications as high as, say, 100 could be reached but could not be exceeded, it would be undesirable to operate so close to the critical conditions. Conditions that are considered to be safe are presented in a reasonably consistent manner in this Handbook. The choice of safety margin is necessarily somewhat arbitrary; but since the data and the methods of calculation are presented, other margins may readily be determined if those used here are considered to be either insufficient or overly restrictive.

There are several other compilations of data and safety guides to which the reader may wish to refer for the treatments of critical mass data or for data, e.g. on aqueous solutions of U^{233}, not included in this Handbook. Notable among these are the K-1019 series of reports, the "Guide to Shipment of Uranium Materials" prepared by H. F. Henry et al., of the Oak Ridge Gaseous Diffusion Plant, and the Nuclear Safety Guide, which is a product of a committee on industrial criticality problems composed of members from various sites. The last report is fairly general in that safe conditions for all fissionable materials are included; however, data and methods of calculation are generally not present.

CONTENTS

LIST OF TABLES

LIST OF FIGURES

GLOSSARY

k_{eff} — Effective neutron multiplication constant. Represents the average number of neutrons resulting from fission that are captured in fissionable material to cause another fission.

ϕ — Neutron flux. In general it is a function both of position $\vec{r}$ and neutron energy E.

Σ — Macroscopic cross section. It is equal to the product of the microscopic cross section σ and the number of atoms per unit volume. Subscripts a, s, f, and t denote absorption, scattering, fission, and total, respectively.

D — Diffusion constant. The Laplacian of the flux, $\nabla^2\phi$ when multiplied by -D gives the neutron leakage from a differential element of volume.

k — Neutron multiplication constant. Represents the average number of neutrons produced by fission per neutron absorbed.

M^2 — Migration area defined by $M^2 = \dfrac{\iint D(E,\vec{r})\phi(E,\vec{r})\,dE\,d\vec{r}}{\iint \Sigma_a(E,\vec{r})\phi(E,\vec{r})\,dE\,d\vec{r}}$

B^2 — Buckling. The subscript m denotes the material buckling defined as $B_m^2 = \dfrac{k-1}{M^2}$. The subscript g denotes the geometric buckling defined as

$$B_g^2 = \frac{\pi^2}{(R+S)^2} \quad \text{for a sphere,}$$

$$B_g^2 = \frac{(2.405)^2}{(R+S)^2} \quad \text{for a cylinder, and}$$

$$B_g^2 = \frac{\pi^2}{(X+2S)^2} + \frac{\pi^2}{(Y+2S)^2} + \frac{\pi^2}{(Z+2S)^2} \quad \text{for a rectangular parallelepiped}$$

where R represents radius and X, Y, and Z the dimensions of the parallelepiped and where S is the reflector saving or extrapolation distance, namely the distance beyond the physical boundaries at which the flux would become zero if extended analytically. In a critical assembly $B_m^2 = B_g^2$.

S — Reflector saving or extrapolation distance (see B^2).

ν — Number of neutrons released per fission.

f Thermal utilization. The fraction of the thermal absorptions that occur in fissionable material. In heterogeneous systems the fissionable material may be considered to be the material of the fuel element even though it is an alloy of fissionable and nonfissionable material.

η The number of neutrons released per absorption in fissionable material.

ϵ Fast fission factor. The factor by which the neutrons released by fissions in U^{235} are increased as the result of fissions in U^{238}.

p The fraction of the fission neutrons that escapes capture in the resonances of U^{238} during moderation to thermal energies.

d Disadvantage factor. The relative value of the average neutron flux in a material.

L^2 Thermal diffusion area defined by $\dfrac{\iint_{Th} D(E,\vec{r})\phi(E,\vec{r})\,dE\,d\vec{r}}{\iint_{Th} \Sigma_a(E,\vec{r})\phi(E,\vec{r})\,dE\,d\vec{r}}$

where the integral is taken over thermal energies only.

τ Neutron age defined so that $L^2 + \tau = M^2$. The age may be divided into as many parts as desired so that $M^2 = L^2 + \sum_i \tau_i$.

β Albedo. The ratio of the neutrons returned by a medium to the neutrons entering it.

CHAPTER I - INTRODUCTION

1.1 FACTORS THAT DETERMINE A CRITICAL MASS

An assembly of fissionable material is critical, i.e., the neutron chain reaction is self-supporting, when on the average exactly 1.0 of the 2.5 to 3 neutrons that result from a fission is absorbed to produce another fission. If more than 1.0 neutron is absorbed to produce fission the number of fissions per unit time rises exponentially with time; if less than 1.0 neutron is absorbed to produce fission a single fission may on the average result in many fissions, but the chain is eventually terminated.

Besides the path by which a fission neutron is absorbed to produce another fission, the other paths that compete for it are absorption by fissionable material without causing a fission, absorption by other materials, and escape from the assembly. The distribution of the neutrons among these paths is dependent on the size and shape of the assembly and on the neutron cross sections of the materials present. These cross sections, in turn, are dependent on the neutron energy.

At the high energy ($\sim$2 Mev) at which the neutrons are born in fission, absorption cross sections are small; hence mean free paths for absorption are long. Thus a large amount of fissionable material is required to reduce the probability of escape to the point where k_{eff}, the effective neutron multiplication constant, is unity. At low energies cross sections are much larger and less material is needed.

High energy neutrons lose energy by inelastic or elastic scattering collisions with nuclei. If the nuclei are light, the average loss in neutron energy per collision is large, and only a few collisions are required to thermalize the neutrons, i.e., to moderate their energies to the point ($\sim$0.025 ev) where, on the average, collisions with nuclei result in no change in energy. Mixing fissionable materials with moderating materials dilutes the former and hence increases the mean free path for fission for the fast neutrons. The moderator also competes with the fissionable material for the capture of neutrons. However, the large increase in fission cross section at low energies more than compensates for these effects, and the net result is a much lower critical mass when a good moderator is present.

In general, as nonfissionable material is mixed with fissionable material, the first effect is an increase in the critical mass as the result of dilution. Then, as more nonfissionable material is added, moderation becomes more effective and the critical mass falls if the absorption cross section of the added material is not too great. Finally, the critical mass rises again, and criticality becomes impossible when the amount of nonfissionable material present reaches

the point where the fraction of neutrons absorbed in it is sufficient to make k_{eff} less than unity, regardless of the size of the assembly.

The effect of the size or shape of the assembly on its critical mass is fairly obvious. If one or more dimensions are made sufficiently small, the fraction of the neutrons escaping is so large that k_{eff} is less than unity. Since for a given volume a sphere has the smallest surface of any shape, the neutron leakage and hence the critical mass is least for a sphere. The critical mass increases as the shape deviates from being spherical.

The neutron leakage is reduced, and hence the critical mass, if some fraction of the neutrons escaping from an assembly of fissionable material is returned to it. Placing a reflector adjacent to an assembly has this result. The same result can also be achieved by the juxtaposition of two or more assemblies of fissionable material.

Another factor that affects the neutron leakage and hence the critical mass is the density of the fissionable material. It can be shown theoretically that for an unreflected sphere the critical mass varies inversely as the square of the density. Thus the critical mass of δ-phase plutonium is $\left(\frac{19.6}{15.8}\right)^2 = 1.54$ times as great as that of α-phase plutonium.

Finally, when fissionable material is mixed with moderating materials, clumping of the fissionable material increases the critical mass. Neutrons thermalized in the moderator have difficulty in penetrating to the center of the clumps because of the large neutron cross section of the fissionable material. As the result of this self-shielding, the fraction of the neutrons absorbed in the moderator is greater than it would be if the two materials were mixed uniformly.

In Table I.1 critical masses of U^{235} taken from the chapters that follow are presented to illustrate the dependence of the critical mass on some of the factors just discussed.

TABLE I.1

Critical Masses of U^{235}

Form	Mass, kg of U^{235}
Unreflected sphere of uranium containing 93.5% U^{235}	48.6
Water-reflected sphere of uranium containing 93.5% U^{235}	22.8
Unreflected sphere containing a water solution of U^{235} at about 75 g/liter	1.440
Water-reflected sphere containing a water solution of U^{235} at about 52 g/liter	0.840
Unreflected infinite 8.70-inch-diameter cylinder containing water solution of U^{235}	∞
Water solution of U^{235} at 11.94 g/liter	∞

1.2 CONSEQUENCES OF ATTAINING A CRITICAL MASS

When a fission occurs, the energy released is approximately 190 Mev (8.3×10^{-18} kw hours, 7.3×10^{-12} calories). Most of this energy appears as kinetic energy of the fission fragments and is dissipated in heating the assembly of fissionable material. Approximately 7.8 Mev of prompt γ radiation is emitted, and nearly an equal amount of delayed γ radiation is associated with the decay of fission products. At a distance of one foot from a fission the gamma dose is thus about 7.2×10^{-13} rem/fission*. The fast neutron dose at this same distance is about 6.8×10^{-12} rem/fission. In an assembly of fissionable material the doses are reduced considerably by self-absorption, but may still be sufficient to be lethal in even the mildest of nuclear incidents.

When an assembly of fissionable material is supercritical, the number of fissions per unit time increases exponentially at a rate that depends upon the amount by which k_{eff} exceeds unity. The generation of heat causes the assembly to expand, thus increasing the neutron leakage and hence reducing k_{eff}. In solutions, radiolytic gas generated by the fission fragments is responsible for most of the expansion until the solution boils. The number of fissions that will have occurred by the time expansion has made the system subcritical depends upon the rate at which k_{eff} increases and upon any constraints on the expansion of the system. In a nuclear weapon these factors are adjusted so as to make this number exceedingly large. In any accidental assembly of a critical mass, however, it is unlikely that the burst would approach within several orders of magnitude that of a weapon. Calculations of radiation bursts have been made for solutions of U^{235} on the basis of a simplified model[1.1]. These calculations show that even for fairly well constrained systems the magnitude of the burst is not greatly dependent on the rate of assembly until rates of increase in k_{eff} of the order of one per cent per second are approached. At lower rates (and even at rates this high for unconstrained systems), the number of fissions in the initial burst was calculated to be about 10^{17}.

This result is in general agreement with the magnitudes of the bursts that have been observed in the few accidents that have occurred. Accidents that have occurred in critical experiment laboratories[1.2] have generally been terminated within a short interval of time by safety devices. In the absence of such devices (particularly in the case of solutions), bursts can occur one after another until sufficient material is expelled or the concentration or shape is sufficiently altered to keep k_{eff} less than unity. The incident that occurred[1.3] in a production area at Oak Ridge had a duration of about 20 minutes,

---

* 1 roentgen equivalent man (rem) is defined as: that amount of radiation absorbed in tissue which has the relative biological equivalence in man of 1 roentgen of X- or gamma rays.

during which interval a total of 1.3×10^{18} fissions occurred in a series of bursts. The man closest to the incident owes his life to his prompt departure from the area immediately following his observance of the blue glow characteristic of such incidents. The incident at Los Alamos[1.4] resulted in 1.5×10^{17} fissions and in the death of one operator. The violent disturbance created by the burst caused the termination of the accident.

The situation is changed somewhat if the fissionable material is confined in shielded areas that are inaccessible to personnel. In such areas contamination from radioactive materials is expected; hence cleanup following a nuclear incident that expels radioactive material is no great problem. The shielding is generally sufficient to prevent radiation doses from being serious, particularly if alarms are used in the event of an incident to warn personnel to evacuate nearby areas. In such areas somewhat smaller safety margins may be tolerated, and more reliance may be placed on procedures. In the incident that occurred at the Idaho Chemical Processing Plant[1.5] the shielding limited the maximum radiation exposure to 50 rem despite the occurrence of about 10^{19} fissions, and this dose, which was chiefly due to beta radiation, is believed to have resulted from airborne fission and decay products released through a sampler opening and through floor drains.

1.3 THEORY

In a critical assembly of fissionable material the number of neutrons produced by fission per second exactly balances the number absorbed and the number that escape, i.e., $k_{eff} = 1$. In describing these events mathematically it is convenient to express them in terms of the neutron flux, the product of the neutron density in neutrons/cm^3 and the neutron speed in cm/sec. The neutron flux is a function both of the neutron energy and of position within the critical assembly. For a particular assembly it is possible to find energy intervals, or groups, within which the flux may be considered to be separable into a product of a function of energy, $\phi(E)$, and a function of position, $\phi(\vec{r})$. Within an energy group the absorption of neutrons per second per unit volume of the assembly is represented by $(\Sigma_a + \Sigma_r)\,\phi(\vec{r})$ where Σ_a is the true macroscopic absorption cross section of the material of which the assembly is composed, and where Σ_r is a fictitious absorption cross section that, when multiplied by the flux, gives the number of neutrons lost from the group as the result of energy changes resulting from collisions between neutrons and the materials of the assembly. The escape or leakage of neutrons from a unit volume is given, according to the diffusion approximation, by $-D\nabla^2\phi(\vec{r})$ where D is the diffusion constant. The production of neutrons per unit volume includes neutrons entering from other groups as the result of the energy changes just mentioned and neutrons in that fraction of the fission spectrum encompassed by the group that result from fissions occurring in all groups. Within a group and within a region in which they are independent of position the constants Σ_a, Σ_r, and D are given by

$$\Sigma_a = \frac{\int \Sigma_a(E)\phi(E)\,dE}{\int \phi(E)\,dE}, \quad \Sigma_r = \frac{\int \Sigma_r(E)\phi(E)\,dE}{\int \phi(E)\,dE},$$

and

$$D = \frac{\int D(E)\phi(E)\,dE}{\int \phi(E)\,dE}.$$

This representation of the fissionable assembly is known as the multigroup model. A second-order differential equation describes the neutron diffusion within each group. The equations are coupled through the source and fictitious absorption terms which give the neutrons transferred from one group to another. The boundary conditions satisfied by the various $\phi(\vec{r})$ at the interfaces between regions, as for example between two fissionable materials of different properties or between fissionable material and reflector, are that the neutron flux $\phi(\vec{r})$ and the net neutron current $-D\nabla\phi(\vec{r})$ be continuous. At the external boundary of an assembly where for every neutron escaping none is returned, the boundary condition is that the flux extrapolate (by analytic continuation) to zero beyond the physical boundary at a distance that depends upon the properties of the assembly.

For uniform assemblies in which the properties are independent of position the energy band over which the flux may be considered separable into a product of a function of energy by a function of position comprises the entire energy region for a major portion of the core. This one-group representation results in a considerable simplification since only one differential equation is required and the production term can be written simply as $k\Sigma_a\phi$ where k represents the number of neutrons produced by fission per neutron absorbed. The one-group equation is

$$D\nabla^2\phi - \Sigma_a\phi + k\Sigma_a\phi = 0. \tag{1.1}$$

The constants D and Σ_a are obtained by integrating over the entire energy region. The neutron multiplication constant k is given by

$$k\Sigma_a = \frac{\int k\Sigma_a\phi(E)\,dE}{\int \phi(E)\,dE}.$$

Even with the one-group model the calculation of D, Σ_a, and k may be difficult because of the difficulty in obtaining $\phi(E)$. The flux as a function of energy is determined by the scattering and absorption cross sections as functions of energy. In moderated systems with low absorption the neutron energy distribution at thermal energies is nearly Maxwellian and at higher energies $\phi(E)$ is proportional to 1/E. For other systems $\phi(E)$ has a more complicated form. It is often convenient to obtain $\phi(E)$ by a multigroup calculation in which $\phi(\vec{r})$ is assumed to be the same for all groups. In effect, this procedure breaks the flux-weighted integrals for k, Σ_a, and D into summations over the number of groups employed.

Equation 1.1 may be rewritten as

$$\nabla^2\phi + B^2\phi = 0 \tag{1.2}$$

where $B^2 = \frac{k-1}{M^2}$ and $M^2 = \frac{D}{\Sigma_a}$. The migration area, M^2, can be shown to be one-sixth the mean square distance travelled by a neutron from the point at which it is born to the point at which it is captured, and hence its magnitude is a measure of the probability that a neutron will escape from an assembly of given size.

Solutions to Equation 1.2 are

$$\text{Sphere:} \quad \phi = A\,\frac{\sin Br}{r} \tag{1.3}$$

$$\text{Infinite cylinder:} \quad \phi = A'\,J_o\,(Br) \tag{1.4}$$

$$\text{Infinite slab:} \quad \phi = A''\cos Bx \tag{1.5}$$

where A, A', and A" are constants and r and x are distances measured from the center of the assemblies. The boundary condition that the flux extrapolate to zero beyond the physical surface of the assembly of fissionable material leads to the following relations between the buckling (B^2), the extrapolation distance (S), and the physical radii (R) or half-thickness (X).

$$\text{Sphere:} \quad B^2 = \frac{\pi^2}{(R+S)^2} \tag{1.6}$$

$$\text{Infinite cylinder:} \quad B^2 = \frac{(2.405)^{2*}}{(R+S)^2} \tag{1.7}$$

$$\text{Infinite slab:} \quad B^2 = \frac{\pi^2}{4(X+S)^2} \tag{1.8}$$

Thus in a critical assembly, one of the three parameters R(or X), S, and B is determined by the other two.

For finite cylinders and parallelepipeds the flux is assumed to be separable as $\phi(r)\,\phi(z)$ or $\phi(x)\,\phi(y)\,\phi(z)$. If S is assumed to be the same in all directions, the results are

$$\text{Cylinder:} \quad B^2 = \frac{(2.405)^2}{(R+S)^2} + \frac{\pi^2}{4(X+S)^2} \tag{1.9}$$

$$\text{Parallelepiped:} \quad B^2 = \frac{\pi^2}{4(X+S)^2} + \frac{\pi^2}{4(Y+S)^2} + \frac{\pi^2}{4(Z+S)^2}. \tag{1.10}$$

Reflected assemblies may also be handled with Equation 1.2, provided the flux is separable into space and energy components over the central portion of the fissionable core. A buckling can be determined for this region. The critical size is then determined from Equations 1.6-1.10 with the proper choice of S. The effect of the reflector is to increase S and hence to decrease the critical size. In this Handbook the term reflector saving rather than extrapolation distance will generally be applied to S for reflected systems. To calculate the reflector saving requires a calculation of the critical size, in which case several energy groups may be required, but only a few such calculations are required since the reflector saving varies slowly with shape.

It is customary to speak of the geometric buckling (B_g^2) as being defined by Equations 1.6-1.10 (or similar equations for more complicated shapes) and the material buckling (B_m^2) as being defined by $\frac{k-1}{M^2}$. The critical equation is then

$$B_m^2 = B_g^2. \tag{1.11}$$

*The first zero of $J_o(y)$ is at $y = 2.405$.

1.4 EXTENSIONS OF EXPERIMENTAL DATA

Many data exist that give experimentally determined critical conditions for fissionable material; that is, conditions for which Equation 1.11 is satisfied. In many cases direct reference to such data is sufficient to indicate the conditions that may be considered safe. In other cases extrapolations or interpolations of the data are required.

It is desirable to have a theoretical basis for making such extensions. In this Handbook two methods are used. For large bucklings, and hence small assemblies, the material buckling corresponding to a particular set of critical conditions is calculated, sometimes by fairly simple and approximate methods, and the reflector saving S is determined from Equation 1.11 and the proper equation among Equations 1.6-1.10. Such values of S serve as parameters to relate theory and experiment. They vary slowly with shape and composition; hence extrapolations of experimental data can be made with a high degree of confidence. For small bucklings, S is very sensitive to errors in the buckling, and conversely the buckling is insensitive to S. In this range either calculated or experimental values of S are employed or S is chosen to minimize the variation of buckling with shape. Extensions of the data are then made by calculating the expected changes in S and B_m^2, which can be calculated by simple methods to higher accuracy than the absolute magnitudes of S and B_m^2. For intermediate bucklings either approach is satisfactory, and the one employed depends upon factors such as the accuracy with which the buckling can be calculated.

In either approach, B_m^2 and S are mutually dependent. If someone wishes to use what he considers to be a more accurate value of B_m^2 than the one used in this Handbook, he must also use different values of S obtained by fitting the data to his buckling. Similarly, small bucklings, corresponding to a particular value of S, are altered if the value of S is changed.

For large bucklings (≥ 0.003 cm^{-2}) the first procedure is not greatly dependent on whether or not the correct B_m^2 is used. In test calculations, S was assumed independent of shape, and a number of dimensions were chosen consistent with an S of 6.50 cm and bucklings of 0.003, 0.01, and 0.03 cm^{-2}. Variations in S corresponding to bucklings higher and lower than these values by 5 and 10% were then calculated. The results are presented in Figure 1.1. The principal effect of changing the buckling is to change the general level of S. Variations in S become appreciable only for the extreme shapes. One clearly must be careful, however, in extrapolating S very far outside the range of shapes for which it has been determined. For example, if values of S determined from experiments with spheres are to be used to obtain critical or safe dimensions of slabs, it would be wise to err on the side of using too small a B_m^2.

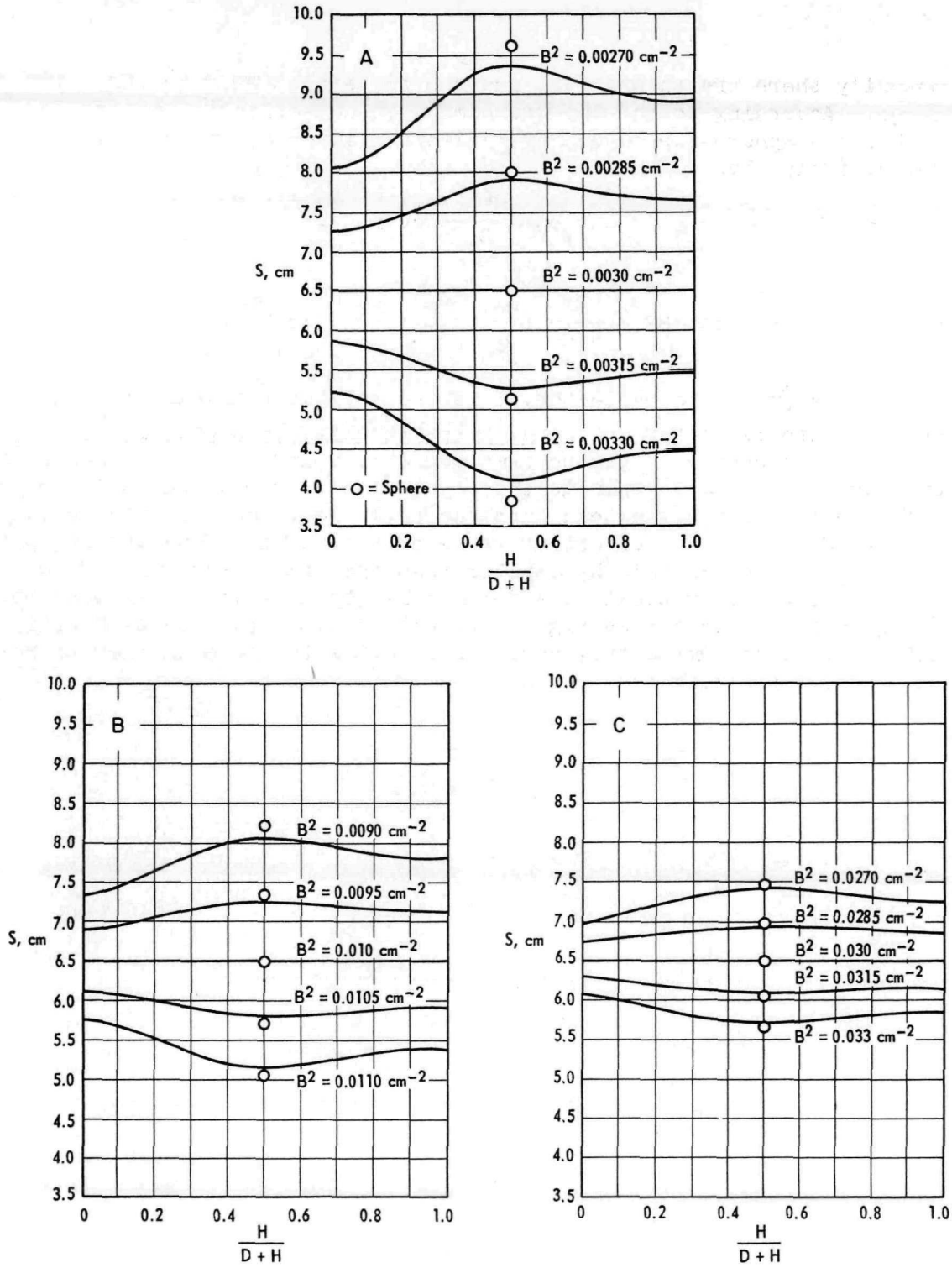

FIG. 1.1 DEPENDENCE OF REFLECTOR SAVING ON BUCKLING AND SHAPE
Dimensions were chosen so that S would be independent of shape for $B^2 = 0.003$, 0.010, and 0.03 cm^{-2}. The effect on S of ± 5% and ± 10% changes in B^2 are presented.

Actually there are theoretical reasons for expecting S to vary with shape. According to the one-group model, the reflector savings for a slab and a sphere surrounded by reflecting material are given, respectively, by

$$\cot BS = \frac{D_r\ \kappa}{D_c\ B} \coth \kappa t, \tag{1.12}$$

and

$$\cot BS = \frac{1}{\pi - BS} \left(\frac{D_r}{D_c} - 1\right) + \frac{D_r\ \kappa}{D_c\ B} \coth \kappa t, \tag{1.13}$$

where $\kappa^2 = \frac{1}{M^2}$ in the reflector, t is the reflector thickness, and r and c denote reflector and core, respectively. Thus only if $D_r = D_c$ would S be expected to be the same for a slab and a sphere. For finite cylinders and parallelepipeds the separation of variables employed in the core cannot truly extend into the reflector, and corner effects must tend to make the effective value of S smaller. Thus the reflector saving for a cube should be smaller than that for a sphere. If this were not so, the critical mass for a cube would be less than that for a sphere for reflector savings in excess of $0.309\ \frac{\pi}{B}$. It is, therefore, difficult to determine from variations in S with shape whether or not the correct buckling has been used.

1.5 MARGINS OF SAFETY

The effective multiplication constant, k_{eff}, may be defined as

$$k_{eff} = \frac{k}{1+M^2B_g^2} = \frac{1+M^2B_m^2}{1+M^2B_g^2}. \qquad (1.14)$$

Clearly k_{eff} is unity if $B_g^2 = B_m^2$ and is less than unity if $B_g^2 > B_m^2$. Assemblies in which $B_g^2 > B_m^2$ are therefore subcritical.

How much margin should be allowed in B_g^2 for safety or what maximum value of k_{eff} may be considered safe are difficult questions to answer. Even when experimental data are available for a particular case there is some uncertainty in the conditions for which k_{eff} is exactly unity, and this uncertainty increases as situations deviate from those studied experimentally. Particularly uncertain are the effects of interactions between assemblies of fissionable material and/or between such assemblies and nearby reflectors. Aside from these uncertainties it is undesirable on general principles to permit high values of k_{eff} or of the neutron multiplication, $m = \frac{1}{1-k_{eff}}$. Presumably smaller safety margins would be tolerated for situations that are considered unlikely or where an accident would have relatively minor consequences.

In this Handbook three levels of safe conditions are specified corresponding to k_{eff}'s of 0.98, 0.95, and 0.90, i.e., to over-all neutron multiplications of 50, 20, and 10. In situations where very good experimental data are available the maximum value may be acceptable. It may also be acceptable where the data are not quite so good or where some extrapolations are required, provided the fissionable material is located in a shielded area, or provided the attainment of this high a value is considered so unlikely that one is willing to take the risk that a margin of 0.02 in k_{eff} may be insufficient to cover uncertainties in data and calculations. For situations in which appreciably higher multiplications than those existing under normal operating conditions cannot be attained, and in which calculated extensions of data are required, the maximum safe allowable value of k_{eff} should probably be set at 0.90. When the data are good or extensions thereof are small, or where calculations are definitely known to be conservative, perhaps as the result of the omission of certain factors, a value of 0.95 may be acceptable. Admittedly these choices are arbitrary and those using this Handbook may wish to use somewhat different margins, which they may easily do from the data and calculations presented.

To express margins of safety in this way requires a reasonably accurate value for k. If the first method for fitting the data is employed, such a value is necessarily obtained in calculating B_m^2. If the second method is employed, particularly if S is chosen by minimizing variations

in B_m^2 with shape, a value for k may not be available. It can be calculated, however, either from

$$k = \frac{\int k\Sigma_a \phi(E)\,dE}{\int \Sigma_a \phi(E)\,dE}$$

or from $k = 1 + M^2 B_m^2$. The latter method is much simpler, provided satisfactory estimates of M^2 are available. Actually no more than reasonable accuracy in k is required. If Equation 1.14 is solved for B_g^2 (the safe value corresponding to a particular k_{eff}), and if M^2 is replaced by $\frac{k-1}{B_m^2}$,

$$B_g^2 = \frac{\frac{k}{k_{eff}} - 1}{k-1} B_m^2 \qquad (1.15)$$

and errors in k tend to cancel out.

REFERENCES

1.1 Clark, H. K. Radiation Bursts in U^{235} Solutions. E. I. du Pont de Nemours & Co., Savannah River Laboratory, Aiken, S. C. AEC Research and Development Report DP-311, 24 pp. (Sept. 1958).

1.2 Thomas, J. T. and D. Callihan. Radiation Excursions at the ORNL Critical Experiments Laboratory. Union Carbide Corporation, Oak Ridge National Laboratory, Oak Ridge, Tenn. AEC Research and Development Report ORNL-2452, 33 pp. (May 1958).

1.3 Accidental Radiation Excursion at the Y-12 Plant. Union Carbide Nuclear Co., Y-12 Plant, Oak Ridge, Tenn. AEC Research and Development Report Y-1234, 77 pp. (July 1958).

1.4 Paxton, H. C., et al. Nuclear-Critical Accident at the Los Alamos Scientific Laboratory. New Mexico, AEC Research and Development Report LAMS-2293, 34 pp. (May 1958).

1.5 Ginkel, W. L., et al. Nuclear Incident at the Idaho Chemical Processing Plant on October 16, 1959. Phillips Petroleum Co., Atomic Energy Div., Idaho Falls, Idaho, AEC Research and Development Report IDO-10035, 97 pp. (Feb. 1960).

CHAPTER II - METAL SYSTEMS

2.1 INTRODUCTION

In this chapter critical and safe conditions are given for fissionable materials both as pure metals and when alloyed with other metals. Dispersals of fissionable material in materials commonly known as moderators are relegated to Chapters III and IV, but the effects of such materials as reflectors are included here. The interaction of units of fissionable material in air is treated in Chapter V as part of a general treatment of interaction problems that include solutions as well as pure metal. The most extensive treatment is given to U^{235}, since the most data are available for this material, and since the general treatment of this material is applicable also to plutonium and U^{233}.

2.2 URANIUM-235

2.2.1 HIGHLY ENRICHED URANIUM

A large amount of data exists[2.1-2.4,2.6] for uranium that contains about 93.5% U^{235}. This has been chosen as a standard concentration, and data obtained for slightly different enrichments have been adjusted[2.2] to this value. The standard density has been taken to be 18.8 g/cm^3 and again adjustments[2.2] in the data to this figure have been made where necessary.

From the critical mass of a bare sphere of uranium (93.5% U^{235}) and from an extrapolation distance of 2.15 cm (consistent with theory) a buckling of 0.0837 cm^{-2} is calculated for this material. This buckling is in good agreement with the value (0.0836 cm^{-2}) calculated for this Handbook from a six-group diffusion theory model employing constants given in Reference 2.7. The six-group calculation gives a k of 2.300. The migration area, M^2, consistent with $B_m^2 = 0.0837$ and k = 2.300 is 15.53 cm^2.

2.2.1.1 Spheres

For spheres the values of R + S corresponding to k_{eff}'s of 1, 0.98, 0.95, and 0.90, obtained from Equations 1.6 and 1.15, are, respectively, 10.86, 10.67, 10.39, and 9.93 cm. The radii corresponding to these values of k_{eff} are obtained by subtracting the appropriate value of S. The minimum value of S is that for a bare sphere far from reflectors, namely 2.15 cm. Reflectors or nearby units of fissionable material increase S, and hence decrease R and the mass. Reflectors are most effective when they are in contact with the sphere, but reflectors even some distance away may contribute significantly to S.

In Figure 2.1 masses of U^{235} in uranium (93.5% U^{235}) spheres are plotted versus S for the four values of k_{eff} given. Experimental data giving the critical mass as a function of reflector material and thickness are expressed as reflector savings in Figures 2.2 and 2.3. Given an S, determined from Figures 2.2 or 2.3, or from estimates of interactions with other units or with nearby reflectors (see Chapter V), one obtains from Figure 2.1 the critical or the safe mass (with various margins of safety) of U^{235} in a sphere of uranium (93.5% U^{235}).

2.2.1.2 Other Shapes

Most of the critical mass data have been obtained with, or have been adjusted to, spherical shapes, since a sphere has the smallest critical mass of any shape. In handling fissionable materials, however, other shapes may be encountered and one may wish to take advantage of the deviation from the spherical shape in setting safe mass limits. Data are available[2.1] that give the critical heights of cylinders of various diameters, surrounded by various materials as reflectors.

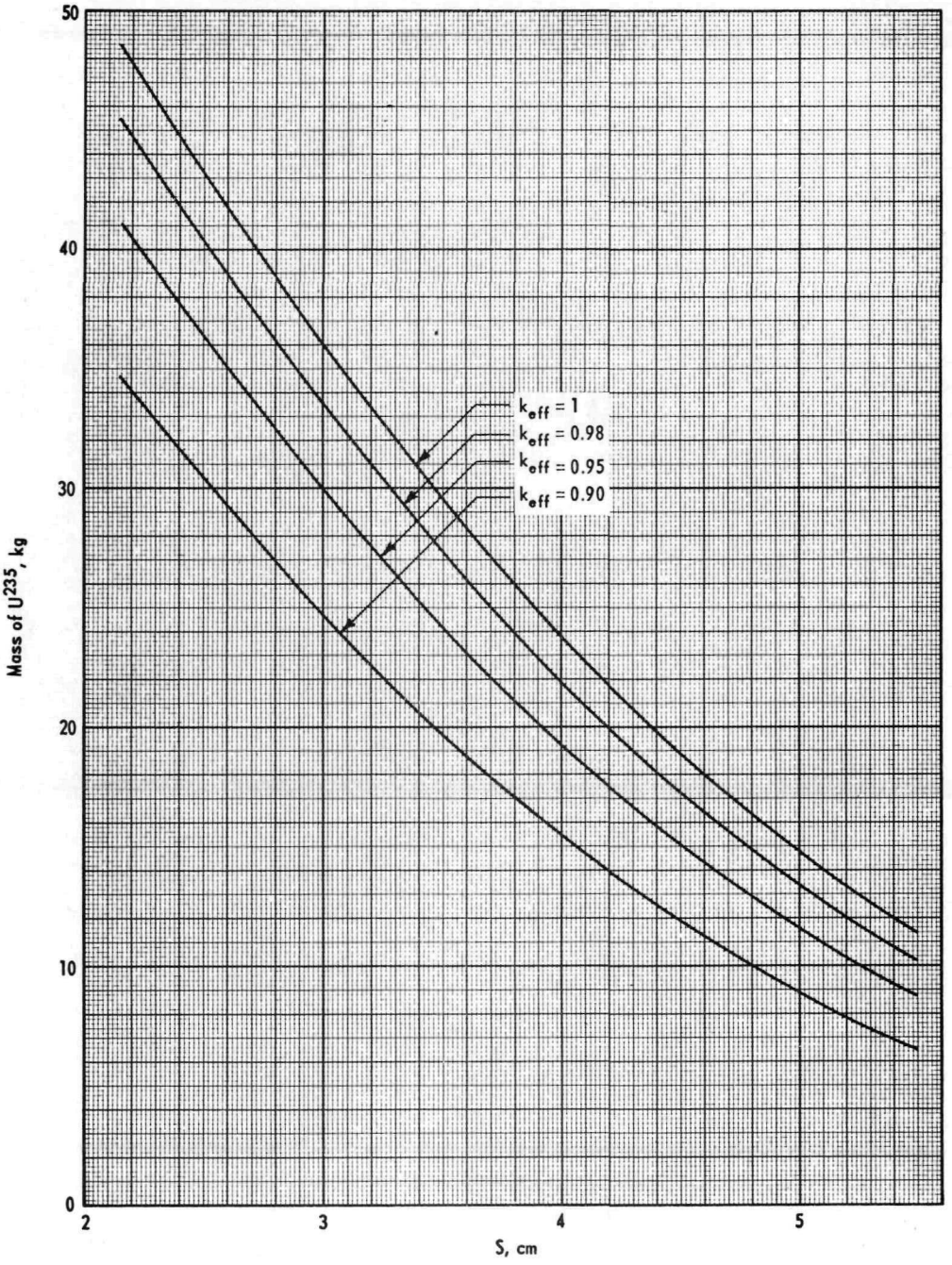

FIG. 2.1 DEPENDENCE OF THE MASS OF U^{235} IN A SPHERE OF URANIUM (93.5% U^{235}) ON S AND k_{eff}

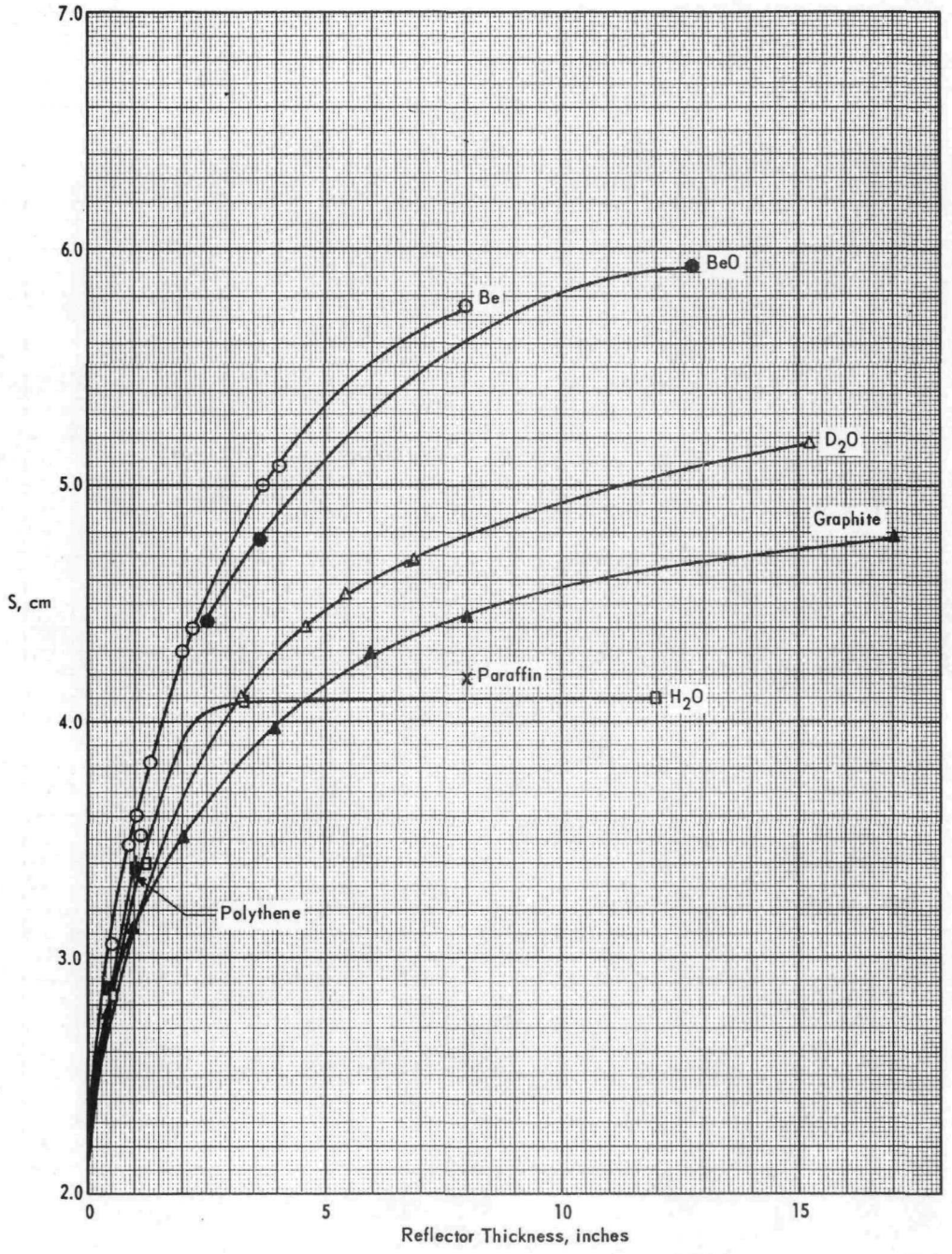

FIG. 2.2 REFLECTOR SAVINGS OF MODERATING MATERIALS FOR URANIUM (93.5% U^{235})

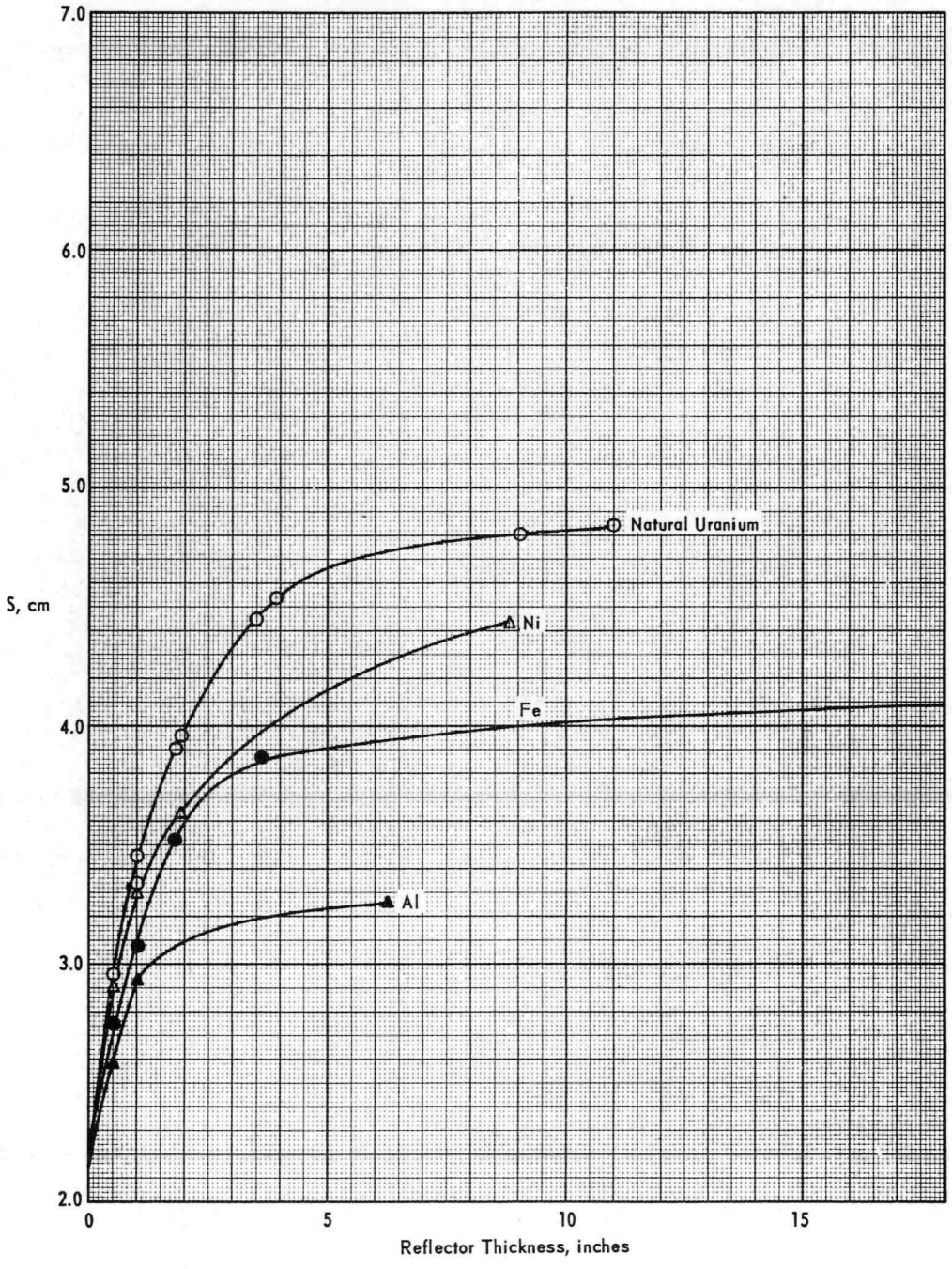

FIG. 2.3 REFLECTOR SAVINGS OF NONMODERATING MATERIALS FOR URANIUM (93.5% U^{235})

Subcritical experiments[2.8,2.9] have been performed with rectangular parallelepipeds, with multiplications in some cases in excess of 10, and the results may be extrapolated to give critical conditions. The critical mass of a cube has been determined.[2.10] As in the case of spheres, these data, obtained with various reflectors, may be expressed as effective reflector savings by equating geometric and material bucklings, with the assumption that S is the same on all surfaces. Values so obtained are plotted for cylinders in Figure 2.4 and are tabulated for rectangular parallelepipeds in Table II.1. These values are somewhat dependent on shape. For cylinders with height approximately equal to diameter, as might be expected (see Section 1.4), the values are smaller than the corresponding ones for spheres.

TABLE II.1

Reflector Saving, S, for Rectangular Parallelepipeds of Uranium (93.5% U^{235}) in Water

Dimensions, in.	Max Multiplication	S, cm
2.70 x 5 x 8	~ 14	3.81
1.31 x 10 x 16	~ 6	4.23
1.14 x 16 x 20	~ 2.8	4.22
4.295 x 4.295 x 4.295	~100	3.95

Determining safe conditions for shapes other than spheres is more complicated since there are two (or three) dimensional parameters to adjust and since the reflector saving is dependent on shape. Corresponding to k_{eff}'s of 1, 0.98, 0.95, and 0.90 the geometric bucklings are, respectively, 0.0837, 0.0867, 0.0915, and 0.1002 cm^{-2}. For cylinders the heights and diameters consistent with these bucklings are obtained from Equation 1.9.

$$B_g^2 = \frac{\pi^2}{(H+2S)^2} + \frac{23.1361}{(D+2S)^2}$$

(Equation 1.10 is used for parallelepipeds.) The reflector saving, S, is obtained from experimental data (e.g., Figure 2.4) or extensions thereof, or from interaction calculations or measurements. In Figure 2.5, H + 2S is plotted versus D + 2S on a reciprocal scale for the four values of k_{eff}. Corresponding to given D and S, the critical or safe value of H + 2S and hence of H is read from the graph.

Since the data for nonspherical shapes are not so extensive as for spheres, extrapolations of the data may often be necessary. Figures 2.2 and 2.3 giving the reflector savings for spheres may be used in these extrapolations, attention being paid to the effect shape has on S by taking ratios between values read from Figure 2.2 or 2.3 and Figure 2.4. In such cases one should use somewhat larger safety margins to allow for

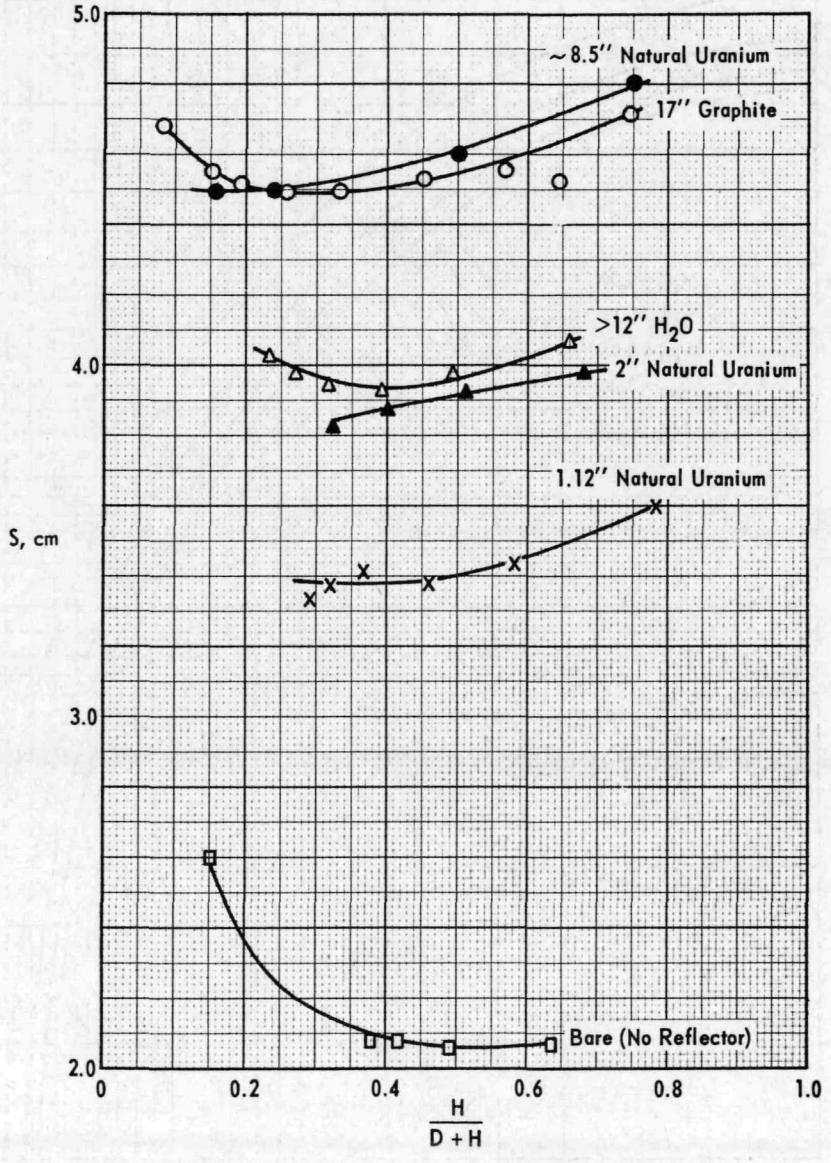

FIG. 2.4 REFLECTOR SAVINGS OF MATERIALS FOR CYLINDERS OF URANIUM (93.5% U^{235})

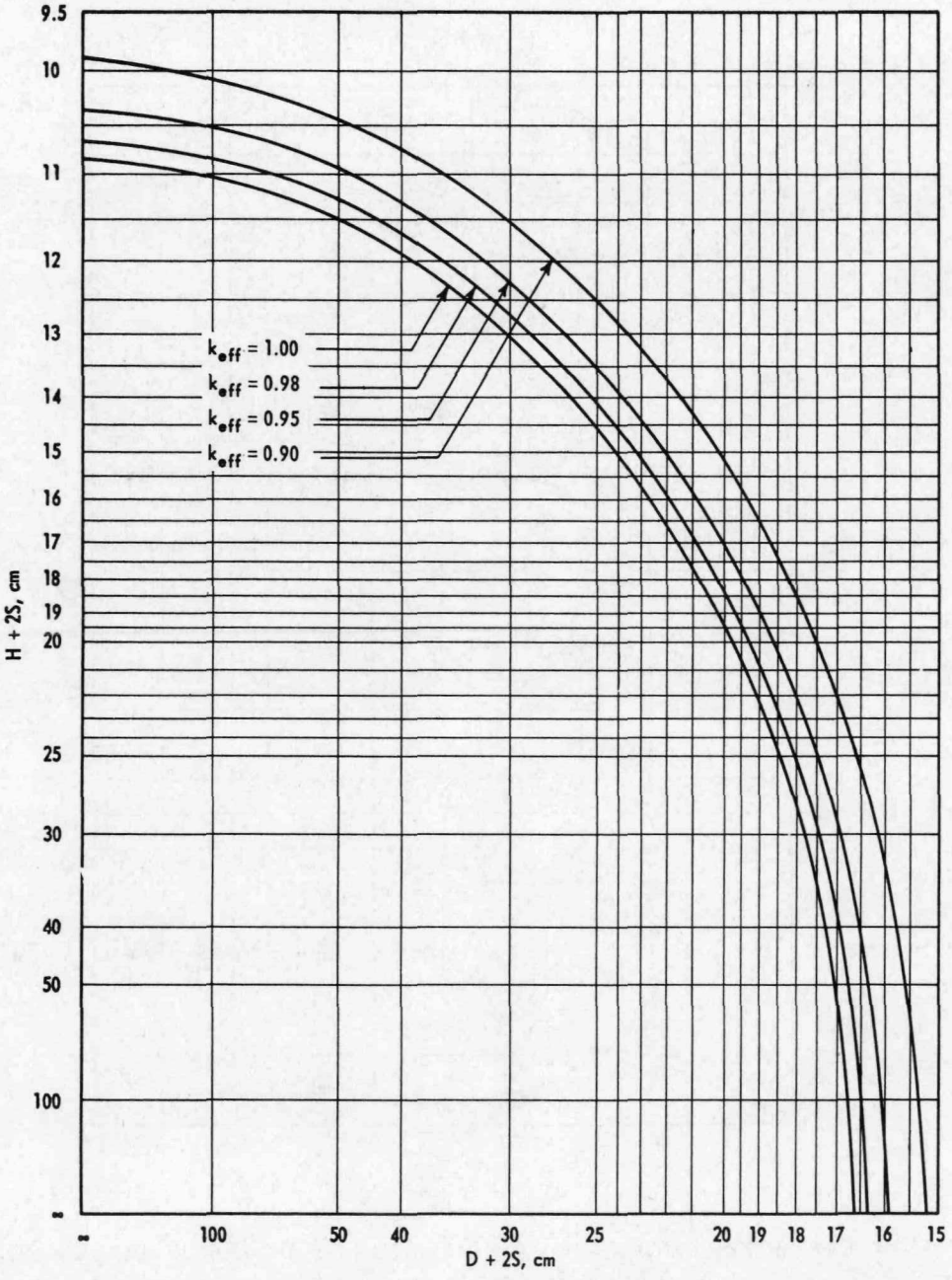

FIG. 2.5 DIMENSIONS OF A URANIUM (93.5% U^{235}) CYLINDER AS A FUNCTION OF S AND k_{eff}

errors. The margin in k_{eff} associated with margins in S is readily apparent from Figure 2.5 and a sufficient margin should be allowed in k_{eff} to cover the estimated uncertainty in S in addition to the margin allowed on general principles.

2.2.2 OTHER ENRICHMENTS

The buckling and the multiplication constant as functions of enrichment were determined for this Handbook by six-group diffusion theory calculations, again based on the constants given in Reference 2.7. These calculations, together with geometric bucklings corresponding to k_{eff}'s of 0.95 and 0.90, are presented in Table II.2 and are plotted in Figure 2.6. At any particular concentration of U^{235}, critical and safe conditions can be determined in the same manner as at 93.5%, U^{235} provided the reflector saving is known. A limited amount of critical mass[2.1] data exist for unreflected uranium and for uranium reflected by a thick layer of natural uranium. These data have been fitted to the calculated bucklings to obtain effective values of S with the results shown in Table II.3 and in Figure 2.7. The increase in S with decreasing concentration may be the result of errors in the calculated buckling, errors in the experiments, or a real effect associated perhaps with the increased radius of the assembly. Equation 1.12 indicates that S increases as the buckling decreases. In any case this increase must be taken into account in determining safe conditions.

Bucklings have been measured in exponential experiments[2.11] at low concentrations. The experiments indicate that the buckling is zero at a concentration of 4.2 to 5.4% U^{235}. The higher value is believed to be more realistic and compares well with the calculated value of 5.66%. At a concentration of 9.18% experimental bucklings of 0.00517 cm^{-2} and 0.00649 cm^{-2} are reported, the lower buckling being believed to be more reliable. From Figure 2.6 the corresponding calculated buckling is 0.0048 cm^{-2}. The experimental values of S determined from radial flux traverses are 1.9 cm with no reflector and 7.1 cm for a 3-inch-thick natural uranium reflector (determined at a concentration of 9.18%). In this range of low concentration the second method (see Section 1.4) of extending data should be used in which experimental bucklings are employed.

When the experimental critical mass data are plotted as critical mass of U^{235} versus per cent concentration of U^{235} in uranium metal, a straight line is obtained on a log-log plot for concentrations greater than 20% for both the bare uranium and the uranium reflected by thick natural uranium. At lower concentrations the plot curves upward toward infinite mass between 5 and 6% U^{235}. The slope of the straight line portion is such that the critical mass of U^{235} is proportional to the -0.73 power of the concentration.

TABLE II.2

Uranium Bucklings Versus Concentration of U^{235}

% U^{235}	B_m^2 (k_{eff} = 1)	B_g^2 (k_{eff} = 0.95)	B_g^2 (k_{eff} = 0.90)	k
100	0.0896 cm^{-2}	0.0979	0.1072	2.314
93.5	0.0836 cm^{-2}	0.0913	0.1000	2.300
60	0.0534 cm^{-2}	0.0585	0.0643	2.191
30	0.0263 cm^{-2}	0.0292	0.0323	1.943
10	0.0058 cm^{-2}	0.0070	0.0083	1.347
5.66	0	-	-	1.000
5.05	-	0	-	-
4.50	-	-	0	-

TABLE II.3

Reflector Saving, S, Versus Concentration of U^{235}

No Reflector		Thick Natural Uranium Reflector	
% U^{235}	S, cm	% U^{235}	S, cm
93.5	2.15	93.5	4.80
53.5	2.41	80.5	5.13
37.5	2.64	67.6	5.53
29.0	2.89	66.6	5.53
16.2	2.86	47.3	6.27

The calculated buckling is nearly a linear function of concentration. In the range of 93.5 ±6.5% U^{235}, relations can be derived that permit the calculation of the effect of changes in concentration from the standard 93.5%. These relations are

$$B^2 = 0.0009323\ y - 0.00361,$$

$$k = 0.4796 \log_{10} y + 1.3548$$

where y is per cent of U^{235} by weight in uranium of density 18.8 g/cm^3.

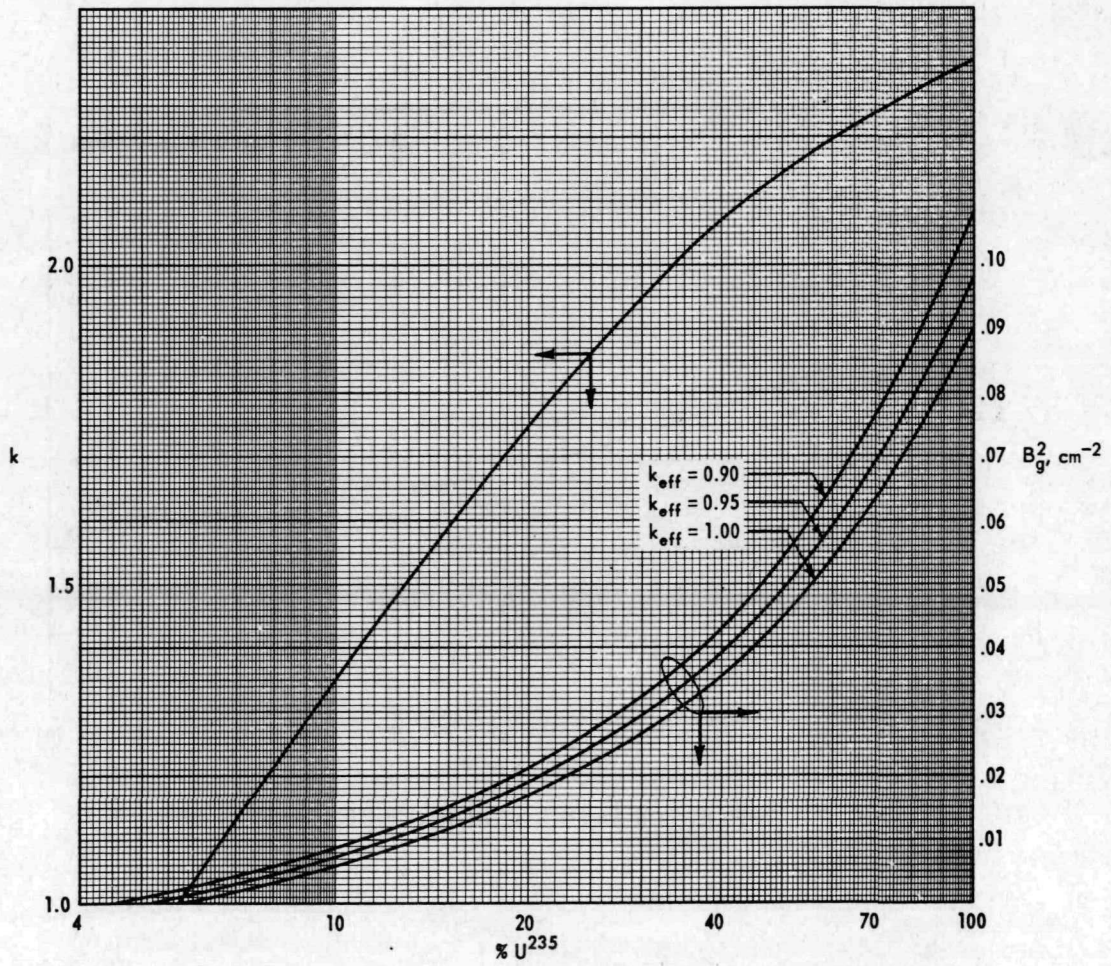

FIG. 2.6 MULTIPLICATION CONSTANT AND BUCKLING OF URANIUM AS A FUNCTION OF THE U^{235} CONCENTRATION

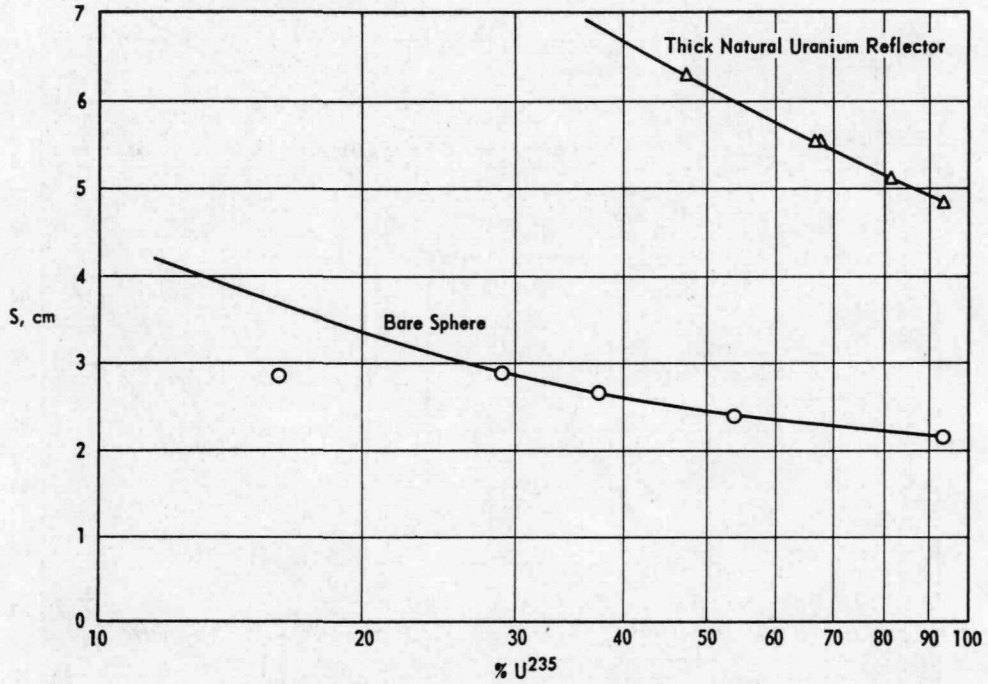

FIG. 2.7 REFLECTOR SAVING VERSUS CONCENTRATION OF U^{235}

2.2.3 DENSITY

The migration area, M^2, in any material is inversely proportional to the square of the density; hence the material buckling of uranium is directly proportional to the square of the density. If there are no effects associated with the curvature of the boundary, the reflector saving due to any material is inversely proportional to the density of the uranium. Thus the critical mass of a sphere of uranium as a function of density is given by

$$m = \rho \frac{4}{3} \pi \left(\frac{\rho_o \pi}{\rho B_o} - \frac{\rho_o S_o}{\rho} \right)^3 = m_o \frac{\rho_o^2}{\rho^2},$$

where m is the mass and ρ the density and where the subscript zero denotes the reference state.

According to Equation 1.13, the reflector saving for a critical sphere of uranium surrounded by a reflector is given by

$$\cot BS = \frac{1}{\pi - BS} \left(\frac{D_r}{D_c} - 1 \right) + \frac{D_r \kappa}{D_c B} \coth \kappa t.$$

As the core density decreases, B decreases in a manner proportional to the density and D_c increases in a manner inversely proportional to the density, hence the product $D_c B$ is unchanged. If the reflector density remains constant, the decrease in D_r/D_c with decreasing core density requires that S increase more than if inversely proportional to the density.

This effect has been observed experimentally[2.1] for uranium (93.5% U^{235}) cores surrounded by a thick reflector of natural uranium with the results given in Table II.4. In the range of densities covered by the experiment, S varies with the -1.28 power of the density rather than the -1 power. In terms of critical mass these data show the mass to vary as the -1.2 power of the density. Experiments performed with beryllium reflectors[2.6] show that the mass varies with a power from -1.2 for a very thick reflector to -2.0 for no reflector, the intermediate points being at -1.6 for a 5-cm-thick reflector and at -1.8 for a 2-cm-thick reflector. Clearly, in extending data obtained at one density to a lower density, the increase in reflector saving must be allowed for. In proceeding in the opposite direction it is, of course, conservative merely to decrease the reflector saving in a manner inversely proportional to the density.

TABLE II.4

Reflector Saving, S, Versus Density of Uranium Core

The reflector is natural uranium and the core is uranium (93.5% U^{235}).

Relative Density, ρ/ρ_o	Critical Mass, kg U^{235}	Critical Radius, cm	S, cm	4.81 ρ_o/ρ, cm
1	16.17	6.03	4.81	4.81
0.854	19.67	6.79	5.90	5.63
0.846	20.06	6.85	5.96	5.69
0.702	25.31	7.88	7.57	6.85
0.500	36.98	10.01	11.67	9.62

If the density of the reflector decreases to the same extent as that of the core so that D_r/D_c remains unchanged, and if its thickness increases inversely with the density so that κt remains unchanged, Equation 1.13 indicates that S increases inversely as the density. Thus for bare systems and for ones in which the density of both reflector and core are changed and the thickness of the reflector is increased inversely with the density, the critical mass is inversely proportional to the square of the density.

For an infinite slab of uranium, S varies inversely with its density regardless of whether or not the reflector density varies, provided the amount of reflector per unit area of slab remains constant. The critical thickness thus varies inversely with density and the critical mass of uranium per unit area of surface is unchanged. For an infinite cylinder, if S varies inversely with density, the critical radius does likewise and hence the critical mass per unit length varies inversely with the density. However, as in the case of the sphere, the radius is involved in the equation for the reflector saving, and for a reflected cylinder S would be expected to increase more than inversely with the density and hence the mass per unit length somewhat less if the density of the reflector remained the same.

2.2.4 DILUTION

Estimates have been made[2.12] of the critical mass of U^{235} in the form of bare spheres of uranium (93.5% U^{235}) diluted with various materials as a function of the concentration of diluent. These are presented in Figure 2.8. For reflected spheres the masses should be scaled downward by the ratio of the critical masses of reflected and bare undiluted uranium spheres.

Since these masses are estimates and except for small dilutions are not directly confirmed by experiment, generous margins of safety should be allowed.

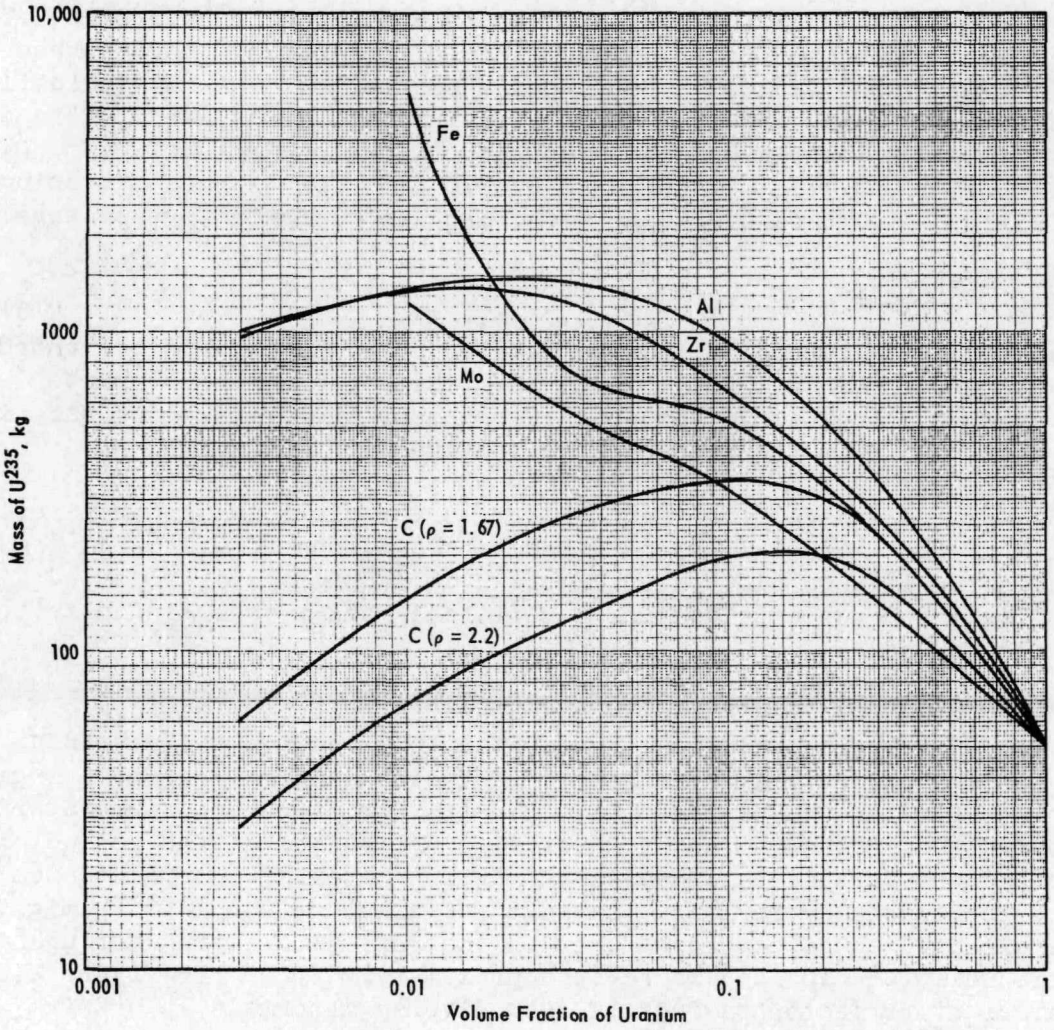

FIG. 2.8 CRITICAL MASS OF U^{235} IN BARE SPHERES OF URANIUM (93.5% U^{235}) DILUTED WITH OTHER MATERIALS

2.3 PLUTONIUM

Data for plutonium systems[2.1,2.3,2.5] are much less extensive than for uranium. Moreover, there are two forms of plutonium to be considered, namely the δ phase with a density of 15.8 g/cm^3 and the α phase with a density of 19.6 g/cm^3. The Pu^{240} concentration is an additional variable, but in amounts less than 10% it may be considered[2.2] equivalent to Pu^{239}.

A six-group calculation (based on constants given in Reference 2.7) for plutonium gives material bucklings of 0.1469 cm^{-2} for δ-phase plutonium and 0.2261 cm^{-2} for α-phase plutonium. The multiplication constant is 2.916 and the respective migration areas are 13.04 and 8.47 cm^2. Geometric bucklings corresponding to k_{eff}'s of 0.98, 0.95, and 0.90 are 0.1515, 0.1587, and 0.1718 cm^{-2} for δ-phase plutonium and 0.2332, 0.2443, and 0.2645 cm^{-2} for α-phase plutonium, respectively.

2.3.1 SPHERES

In Figure 2.9 curves of mass versus reflector saving are presented for the four values of k_{eff} for spheres of both δ-phase and α-phase plutonium. Thus as in the case of uranium, the critical or safe mass can be read from the proper curve provided one knows S.

The available data[2.1,2.3,2.5] for δ-phase plutonium spheres reflected with various materials when fitted to a buckling of 0.1469 cm^{-2} give the reflector savings plotted in Figure 2.10. The data as reported indicate some uncertainty in the critical mass with an infinite reflector of H_2O.

The uranium (93.5% U^{235}) data expressed as reflector savings (Figures 2.2, 2.3, and 2.4) are useful in extending the plutonium data. There are theoretical reasons[2.7] for expecting reflector savings of thin reflectors to have a constant ratio for different core materials regardless of the reflector material. The ratios of the reflector savings of various thicknesses of various materials for plutonium to the corresponding reflector savings for uranium (93.5% U^{235}) might thus be expected to be dependent only on the reflector saving for uranium. This relationship appears to be approximately true. In Figure 2.11 ratios of reflector savings of such diverse materials as uranium (93.5% U^{235}) and carbon are plotted versus reflector savings for uranium (93.5% U^{235}). Reflector savings ratios for both δ-phase and α-phase plutonium with respect to the uranium are presented. In the case of α-phase plutonium, the graph[2.3] from which these ratios were determined was for a density of 19.5, and no correction was made to the standard value of 19.6 being used in this Handbook.

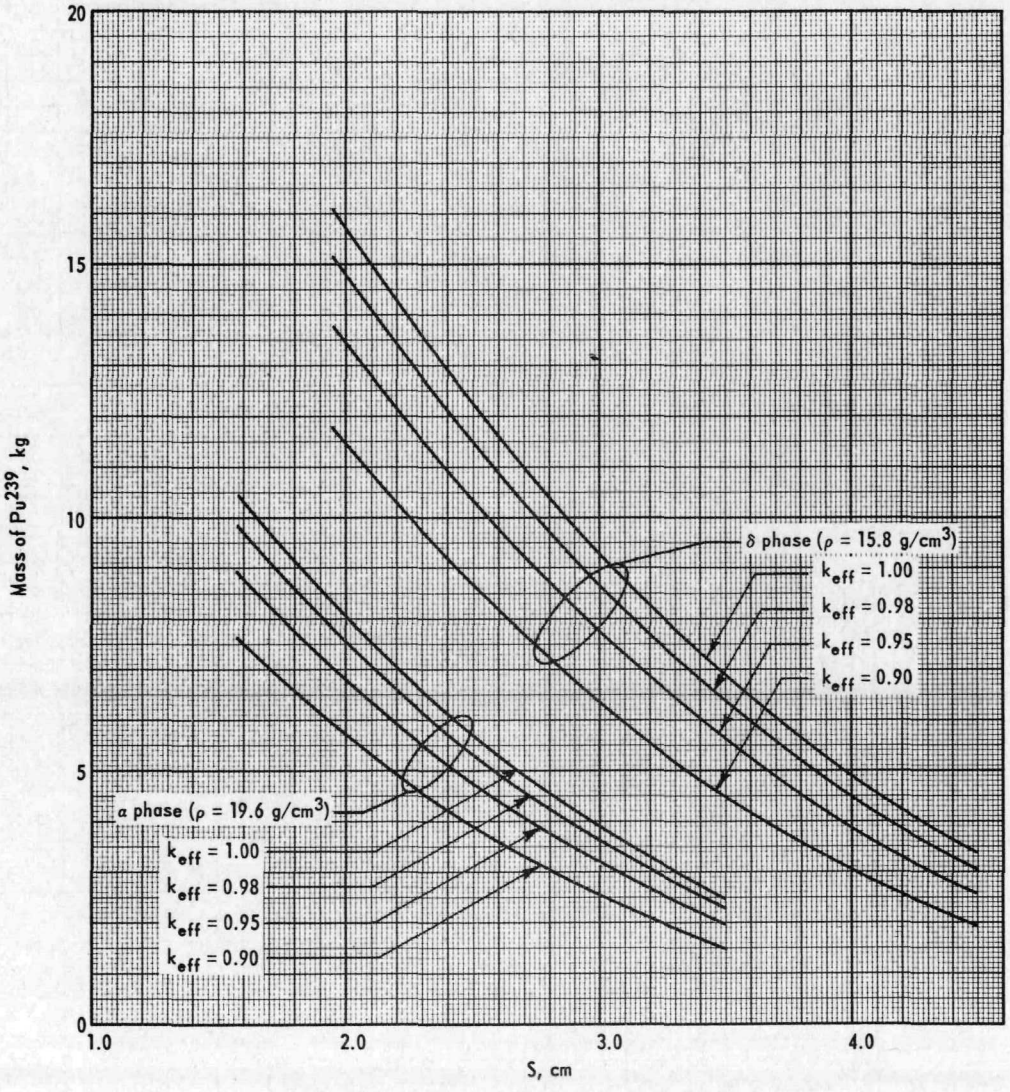

FIG. 2.9 DEPENDENCE OF THE MASS OF A Pu^{239} SPHERE ON S AND k_{eff}

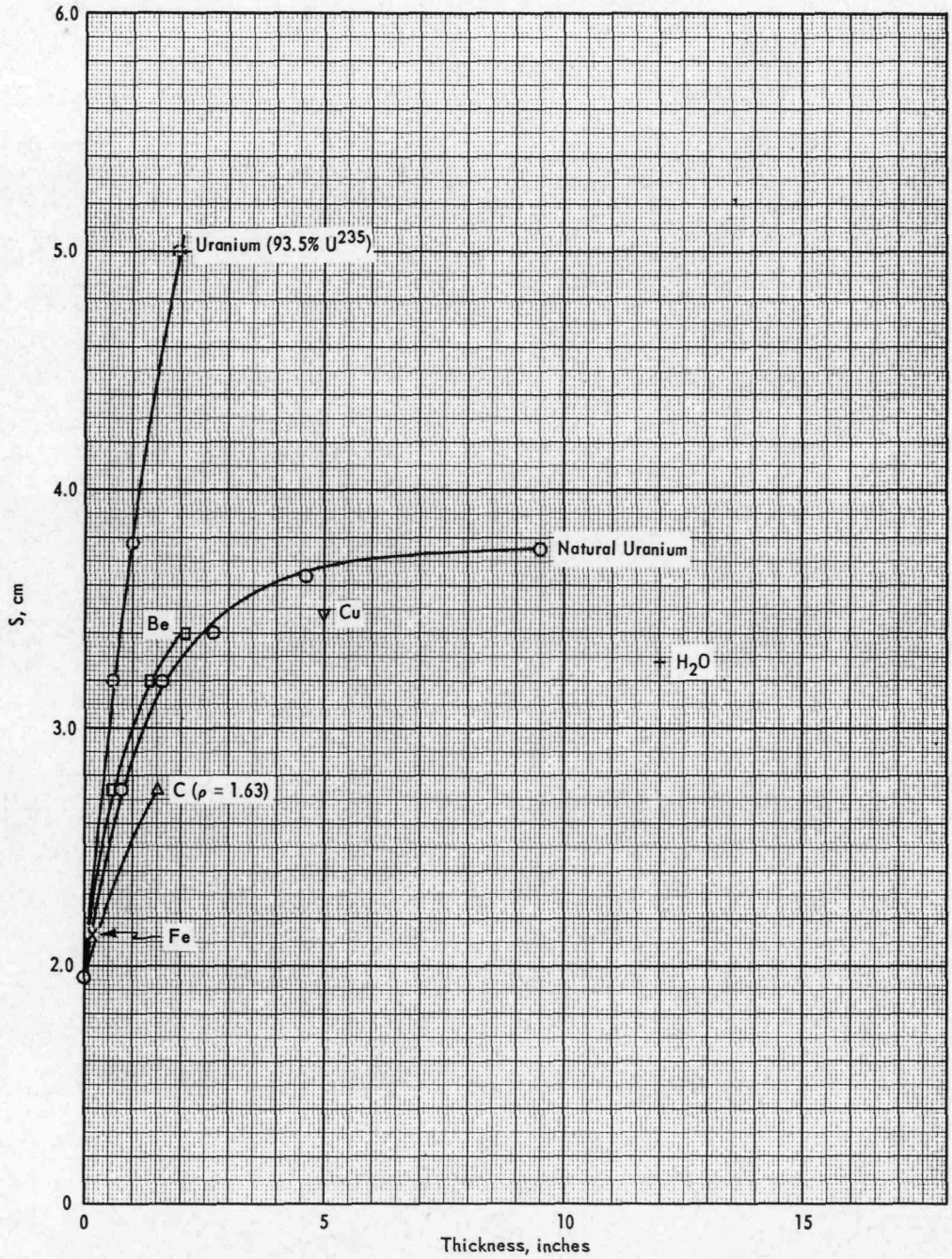

FIG. 2.10 REFLECTOR SAVINGS OF MATERIALS FOR δ-PHASE (ρ = 15.8 g/cm^3) PLUTONIUM

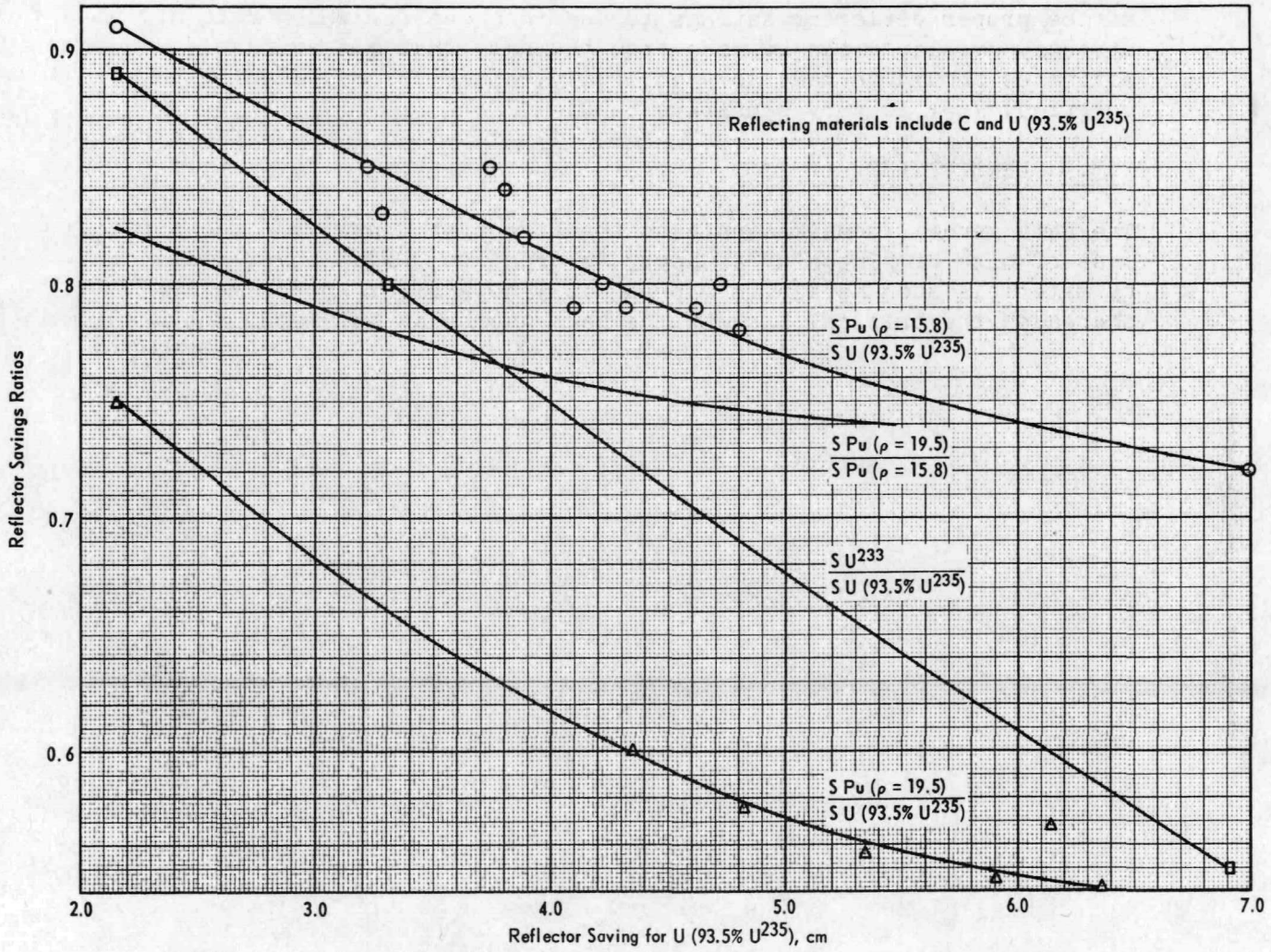

FIG. 2.11 RATIOS OF S FOR Pu AND U^{233} TO S FOR URANIUM (93.5% U^{235})

2.3.2 OTHER SHAPES

Some data[2.6] have been obtained with δ-phase plutonium cylinders surrounded by various reflectors. Expressed as reflector savings, these data are plotted in Figure 2.12. Graphs of H + 2S versus D + 2S are presented in Figure 2.13 for both δ- and α-phase plutonium for k_{eff}'s of 1.0, 0.95, and 0.90. As in the case of uranium, estimates of the proper reflector savings to use in cases for which data are not directly available can be made from the data that are available. Such estimates should be made very carefully, since, as may readily be verified, k_{eff} is very sensitive to S.

2.3.3 DENSITY AND DILUTION

The same general remarks apply to the effect of density on the critical mass of size of plutonium as apply to uranium. Dilution of plutonium by materials such as aluminum presumably to a first approximation increases the critical mass by the same factor as estimated for uranium.

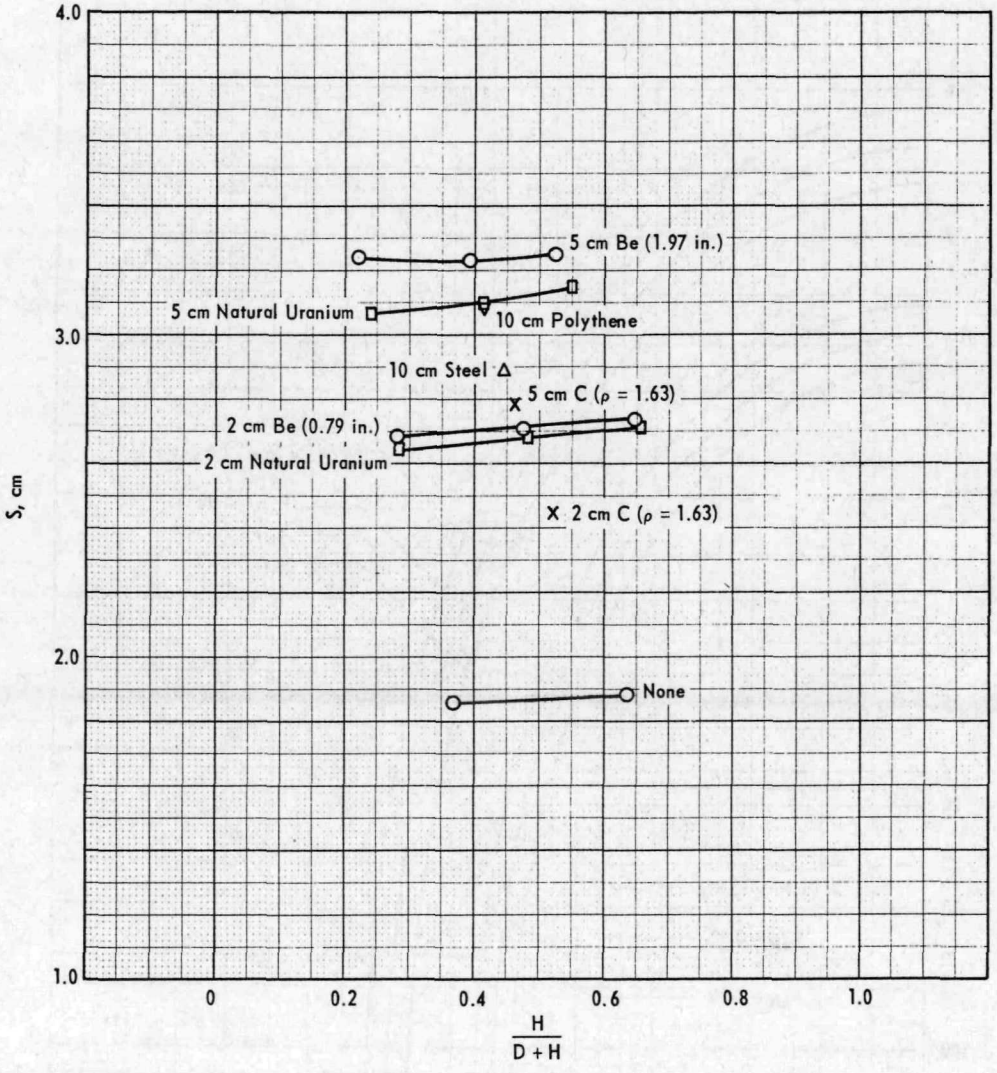

FIG. 2.12 REFLECTOR SAVINGS OF MATERIALS FOR CYLINDERS OF δ-PHASE PLUTONIUM

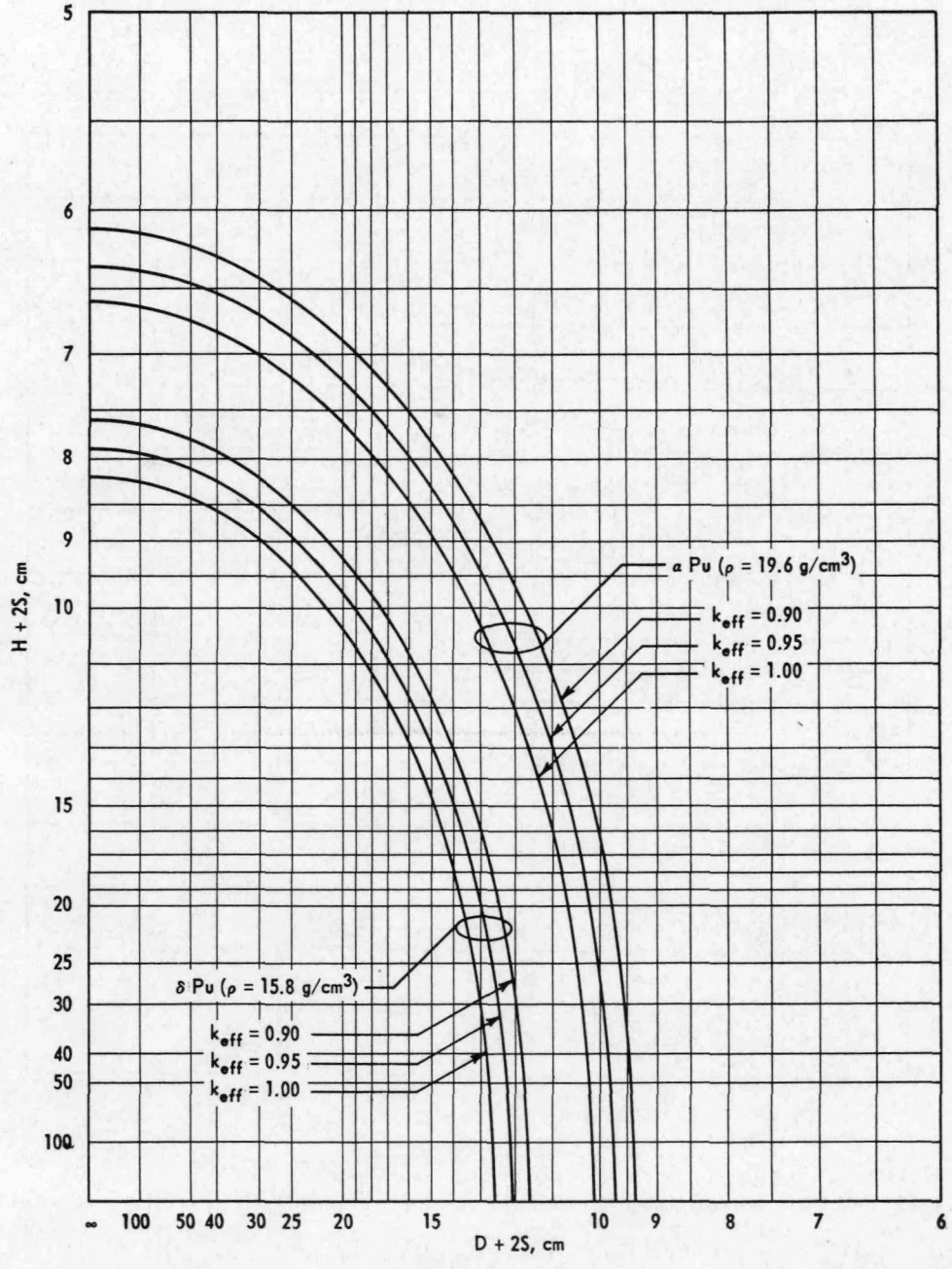

FIG. 2.13 DIMENSIONS OF PLUTONIUM CYLINDERS AS A FUNCTION OF S AND k_{eff}

2.4 URANIUM - 233

Data for U^{233} are very meager. Six-group calculations give $B_m^2 = 0.1672\ cm^{-2}$, $k = 2.547$, and $M^2 = 9.25$. In Figure 2.11 reflector savings ratios of U^{233} to uranium (93.5% U^{235}) are plotted versus the reflector saving for uranium (93.5% U^{235}). Estimates of S can thus be obtained from this graph and the reflector savings reported for uranium (93.5% U^{235}). Plots of mass versus S for k_{eff} values of 1.0, 0.95, and 0.90 are presented in Figure 2.14. In Figure 2.15, H + 2S is plotted versus D + 2S for cylinders on a reciprocal scale for the same three k_{eff} values. The standard density for U^{233} is taken[2.3] as $18.5\ g/cm^3$.

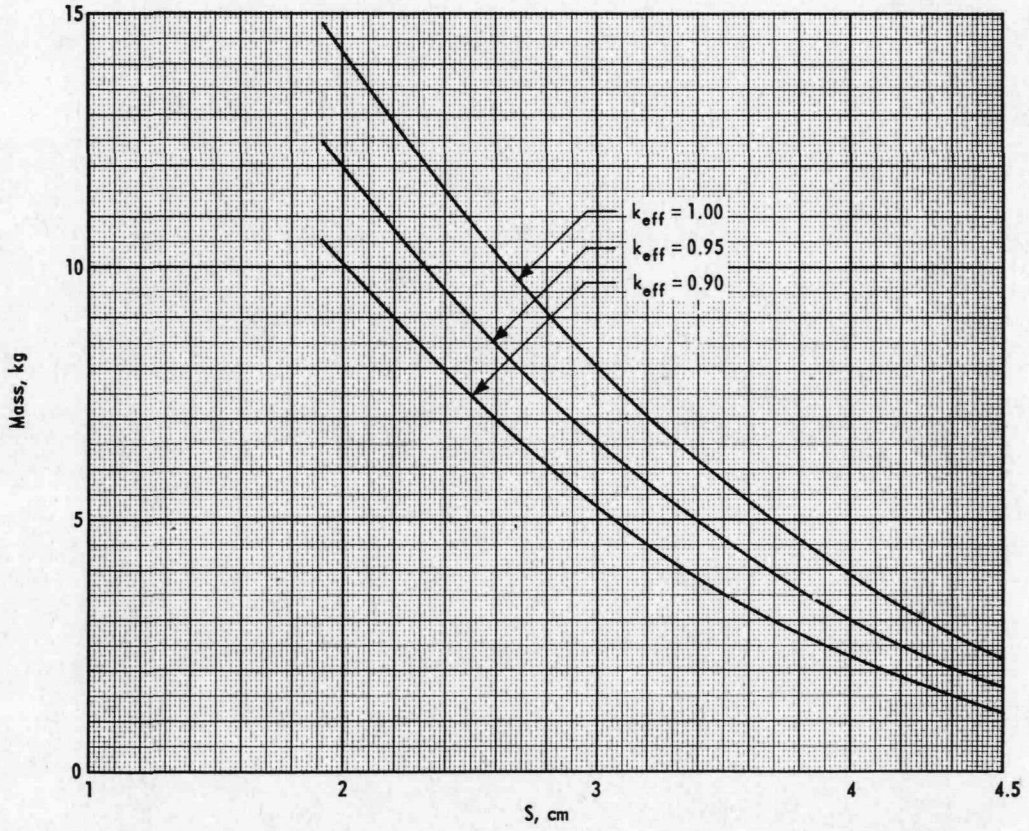

FIG. 2.14 DEPENDENCE OF THE MASS OF A U^{233} SPHERE ON S AND k_{eff}

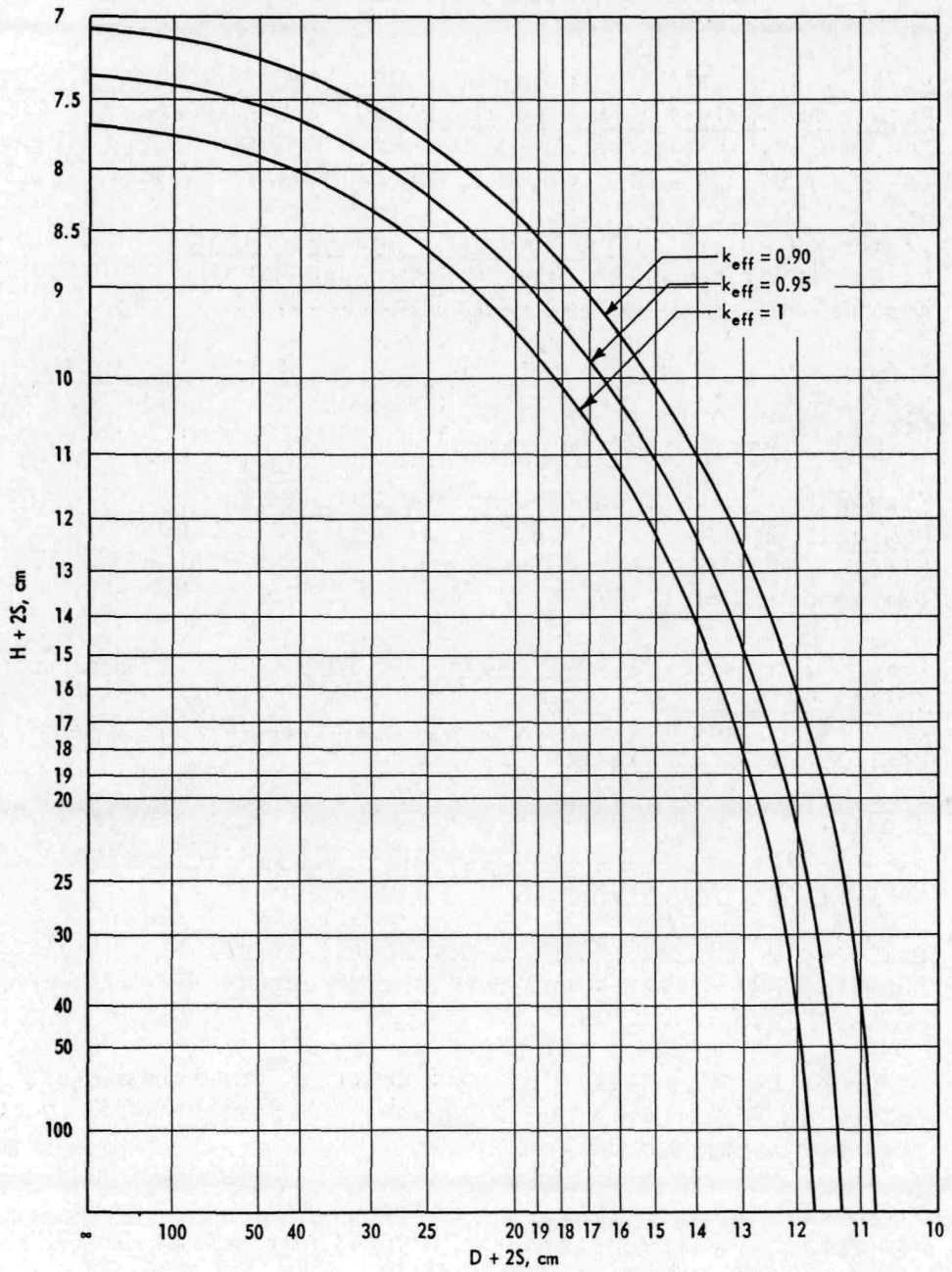

FIG. 2.15 DIMENSIONS OF A U^{233} CYLINDER AS A FUNCTION OF S AND k_{eff}

REFERENCES

2.1 Shapiro, M. M. "Reactor Statics; Experimental and Numerical Results". The Reactor Handbook, Volume 1, Physics. First Edition, Chapter 1.5, March 1955.

2.2 Paxton, H. C. and G. A. Graves. Critical Masses of Fissionable Metals as Basic Nuclear Safety Data. Los Alamos Scientific Laboratory, New Mexico. AEC Research and Development Report LA-1958, 24 pp. (January 1955). (Declassified August 17, 1957).

2.3 Paxton, H. C. Critical Data for Nuclear Safety. Los Alamos Scientific Laboratory, New Mexico. AEC Research and Development Report LAMS-2415, 68 pp. (February 1960).

2.4 Hansen, G. E., et al. Critical Masses of Oralloy in Thin Reflectors. Los Alamos Scientific Laboratory, New Mexico. AEC Research and Development Report LA-2203, 33 pp. (January 1958).

2.5 Kloverstrom, F. A. Spherical and Cylindrical Plutonium Critical Masses. University of California Radiation Laboratory, Livermore Site. AEC Research and Development Report UCRL-4957, 17 pp. (September 1957).

2.6 Ralston, H. R. Critical Masses of Spherical Systems of Oralloy Reflected in Beryllium. University of California Radiation Laboratory, Livermore Site. AEC Research and Development Report UCRL-4975, 7 pp. (October 1957).

2.7 Hansen, G. E. "Properties of Elementary Fast-Neutron Critical Assemblies". Proc. U. N. Intern. Conf. Peaceful Uses Atomic Energy, 2nd, Geneva, 12, 84-88 (1958) P592.

2.8 Schuske, C. L., et al. The Dow Chemical Co., Rocky Flats Plant, Denver. AEC Research and Development Report RFP-66, 22 pp. (August 1956)(Secret).

2.9 Schuske, C. L., et al. The Dow Chemical Co. Rocky Flats Plant, Denver. AEC Research and Development Report RFP-69, 19 pp. (October 1956)(Secret).

2.10 Hoogterp, J. C., et al. Los Alamos Scientific Laboratory, New Mexico. AEC Research and Development Report LA-2026, 56 pp. (March 1957). (Confidential).

2.11 Neuer, J. J., et al. Preliminary Survey of Uranium Metal Exponential Columns. Los Alamos Scientific Laboratory, New Mexico. AEC Research and Development Report LA-2023, 44 pp. (January 1956).

2.12 Paxton, H. C. Los Alamos Scientific Laboratory, Los Alamos, New Mexico, Private Communication.

CHAPTER III - HETEROGENEOUS MODERATED SYSTEMS

3.1 INTRODUCTION

Fissionable material must often be handled when mixed with moderating materials. In the Purex process, plutonium is separated from uranium and from fission products in aqueous and organic solutions. Spent fuel elements are stored under water, and fissionable material is recovered from such elements by dissolving them in acid. In fuel element fabrication processes cleaning and etching baths may be employed.

Even when the fissionable material is handled in air, attention must be given to the possibility that moderators may inadvertently be permitted to intermingle with it. As pointed out in Chapter I, such intermingling can lead to a drastic reduction in the critical mass. The principal moderator one needs to be concerned about is H_2O (or other hydrogenous substances). Carbon may also be of importance in some special cases, but moderators such as Be and D_2O are ordinarily not encountered in nuclear safety problems. Hydrogenous materials are both excellent moderators and very common substances, and guaranteeing their exclusion may be difficult if not impossible. It is, therefore, often customary to handle fissionable material as though it actually were moderated by water, although this means that in the absence of moderation the margins of safety are very large.

A considerable simplification results if the fissionable material and moderator are homogeneously mixed as in the case of solutions or of mixtures of very fine machining chips and moderator. In these cases there is no self-shielding of the fissionable material for thermal or resonance neutrons. Data for solutions are very extensive because of their importance in separations and recovery processes. A separate chapter (Chapter IV) is therefore devoted to the treatment of solutions and homogeneous moderated systems; the present chapter is restricted to heterogeneous systems.

3.2 THEORY

3.2.1 EFFECT OF MODERATION

When moderator and fissionable materials intermingle, the neutron energies become degraded. For most moderators the degradation is not sufficient for moderator to replace fissionable material on a volume-per-volume basis, hence the critical volume increases and the critical buckling decreases. The energy degradation is sufficient, however, to reduce the critical mass at optimum moderation by a large factor because of the increase in fission cross section with decreasing neutron energy. In a fission spectrum the average fission cross section of U^{235} is 1.22 barns. In a neutron spectrum with a Maxwellian distribution of energies about the room temperature thermal value of 0.025 ev the average fission cross section is 504 barns. Moderation, however, cannot reduce the critical mass by as large a factor as the ratio of the cross sections indicates because (1) the migration area of the neutrons is greater in the moderated system than in pure U^{235}, (2) some fraction of the neutrons is absorbed in the moderator, and (3) the number of neutrons produced per neutron absorbed in fissionable material is less at thermal energies.

Besides increasing the cross sections, moderation changes their relative values. For unmoderated uranium metal, the neutron multiplication factor (k) was calculated in Chapter II to be unity at a U^{235} concentration of 5.66%. Lower concentrations are subcritical because the fraction of neutrons with energies below the fission threshold of U^{238} (~1 Mev) absorbed to produce fissions in U^{235} is too small. In a Maxwellian thermal neutron spectrum, however, the fission cross section of U^{235} is enough larger than the U^{238} absorption cross section that in a moderated system employing natural uranium (0.714% U^{235}) k would be 1.327, were it not for the resonance absorption of neutrons in U^{238} during moderation and the absorption of neutrons by the moderator. In a homogeneous H_2O-moderated system of optimum concentration an enrichment to only about 1% U^{235} is required to make k unity.

Distribution of the fissionable material throughout the moderator in clumps rather than homogeneous dispersion decreases the probability that a fission neutron will be moderated, and also decreases the probability that if a fission neutron is moderated it will be absorbed in fissionable material. For high concentrations of U^{235} the result is an increase in the minimum critical mass obtainable at optimum moderation, with the mass approaching that of reflected metal as the size of the clump increases. For low concentrations of U^{235} the high energy fissions in U^{238} are increased and the absorption of moderated neutrons in U^{238} and U^{235} is reduced. The greatest reduction in absorption occurs in the resonance energy region (~5 to ~10,000 ev) where the effective absorption cross section of U^{238} is much higher with respect to the fission cross section of U^{235} than at thermal energies. As a result, for optimum moderation and clumping, uranium

can be made critical in H_2O when the U^{235} concentration is only slightly in excess of that of natural uranium.

3.2.2 EXTENSION OF DATA AND CALCULATION OF SAFETY MARGINS

Because of the much wider energy region for moderated systems, and because of the added complication of heterogeneity, multigroup calculations of the buckling are much more difficult than for pure metal systems and may be less accurate. Moreover, especially for low concentrations of U^{235}, the bucklings may be small, and hence reflector savings that are determined by fitting data to calculated bucklings may be very sensitive to the particular buckling employed. Accordingly, for heterogeneous moderated systems the second approach outlined in Section 1.4, in which the data are fitted to calculated or experimental reflector savings or to reflector savings that are chosen to minimize the variation of buckling with shape, is much more satisfactory and is the one generally used in this chapter.

Simple formulas may be employed to extend the data or to express margins of safety in terms of k_{eff}. The expression for the geometric buckling corresponding to a particular k_{eff} that is considered to be safe is given by Equation 1.15. A similar expression may be written for an extrapolated buckling B^2 in terms of a known value B_o^2, namely

$$B^2 = \left(\frac{(\frac{k}{k_o})k_o - 1}{k_o - 1} \right) \left(\frac{M_o^2}{M^2} \right) B_o^2. \qquad (3.1)$$

As in Equation 1.15, k_o appears both in the numerator and in the denominator; hence the buckling is not greatly sensitive to small errors in k_o. Although the calculation of accurate values of k or of M^2 may require considerable care, it is not expected that this is so in the case of k/k_o and M_o^2/M^2, since errors should tend to cancel out. It is generally best to calculate k_o itself as $k_o = 1 + M_o^2 B_{mo}^2$, where B_{mo}^2 is the experimental buckling and M_o^2 is either determined experimentally or calculated. In extending data, reflector savings should, of course, be calculated for the extended situation, but for large systems the accuracy of the calculations need not be very great. Equation 1.12 may be employed to estimate the change, although a two-group calculation might be expected to give better results.

In calculating k it is convenient to break it down into several factors. According to the definition given in Chapter I,

$$k = \frac{\int k(E)\Sigma_a(E)\phi(E)dE}{\int \Sigma_a(E)\phi(E)dE}.$$

If the fission cross section is represented by $\Sigma_f(E)$ and the number of neutrons released per fission by $\nu(E)$, $k(E) = \frac{\nu\Sigma_f}{\Sigma_a}$, and

$$k = \frac{\int \nu(E)\Sigma_f(E)\phi(E)dE}{\int \Sigma_a(E)\phi(E)dE} .$$

The absorption cross sections of most substances, including fissionable materials, vary approximately inversely as the neutron velocity in the thermal energy range. For moderators this behavior continues to high energies. Hence, when a large fraction of the fissions is caused by thermal neutrons, it is convenient to separate the 1/v absorptions from the remainder. If Σ_{fo} and Σ_{ao} represent the 1/v portion of the cross section, if ν_o represents the constant thermal value of ν, and if $\Delta\Sigma_f(E)$, $\Delta\Sigma_a(E)$, and $\Delta\nu(E)$ represent deviations from the 1/v cross sections and the thermal value of ν as functions of energy,

$$k = \left[\frac{\nu_o \Sigma_{fo}(E_o)}{\Sigma_{ao}(E_o)}\right] \left[\frac{1 + \dfrac{\int[\nu_o \Delta\Sigma_f + \Sigma_f \Delta\nu]\phi(E)dE}{\int \nu_o \Sigma_{fo}\phi(E)dE}}{1 + \dfrac{\int \Delta\Sigma_a \phi dE}{\int \Sigma_{ao}\phi dE}}\right]$$

where E_o is some convenient reference energy such as 0.025 ev. The particular value of E_o in the thermal range is unimportant if the cross sections vary strictly as 1/v in this region, since the energy dependence cancels out in the flux weighted integrals.

The term $\dfrac{\nu\Sigma_{fo}(E_o)}{\Sigma_{ao}(E_o)}$ is commonly represented as the product of two factors,

$$f = \frac{(\Sigma_{ao})_{\text{fissionable material}}}{(\Sigma_{ao})_{\text{all materials}}} \quad \text{and} \quad \eta = \frac{(\Sigma_{fo})}{(\Sigma_{ao})_{\text{fissionable material}}}\nu .$$

Actually some cross sections deviate slightly from 1/v behavior in the thermal energy range. It is usually customary to include this deviation in the computation of f and of η by means of a "non-1/v" factor, which is of course dependent on the shape of the neutron spectrum at thermal energies. The neutron spectrum often assumed for the calculation of the "non-1/v" factor is Maxwellian[3.1], although in the presence of absorptions this spectrum is only an approximation to that which actually exists.

If the epithermal non-1/v absorptions and fissions occur at approximately equal energies and with approximately the same ratio of fissions to absorptions as at thermal energies, as for example is the case for U^{235}, they tend to cancel each other. They may be allowed for by modifying the thermal value of η, but the error introduced if they are ignored is small. In highly enriched, moderated uranium, then, a two-factor formula for k, namely $k = \eta f$ is adequate.

For low enrichments, additional factors are required to take account of the non-1/v events in U^{238}. Fissions occur in U^{238} at neutron energies in excess of 1 Mev and resonance absorptions occur over the entire epithermal region with major contributions from the resonances of lower energy which start with a large resonance peak at about 7 ev. It is customary to represent these events by the product of two factors, ϵ and p, where ϵ gives the increase in the number of fast neutrons as the result of fissions in U^{238} and p gives the probability that a fast neutron escapes capture in the resonances of U^{238} during its moderation to thermal energies. The multiplication constant is then represented as the product of four factors

$$k = \eta f \epsilon p.$$

In heterogeneous systems the calculation of f requires a knowledge of the self-shielding or disadvantage factors, as well as a knowledge of the thermal cross sections. The disadvantage factor of material i may be defined as

$$d_i = \frac{\overline{\Phi}_i}{\sum_i \overline{\Phi}_i}$$

where $\overline{\Phi}_i$ is the average neutron flux in material i. The thermal utilization, f, is then given by

$$f = \frac{(\Sigma V d)_{\text{fissionable material}}}{\Sigma_{\text{all materials}} (\Sigma_i V_i d_i)}$$

where V_i is the volume of the i^{th} material. Diffusion theory is generally inadequate for computing d_i, although its use in nuclear safety calculations is conservative since it underestimates the self-shielding of the fissionable material. The P_3 approximation to the neutron transport equation gives much more nearly correct values for the disadvantage factors. This is the method used at the Savannah River Laboratory for calculating f; an IBM-650 code is available for calculating f in cylindrical geometry.

The factors ϵ and p are also functions of the heterogeneity of the system. For large clumps ϵ tends to be large because the probability of a fission neutron escaping from the clump without causing a fission in U^{238} is relatively low, and p also tends to be large because the self-shielding against resonance energy neutrons entering from the moderator is large. As the spacing between clumps, and hence the relative amount of moderator present, increases, ϵ decreases because the probability of a fast neutron escaping from one clump and entering another clump without having its energy degraded by collisions with moderator atoms decreases. Two somewhat compensating effects occur in p as the spacing is increased: the increased amount of moderator

increases the probability (p) that a neutron will be thermalized without resonance capture, and the increased spacing decreases the shielding of one clump by another against neutrons of resonance energy. At large spacings the interaction effect in ϵ and the shielding of one clump by another against resonance neutrons are insignificant.

The calculation of ϵ and p is somewhat complicated for close-spaced clumps. J. W. Weil[3.2] describes methods for calculating ϵ in uranium-water lattices, and a Monte Carlo code is available at the Savannah River Laboratory. Experimental values[3.3] also exist, which can be used to normalize the calculations. The calculation of p is described in Reference 3.4 and requires a knowledge of the resonance integral, which has been determined experimentally[3.5] as a function of the surface-to-mass ratio of the uranium. For close-spaced clumps the effective surface of a clump is reduced by the shielding provided by the other clumps. Methods are available[3.6] for computing this effect.

3.3 HIGHLY ENRICHED URANIUM IN WATER

For clumps of uranium (93.5% U^{235}) of a given size, increasing the spacing between clumps, and hence increasing the relative amount of moderator present, decreases the material buckling and thus increases the critical size of the system. The decrease in buckling results from an increase in migration area as it approaches that for pure moderator and from a decrease in k, due to the degradation of neutron energies and to the absorption of neutrons in the moderator. These effects tend to increase the critical mass, but they are opposed by the increase in fission cross section, which results from moderation of the neutrons and tends to reduce the amount of fissionable material required for criticality. The result is that the critical mass has a minimum as the relative amount of moderator increases. As the size of the clump decreases, this minimum critical mass decreases because of the decrease in self-shielding for moderated neutrons, and the relative amount of moderator at the minimum mass increases.

Experiments to determine the critical mass have been performed[3.7] with approximately cubic arrays of 1-inch and 1/2-inch cubes of uranium (~94.4% U^{235}) arranged at various regular spacings in water. In Figure 3.1 the reciprocal of the length of one side of the array (the volume to the -1/3 power) is plotted against the logarithm of the fraction of the volume occupied by the uranium blocks for blocks of both sizes. Interpolations made from these slowly varying curves were used in constructing the graphs of critical mass versus the logarithm of the uranium volume fraction shown in Figure 3.2.

Other experiments[3.7] have been performed with approximately cylindrical arrays of 1/8-inch diameter, 12-inch-long rods of uranium (93.6% U^{235}) arranged at various regular spacings in water. In Figure 3.3 the reciprocal of the diameter of the array and the critical mass are plotted against the logarithm of the volume fraction of uranium in the lattice. Since the rods were all of the same length, varying the spacing introduces a variation in the ratio of height to diameter of the array as well. The minimum mass occurs at a height-to-diameter ratio of about 1.3. For an assembly of 1/8-inch-diameter rods of optimum shape the critical mass is about 10% lower. Some experiments[3.7] were performed in which the arrangement of rods was nonuniform. Although the critical mass in some cases was less than that of a uniform array with the same average volume fraction of uranium, in no case studied was it less than that at optimum spacing.

The minimum critical masses of the arrays of cubes and rods can be plotted against the volume-to-surface ratio of an individual unit to permit interpolations for clumps of other sizes and shapes. As the volume-to-surface ratio approaches atomic dimensions, the minimum critical mass for a solution must be approached. At the other end of the range the minimum critical mass must approach that for solid uranium. Inspection of Figure 3.2 indicates that for blocks larger than 1-inch

cubes there may be a minimum critical mass as a function of volume fraction that lies above the mass of the solid metal. In the range of the experimental data, the minimum critical mass is nearly a linear function of the logarithm of the ratio of volume to surface.

In addition to the experiments with uranium blocks and rods, some experiments[3.8] have been performed in which machining chips were immersed in water at H/U^{235} ratios between 60 and 120. The experiments were performed in 8- and 10-inch diameter cylinders reflected by water. Critical masses were between 18 and 92% higher than for solutions at the same H/U^{235} ratios in the same diameter vessels.

Margins of safety are not given for these systems because of the difficulty of computing k and B^2. Moreover, no variation in shape was made in the experiments so that B^2 and S could be obtained by choosing S to minimize variations in B^2. According to solution data, (see Chapter IV) a reasonable value for S appears to be about 6 cm. With this value bucklings can be obtained and equated to solution bucklings, and the thermal disadvantage factor of the uranium can be obtained. Values of k can then be obtained, and margins of safety calculated in the usual manner. The validity of such an approach is perhaps questionable for the 1-inch blocks, but for the 1/8-inch rods and the machining chips it should give good results. The interest in these data is insufficient, however, to justify presenting the results of such an analysis here.

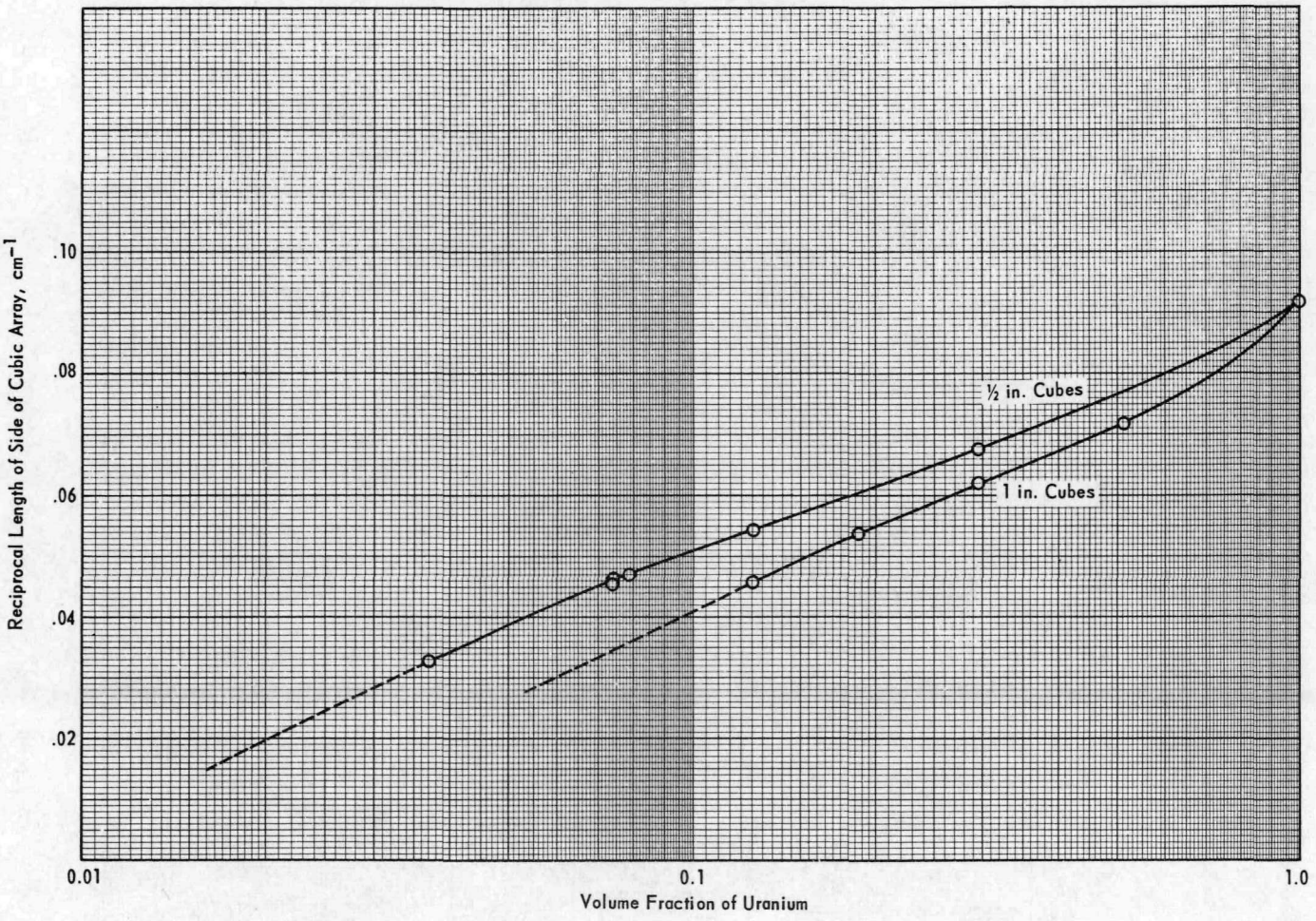

FIG. 3.1 CRITICAL SIZE OF CUBIC ARRAYS OF CUBES OF URANIUM (~94.4% U^{235}) IN WATER

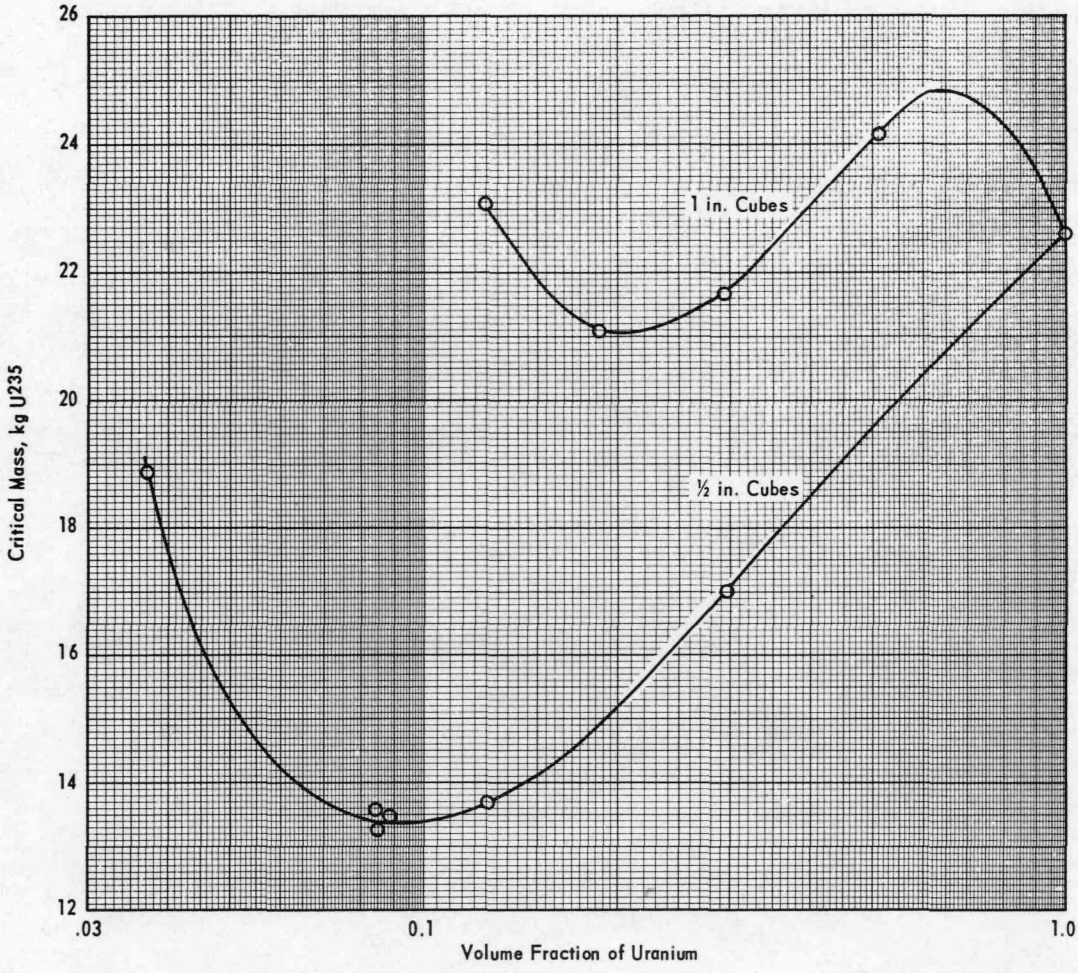

FIG. 3.2 CRITICAL MASS OF U^{235} IN CUBES OF URANIUM (~ 94.4% U^{235}) IN WATER

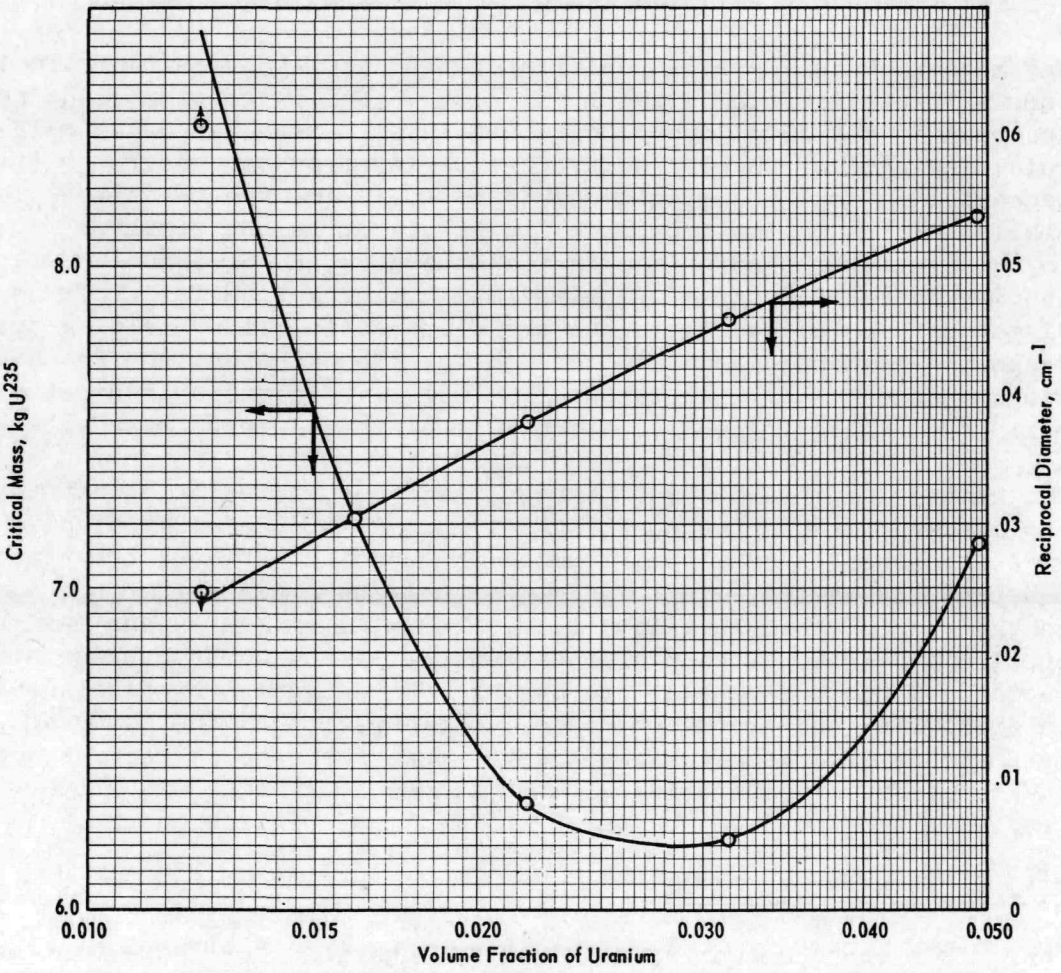

FIG. 3.3 CRITICAL MASS OF U^{235} AND RECIPROCAL DIAMETER OF CYLINDRICAL ARRAYS OF 1/8-INCH DIAMETER, 12-INCH-LONG RODS OF URANIUM (93.6% U^{235}) IN WATER

3.4 SLIGHTLY ENRICHED URANIUM IN WATER

3.4.1 GENERAL CONSIDERATIONS

For arrays of clumps of uranium ($< 5\%$ U^{235}) in water, the buckling has a maximum as the spacing between clumps is varied. The maximum is the result of the opposing effects of the increase in the ratio of U^{235} fissions to U^{238} absorptions and the increase in moderator absorptions (and, for some moderators, the increase in migration area) as the proportion of moderator is increased. The critical mass, of course, passes through a minimum since it approaches infinity both as the spacing approaches zero and as it becomes very large.

The maximum buckling as a function of the water-to-uranium ratio is in turn a function of the size of the clump. For large clumps the neutron spectrum in the clump approaches that in pure metal, and the self-shielding against thermal neutrons entering from the moderator is large; hence the maximum buckling tends to be small or even negative. For smaller clumps the maximum buckling is higher as the result of relatively fewer absorptions in the moderator and of a more nearly thermal neutron spectrum. The maximum buckling then falls off as the clumps become very small, since the decrease in self-shielding against resonance absorptions in U^{238} eventually predominates, and the buckling approaches that for a solution. The relative volume of moderator at maximum buckling increases as the size of the clump decreases.

The critical mass shows much the same sort of variation except that it has minima, whereas the buckling has maxima. For a clump of given size it passes through a minimum as the spacing between clumps in the moderator is varied. This minimum mass in turn passes through a minimum as the size of the clump is varied. The minimum masses and maximum bucklings do not, of course, occur at the same moderator-to-uranium ratios. Since the rate of decrease in concentration of fissionable material with increasing moderator concentration at the point of maximum buckling is generally greater than the rate of decrease of buckling, the minimum critical mass occurs at a higher moderator-to-uranium ratio than that at which the maximum buckling occurs.

3.4.2 EXPERIMENTAL DATA

There is a large amount of data giving bucklings that have been measured with lattices of slightly enriched uranium rods in H_2O. These bucklings are necessarily associated with values of the reflector savings of the essentially infinite H_2O reflector which surrounded the lattices. In the Brookhaven experiments[3.3,3.9,3.10] either lattices of various effective diameters were employed and the reflector saving was chosen that minimized the variation in the buckling, or reflector savings were determined by fitting radial flux traverses to $J_o(B_r r)$. In the Hanford experiments[3.11,3.12] the reflector savings were estimated from the Brookhaven results. In both sets of experiments the lattices

were approximately cylindrical and the effective radius of the cylinder was taken to be $\sqrt{NA/\pi}$, where N is the number of rods in the lattice and A is area of the lattice cell associated with each rod.

The experiments both at Brookhaven and Hanford were exponential rather than critical experiments. A reactor or neutron sources furnished a plane source of thermal neutrons at the base of the cylindrical array of rods, and the attenuation of this source was fitted to the theoretical flux shape $\phi(z) = A \sinh \kappa_z(z + S)$ where z is measured downward from the top of the assembly. In this manner κ_z was determined. The buckling is given by $B^2 = B_r^2 - \kappa_z^2$ where $B_r^2 = \dfrac{(2.405)^2}{\left(\sqrt{\dfrac{NA}{\pi}} + S\right)^2}$.

The data were obtained with aluminum-jacketed rods, and there was generally a small air gap separating the aluminum sheath from the uranium. At the same water-to-uranium ratio the effect of the aluminum on p and ϵ is small and tends to be in opposite directions for the two factors. Extensions of the data to unclad rods can thus be made solely on the basis of the change in M^2 and in f. It is a reasonable assumption that

$$\frac{M^2}{M_{Al}^2} = \frac{\left(1 + \dfrac{V_{H_2O}}{V_U}\right)\left(1 + \dfrac{V_{H_2O}}{V_U} + \dfrac{V_{Al}}{V_U}\right)}{\left(1 + \dfrac{V_{H_2O}}{V_U} + \dfrac{V_{Al}}{V_U} + \dfrac{V_{air}}{V_U}\right)^2},$$

where M_{Al}^2 and M^2 denote respectively migration areas for the lattices of clad and bare rods.

Extensions to bare rods have been made for this Handbook by means of this approximation and by P_3 calculations to determine the f/f_{Al} ratio, use being made of Equation 3.1. The values of M^2 used in computing k_o are either those obtained experimentally[3.3,3.10] or values inferred from these where such data do not exist. For lattices of bare rods the reflector savings are smaller; but the differences are small, and it is conservative to ignore them. For convenience all the experimental bucklings have been adjusted to average values of reflector saving determined from the Brookhaven data. These average values are plotted in Figure 3.4. In making these adjustments it was assumed that the experimental bucklings apply to infinite cylinders.

Extension of the bucklings obtained for bare rods to other enrichments have also been made for this Handbook. A change in enrichment was assumed to affect only f and η, with ϵ, p, and M^2 remaining unaffected. The f ratio was obtained by P_3 calculations made with thermal Maxwellian cross sections, and the η ratio was obtained from thermal values. The

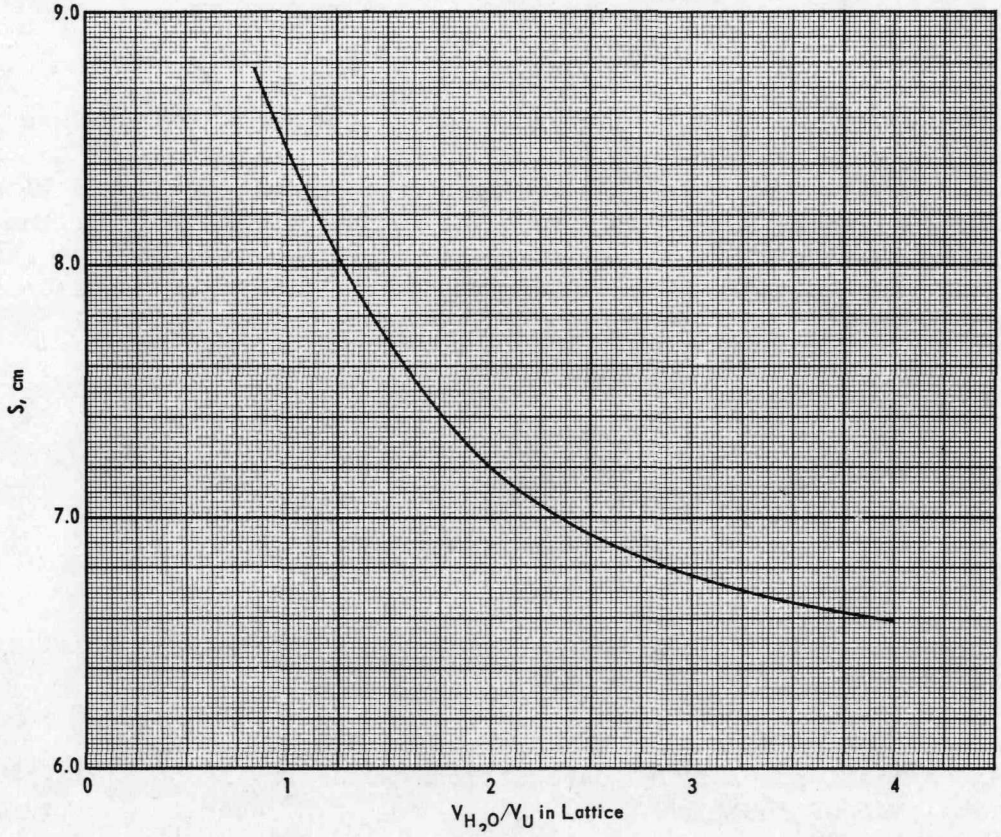

FIG. 3.4 REFLECTOR SAVINGS FOR LATTICES OF URANIUM (< 5% U^{235}) RODS IN WATER
(The arrays are cylindrical and the thickness of the water reflector is effectively infinite.)

reflector savings are considered unchanged from the values plotted in Figure 3.4. In cases where data were obtained at more than one enrichment with the same diameter rod, average values are chosen for the bucklings extrapolated to other enrichments.

In Table III.1 the bucklings of bare rods are presented at the enrichments at which the bucklings for clad rods were measured and at concentrations of 0.714% (natural uranium), 1.0, 2.0, and 3.0% U^{235}. There are numerous ways in which these bucklings can be plotted to furnish useful interpolations and extrapolations.

In Figures 3.5-3.8 graphs of B^2 versus water-to-uranium ratio are presented for each rod size at each of the four enrichments. In constructing these graphs the shapes of the curves, particularly the maxima, were determined by interpolations made on auxiliary graphs of f, k/f, and M^2 against V_{H_2O}/V_U.

3.4.3 MARGINS OF SAFETY

In terms of k_{eff}, the data at these low enrichments are very good. The Brookhaven data give the error in the buckling as generally considerably less than $\pm 10^{-4}$ cm^{-2}. With an average value of M^2 of 32, which is suitable for margin of safety calculations, the corresponding error in k_{eff} is less than ±0.0032. Although there are uncertainties in extending the data to bare rods, the greatest being in the M^2 ratio, the total magnitude of the buckling correction is at most about 10×10^{-4} cm^{-2} or about 0.032 in k_{eff}; and this large a correction applies only to the 0.387-inch-diameter rods at the highest enrichment and to the 1.34-inch-diameter rods at low water-to-uranium ratios. For large rods, low enrichments, and high water-to-uranium ratios, the correction is only a fraction of this. In the extension of the data to the four enrichments chosen, the spread in the three values of buckling obtained by extrapolating the Brookhaven data for enrichments of 1.027, 1.143, and 1.299% is at most about 3×10^{-4} cm^{-2}. For natural uranium at a water-to-uranium ratio of 1.5 and for a rod diameter of 1.1 inches the extrapolation of the data gives a buckling of -3×10^{-4} cm^{-2}. This may be compared with an experimental buckling[3.13], corrected for the presence of cladding, of -0.5×10^{-4} cm^{-2}.

From the foregoing remarks it appears that the maximum safe value of k_{eff} may generally be taken to be as large as 0.98. The corresponding margin in buckling is 6.4×10^{-4} cm^{-2} + 0.02 B^2. For situations that do not deviate greatly from those studied experimentally, even higher values of k_{eff} may be considered acceptable, but one should consult the original data to satisfy himself that this is so.

TABLE III.1

Material Bucklings of Lattices of Uranium Rods in Water

0.387-inch-diameter rods

	Buckling in $cm^{-2} \times 10^4$ at U^{235} concentrations of:						
V_{H_2O}/V_U	0.714%	1.0%	1.027%(a)	1.143%(a)	1.299%(a)	2.0%	3.0%
1	-31.00	4.40	7.10	17.80	28.50	63.60	88.60
1.5	-12.90	24.70	26.40	39.70	51.40	88.60	115.80
2	- 9.70	33.60	36.40	50.90	63.80	108.20	140.40
3	-10.30	35.40	37.50	53.70	68.70	115.80	151.30
4	-20.60	27.00	29.70	46.10	62.10	112.80	151.30

0.600-inch-diameter rods

	Buckling in $cm^{-2} \times 10^4$ at U^{235} concentrations of:						
V_{H_2O}/V_U	0.714%	1.0%	1.027%(a)	1.143%(a)	1.299%(a)	2.0%	3.0%
1	-24.50	11.70	13.40	25.80	37.40	72.30	97.80
1.5	- 8.00	31.10	34.30	45.90	58.20	97.50	125.60
2	- 4.50	37.60	40.60	53.80	67.30	109.90	140.80
3	-13.70	32.80	36.00	51.10	65.80	114.20	149.80
4	-30.00	18.80	22.50	38.10	53.60	106.00	144.70

0.750-inch-diameter rods

	Buckling in $cm^{-2} \times 10^4$ at U^{235} concentrations of:				
V_{H_2O}/V_U	0.714%	1.0%	1.027%(a)	2.0%	3.0%
1.334	- 8.80	29.40	32.30	93.90	121.00
1.584	- 4.60	34.60	37.60	101.00	129.00
1.834	- 3.90	37.10	40.20	107.00	137.00
2.334	- 7.80	36.00	39.30	111.00	144.00
2.834	-13.10	31.70	35.10	110.00	143.00
3.834	-30.50	15.50	19.00	96.90	133.00

TABLE III.1 (Continued)

0.925-inch-diameter rod

V_{H_2O}/V_U	Buckling in $cm^{-2} \times 10^4$ at U^{235} concentrations of: 0.714%	1.007%(a)	2.0%	3.0%
1.37	- 7.10	31.90	95.60	123.00
1.74	- 3.40	37.50	105.00	133.00
1.94	- 6.20	36.10	106.00	136.00
2.15	-10.90	32.20	104.00	135.00

1.34-inch-diameter rod

V_{H_2O}/V_U	Buckling in $cm^{-2} \times 10^4$ at U^{235} concentrations of: 0.714%	1.0%	1.44%(a)	2.0%	3.0%
1.31	-11.40	26.10	61.70	88.40	114.00
1.46	- 9.20	28.90	65.10	92.30	119.00
1.73	-10.70	28.20	65.20	93.20	120.00
2.30	-22.80	17.90	57.00	86.60	116.00
2.92	-37.70	26.50	41.70	71.40	100.00

1.66-inch-diameter rod

V_{H_2O}/V_U	Buckling in $cm^{-2} \times 10^4$ at U^{235} concentrations of: 0.714%	1.007%(a)	2.0%	3.0%
0.86	-19.80	17.50	77.50	103.00
1.33	- 9.90	28.20	89.80	116.00
1.85	-17.00	22.10	85.80	113.00

(a) U^{235} concentrations for which experimental data were obtained

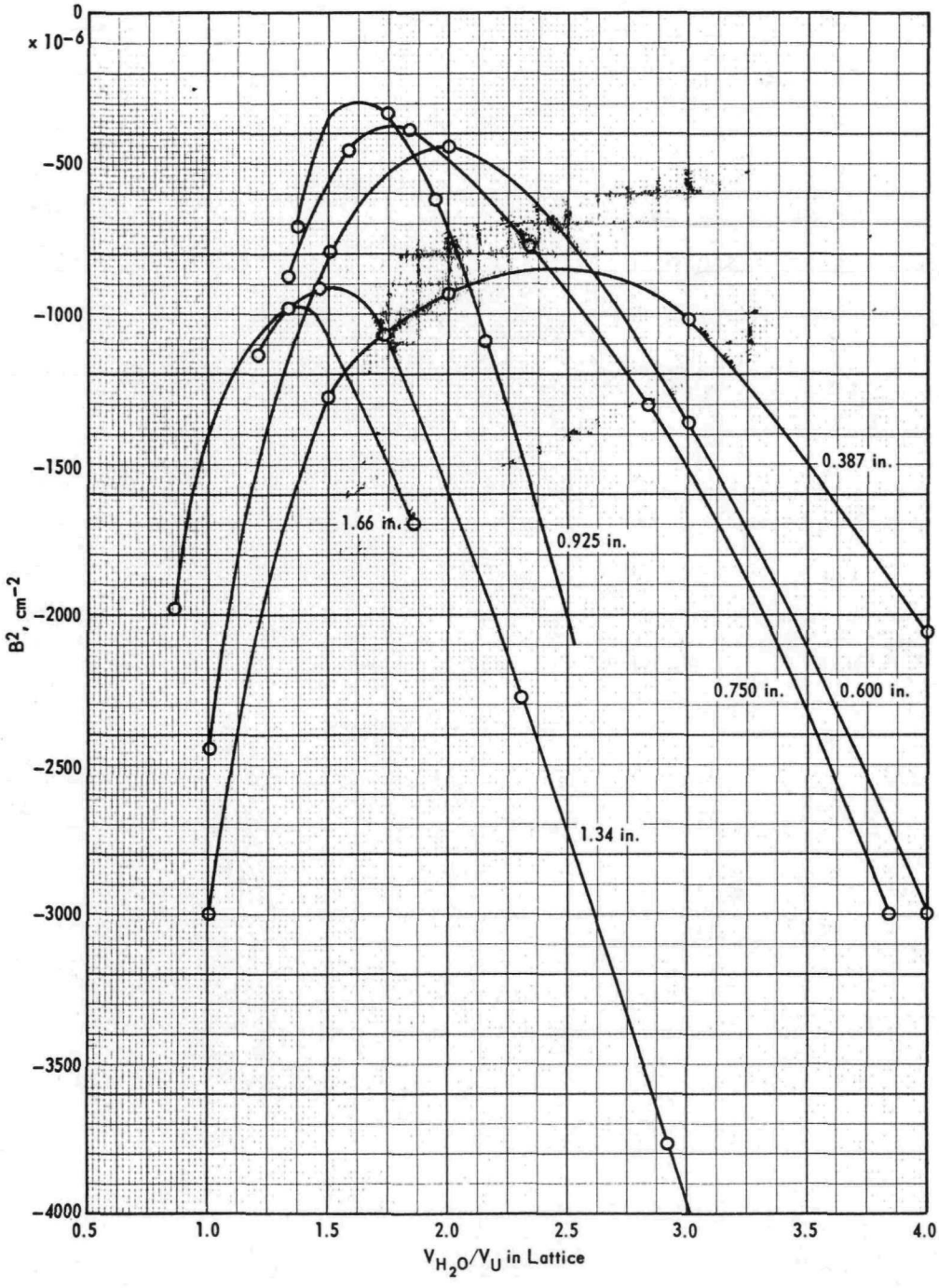

FIG. 3.5 MATERIAL BUCKLINGS OF ARRAYS OF URANIUM (0.714% U^{235}) RODS IN WATER
(The curves are for various rod diameters.)

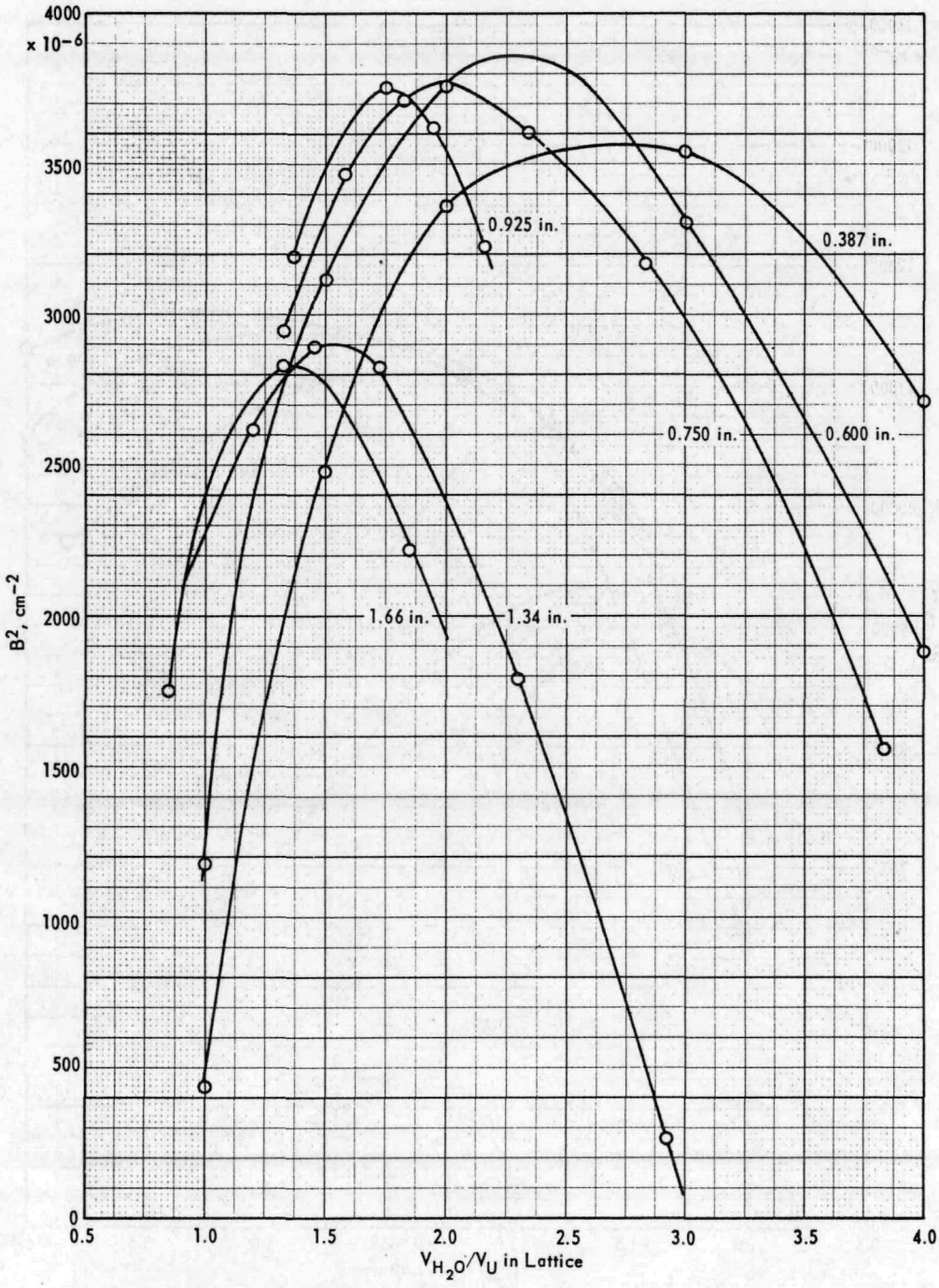

FIG. 3.6 MATERIAL BUCKLINGS OF ARRAYS OF URANIUM (1.0% U^{235}) RODS IN WATER
(The curves are for various rod diameters.)

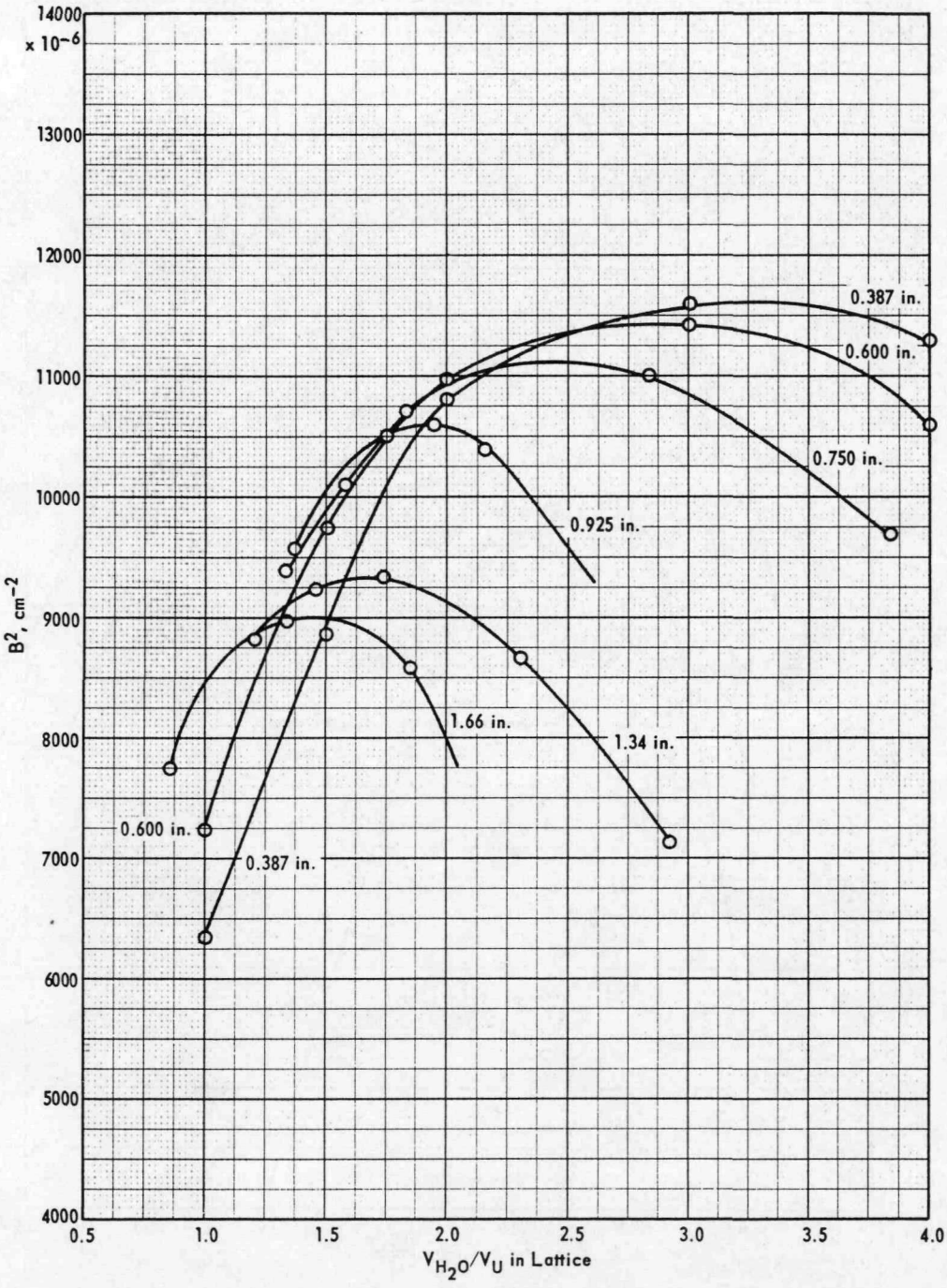

FIG. 3.7 MATERIAL BUCKLINGS OF ARRAYS OF URANIUM (2.0% U^{235}) RODS IN WATER
(The curves are for various rod diameters.)

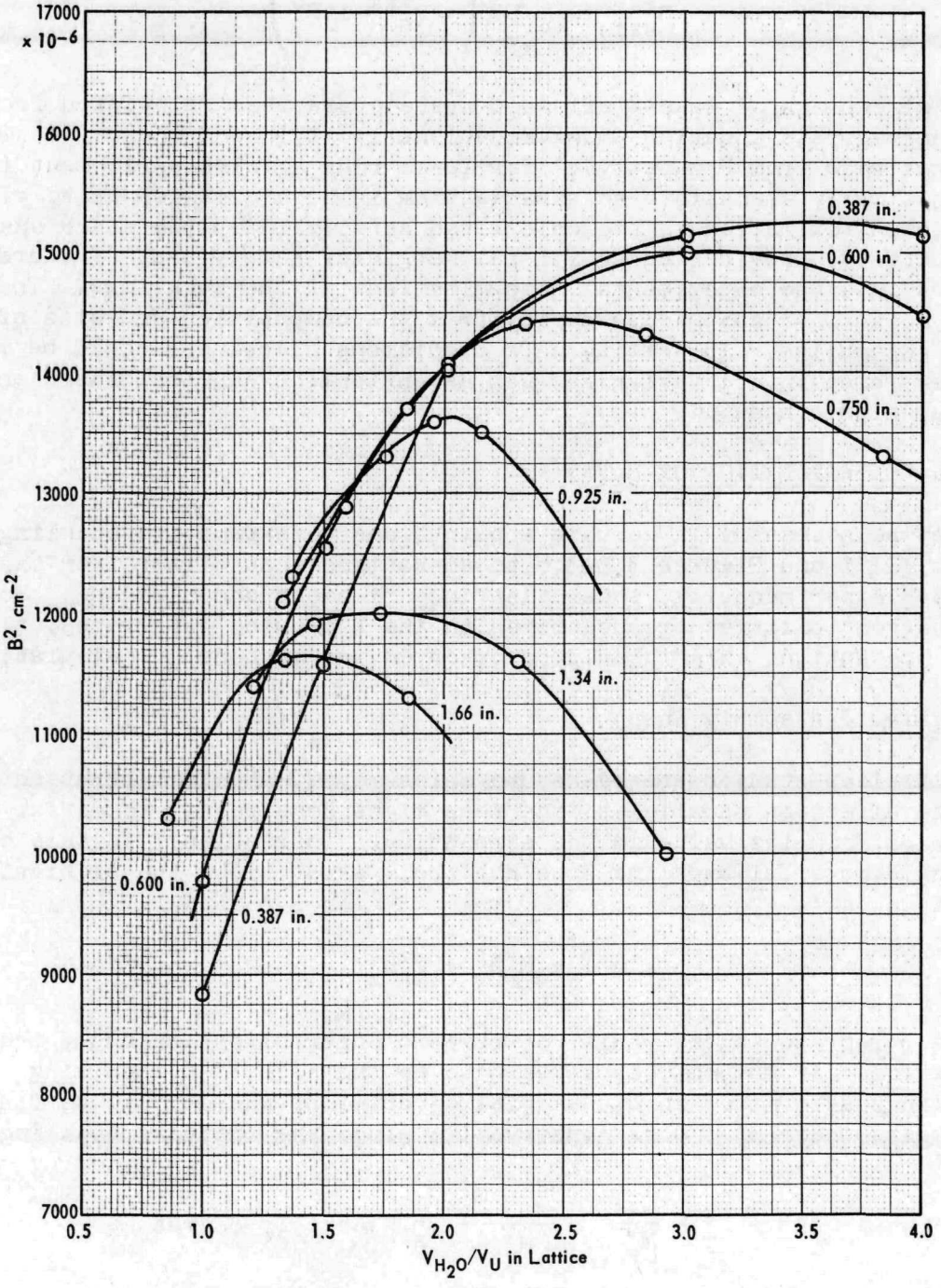

FIG. 3.8 MATERIAL BUCKLINGS OF ARRAYS OF URANIUM (3.0% U^{235}) RODS IN WATER
(The curves are for various rod diameters.)

The safe bucklings corresponding to particular choices of k_{eff} are obtained from Equation 1.15, which with $M^2 = 32$ becomes

$$B^2_{safe} = \frac{1}{k_{eff}} \left(\frac{1-k_{eff}}{32} + B^2 \right).$$

Safe dimensions of water-reflected systems are then calculated from the appropriate equation among Equations 1.6-1.10 and the reflector savings read from Figure 3.4. For large rods at high enrichment it may be physically impossible to arrange them in such a manner as to give a good approximation to the calculated safe cylinder (or other shape). This effect, provides an additional margin of safety and, of course, enters into the experimental determinations of the bucklings. The safe masses are calculated easily from the composition and size of the safe assemblies. In setting safe conditions allowance should be made for extremes in all variables such as enrichment and the dimensions of the uranium pieces.

3.4.4 EXTRAPOLATION OF DATA

It may be necessary in certain applications to extend the bucklings of Table III.1 and Figures 3.5-3.8 to situations that differ from those studied experimentally, other than in enrichment and cladding. Some of the possibilities are described in the following paragraphs, along with precautions which should be observed and methods of calculations.

3.4.4.1 Assembly Shape

The lattices studied are by nature anisotropic, and the migration area in the direction parallel to the rods might be expected to differ somewhat from its value in the perpendicular direction. In this case a single material buckling does not truly exist since the critical equation is

$$k = 1 + M^2_r B^2_r + M^2_z B^2_z$$

where r represents the radial or perpendicular direction and z the axial direction. If $M^2_z > M^2_r$, as appears to be the case,[3.3] applying bucklings determined in exponential experiments where $B^2_z < 0$ to finite cylinders where $B^2_z > 0$ is conservative since the critical buckling,

$$B^2_r + B^2_z = \frac{k-1}{M^2_r} - \frac{M^2_z - M^2_r}{M^2_r} B^2_z, \text{ actually decreases}$$

as B^2_z increases. The anisotropy, however, has not been measured in many cases and is somewhat uncertain. Moreover, there may be changes in S with shape; hence somewhat larger margins of safety should be allowed for assemblies differing considerably in shape from those studied experimentally.

3.4.4.2 Shape of Uranium Clump

The uranium pieces may not be solid rods. To a first approximation the equivalent solid rod is one which has the same surface-to-volume ratio. The probability of a fission neutron escaping the piece without a collision, upon which ϵ depends, is very nearly a function only of surface-to-volume ratio for a uniform source distribution in such diverse shapes as slabs, cylinders, spheres, and hemispheres. The resonance integral, too, is a function of surface-to-volume ratio. However, thermal disadvantage factors and interaction effects between clumps may be shape dependent. At the same water-to-uranium ratio a hollow cylinder with the same volume as a solid cylinder would have lower values of p and ϵ because of the greater surface, but higher values of f because of the higher thermal disadvantage factor in the uranium. It is not known whether it is possible to obtain with different shapes or hollow rods, bucklings greater than the maximum achievable with solid rods; however, allowance should be made for this possibility in setting safe limits. Data exist[3.12,3.14-3.16] for some particular shapes that may be compared with data for solid cylinders of the same volume or surface-to-volume ratio or that may be useful in evaluating methods of calculating the changes in ϵ, p, and f in going from a solid cylinder to some other shape.

3.4.4.3 Arrangement of Pieces

The bucklings in Table III.1 are for arrays of regularly spaced rods. Experiments performed at Hanford[3.17,3.18] with uranium slugs close to the optimum size for maximum buckling indicate that a random arrangement generally has a lower buckling than a regular array at a water-to-uranium ratio corresponding to the average of the random array. This result appears reasonable if the average water-to-uranium ratio is close to the optimum since this ratio is the result of rods with separations on both sides of the optimum. Irregular arrays of very small uranium rods might very well, however, have bucklings larger than regular arrays since grouping several small rods together would tend to approximate a larger rod.

3.4.4.4 Other Reflectors and Moderators

The bucklings in Table III.1 apply to the situation in which a regular lattice of rods is immersed in water and a thick layer of water surrounds the assembly. If the immersion medium is an organic liquid, corrections to these bucklings may be necessary. If the organic liquid has a lower hydrogen density than water, both M^2 and f are larger because relatively fewer neutrons are moderated and captured by hydrogen atoms. Except for very small or negative bucklings the net result is a decrease in buckling. The change in f can be calculated by the diffusion or P_3 approximation. The change in M^2 can be estimated from the approximation

$$M'^2 = \frac{1 + \frac{V_{mod}}{V_U}}{1 + \rho \frac{V_{mod.}}{V_U}} M^2$$

where M'^2 is the migration area with the organic liquid, M^2 the migration area with water, V_{mod} and V_U are the volumes of moderator and uranium, and ρ is the hydrogen density in the organic liquid relative to that in water. The reflector saving, to a first approximation, is unchanged since changes in B are compensated by changes in κ (see Equation 1.12).

In a dissolver the immersion medium may be nitric acid. As dissolution progresses uranium goes into solution and the uranium pieces become smaller. The increase in surface-to-volume ratio decreases p and ϵ, and the decrease in self-shielding increases f. The solution that finally results has a lower buckling than that achievable with pieces of optimum size, but if sufficiently large pieces are dissolved, the buckling may pass through a maximum as the dissolution progresses. It is of course conservative to assume that p and ϵ do not change as dissolution progresses and to calculate f by the P_3 approximation. The poisoning due to nitrogen decreases f. The displacement of hydrogen by nitrogen increases M^2, but it is conservative to ignore this effect.

In some circumstances an array of enriched uranium might be surrounded by natural uranium. The reflector saving provided by the natural uranium is readily calculated from Equation 1.12 with $D_c = D_r$ and $\kappa_r^2 = -B^2$ for natural uranium.

3.4.4.5 Moderator Density

When uranium pieces are handled in air, reliance may be placed on control of the spacing between pieces to ensure that a nuclear incident will not occur in the event of flooding by water. As Table III.1 illustrates, either a close-packed arrangement or a widely spaced arrangement results in a considerable increase in critical mass over the value at optimum spacing. Although it is possible to increase the separation between pieces sufficiently that an infinite mass is subcritical in the event of flooding, there is danger in relying too heavily on this procedure since full flooding is not the worst circumstance. At the large separation the optimum water-to-uranium ratio is achieved by filling only a fraction of the available space around each piece with water, such as flooding with water of density less than 1 g/cm^3. The critical mass is, of course, greater than for an array at optimum moderation with water of full density, but is by no means infinite. Examples of situations in which such partial flooding or its equivalent might occur are the spraying of an array with a hose, or the separation of pieces from each other by wooden or plastic partitions.

The buckling of a partially flooded array, containing voids, can be obtained from that of a compact array of the same water-to-uranium ratio by calculating the change in M^2, which is given by

$$\frac{M^2_{voids}}{M^2} = \left(1 + \frac{V_{void}}{V_{H_2O} + V_U}\right)^2 = \left(\frac{1 + \frac{V_{H_2O}}{V_U}\left(1 + \frac{V_{void}}{V_{H_2O}}\right)}{1 + \frac{V_{H_2O}}{V_U}}\right)^2$$

where M^2_{void} and M^2 denote respectively the migration areas of the arrays with and without voids.

In addition to the change in M^2 there may be changes in k that are functions of the placement of the voids. Thus a positive buckling for natural uranium rods in water has been reported[3.9] when an annular void surrounds the rods. The voids also affect the reflector saving, which increases at least as fast as M; the increase may be even greater if the considerations discussed in Chapter II apply here. In view of these uncertainties generous margins of safety should be applied to such arrangements if partial flooding is considered possible.

REFERENCES

3.1 Hughes, D. J. and J. A. Harvey. Neutron Cross Sections. Brookhaven Neutron Cross Section Compilation Group. AEC Research and Development Report BNL-325, 334 pp. (July 1955).

3.2 Weil, J. W. Fast Fission Effect in Uranium-Water Lattices. General Electric Co. Knolls Atomic Power Laboratory, Schenectady, New York. AEC Research and Development Report KAPL-1043, 31 pp. (January 1954).

3.3 Kouts, H. and R. Sher. Experimental Studies of Slightly Enriched Uranium, Water Moderated Lattices. Part I. 0.600-In.-Diameter Rods. Brookhaven National Laboratory, Upton, N. Y. AEC Research and Development Report BNL-486, 41 pp. (September 1957).

3.4 Glasstone, S. and M. C. Edlund. The Elements of Nuclear Reactor Theory. New York: D. Van Nostrand & Co. 416 pp. (1952).

3.5 Hellstrand, E. "Measurements of the Effective Resonance Integral in Uranium Metal and Oxide in Different Geometries". J. Applied Physics, 28, 1493-1502 (December 1957).

3.6 Dancoff, S. M. and M. Ginsburg. Surface Resonance Absorption in a Close-Packed Lattice. United States Atomic Energy Commission, Technical Information Service Extension, Oak Ridge, Tenn. AEC Research and Development Report CP-2157, 9 pp. (October 1944).

3.7 Hoogterp, J. C. Critical Masses of Oralloy Lattices Immersed in Water. Los Alamos Scientific Laboratory, New Mexico. AEC Research and Development Report LA-2026, 56 pp. (March 1957).

3.8 McLendon, J. D. and J. W. Morfitt. Union Carbide and Carbon Chemicals Co. Y-12 Oak Ridge, Tenn. AEC Research and Development Report Y-A2-71, 17 pp. (February 1952). (Secret).

3.9 Kouts, H., et al. "Exponential Experiments with Slightly Enriched Uranium Rods in Ordinary Water". Proc. U. N. Intern. Conf. Peaceful Uses of Atomic Energy, Geneva, 5, 183-202 (1955) P600.

3.10 Kouts, H. et al. "Physics of Slightly Enriched, Normal Water Lattices (Theory and Experiment)". Proc. U. N. Intern. Conf. Peaceful Uses Atomic Energy, 2nd Geneva, 12, 446-482 (1958). P1841.

3.11 Clayton, E. D. Exponential Pile Measurements in Water Moderated Lattices with Enriched Uranium Rods. Hanford Atomic Products Operation, Richland, Washington. AEC Research and Development Report HW-40930, 45 pp. (January 1956).

3.12 Block, E. Z. and E. D. Clayton. "Buckling Measurements with Enriched Fuel Elements in Light Water". Nuclear Physics Research Quarterly Report - July, August, September 1956. General Electric Co. Hanford Atomic Products Operation, Richland, Washington. AEC Research and Development Report HW-47012, 56 pp. (November 1956). pp. 12-19.

3.13 Kouts, H., et al. "Reactor Parameters of a Light Water-Normal Uranium Lattice". J. of Nuclear Energy, 2-3, 141-142 (1955-56).

3.14 Clayton, E. D. and E. Z. Block. "Buckling Measurements with Enriched Hollow Fuel Elements in Light Water". Physics Research Quarterly Report - April, May, June 1956. General Electric Co., Hanford Atomic Products Operation, Richland, Washington. AEC Research and Development Report HW-44525, 75 pp. (July 1956). pp. 59-67.

3.15 Block, E. Z. "Enriched Uranium-Water Lattices". Nuclear Physics Research Quarterly Report - April, May, June 1957. General Electric Co. Hanford Atomic Products Operation, Richland, Washington. AEC Research and Development Report HW-51983, 81 pp. (August 1957), pp. 49-54.

3.16 Fox, J. K., J. T. Mihalczo, and L. W. Gilley. "Critical Experiments with 2.09% U^{235} Enriched Uranium Metal Plates in Water". Oak Ridge National Laboratory, Tenn. AEC Research and Development Report ORNL-CF-58-8-3, 8 pp. (August 1958).

3.17 Lloyd, R. C. "Buckling Measurements of Fuel Elements in a Random Array, Water Moderated". pp. 35. Nuclear Physics Research Quarterly Report October, November, December 1957. General Electric Co. Hanford Atomic Products Operation, Richland, Washington. AEC Research and Development Report HW-54591, 85 pp. (March 1958).

3.18 Lloyd, R. C. "Buckling Measurements for Fuel Elements in a Random Array". p. 12. Nuclear Physics Research Quarterly Report, January, February, March 1958. General Electric Co. Hanford Atomic Products Operation, Richland, Washington. AEC Research and Development Report HW-55879, 42 pp. (April 1958).

CHAPTER IV - HOMOGENEOUS MODERATED SYSTEMS

4.1 INTRODUCTION

In this chapter critical and safe conditions are given for homogeneous mixtures of fissionable and moderating materials. Only such additional theory as is needed here is included, since a fairly complete presentation of the effect of moderation is given in Chapters I and III. Water solutions of U^{235} receive the most extensive treatment because of the large amount of data available. The general treatment and methods of handling the data apply also to plutonium and U^{233}.

4.2 AQUEOUS SOLUTIONS OF URANIUM (~93.5% U^{235})

4.2.1 THEORY

A large number of critical experiments[4.1-4.4] have been performed at the Oak Ridge National Laboratory with solutions of UO_2F_2 in which the uranium contained approximately 93.5% U^{235}. This compound was chosen because of its high solubility and because of the small neutron capture cross sections of oxygen and fluorine. A somewhat smaller number of experiments[4.5] have been performed with $UO_2(NO_3)_2$ solutions with various amounts of HNO_3 present. Except perhaps for solutions of low concentration, the bucklings of these solutions are large enough that it is practical to use the first method given in Section 1.4 for extending data, in which the reflector savings serve as parameters that relate theory and experiment. Although bucklings calculated by multigroup methods would probably be more accurate and hence preferable, a simple one-group expression is adequate. As pointed out in Section 1.4, even when the correct buckling is used, some variation of reflector saving with shape is expected; hence the small variations (see Figures 1.1-1.3) attributable to an incorrect buckling are not objectionable provided the error in the buckling is not too great.

The expression used for the buckling is

$$B_m^2 = \frac{k-1}{M^2} \tag{4.1}$$

where $k = \eta f$ and $M^2 = \tau + L^2$. Thermal cross sections are employed for η and f, and τ is taken to be the neutron age in pure moderator. The thermal utilization, f, is given by

$$f = \frac{\sigma_{U^{235}}}{\sigma_{U^{235}} + \frac{H}{U^{235}}\sigma_H + \frac{X}{U^{235}}\sigma_X} \tag{4.2}$$

where the σ's are thermal cross sections in barns, X denotes elements other than hydrogen and U^{235} that may be present, and $\frac{H}{U^{235}}$ and $\frac{X}{U^{235}}$

are atomic ratios. The diffusion area, L^2, is approximated by

$$L^2 = (1 - f)L_o^2 \qquad (4.3)$$

where L_o^2 is the diffusion area of the moderator.

Values of thermal cross sections employed in this Handbook are given in Table IV.1, together with the thermal value of η. The U^{235} cross section contains a non-1/v factor calculated for a Maxwellian distribution about 0.025 ev so as to give a nearly correct cross section for dilute solutions. Allowance for the small contributions of U^{234} and U^{238} are included in the U^{235} cross section; hence these isotopes may be ignored for uranium containing approximately 93.5% U^{235}. Resonance absorption in U^{238} is assumed to be compensated by fast fissions in U^{238}. The only substance other than hydrogen and uranium considered to contribute significantly to f is nitrogen. Fluorine and oxygen have such small cross sections that they may be ignored. Absorbers such as boron or cadmium might be present in special cases, but they are not considered here.

TABLE IV.1

Parameters Employed in Calculating k for U^{235} Solutions

Material	σ, barns	η
U^{235}	678	2.07
H	0.332	
N	1.88	

For UO_2F_2 solutions the pure moderator is taken to be H_2O; for $UO_2(NO_2)_2$ solutions it is taken to be a nitric acid solution with the same acid normality as that of the uranyl nitrate solution. The diffusion area in nitric acid solutions is plotted in Figure 4.1 against the acid normality. In Figure 4.2 a similar graph is presented for the neutron age. Both curves are calculated, and they are based on values for pure H_2O that are consistent with experiment.

4.2.2 URANYL FLUORIDE SOLUTIONS

4.2.2.1 Spheres

Some experiments[4.4,4.6,4.7,4.15] have been performed in which bare and water-reflected spheres were made critical by adjusting the concentration of the solution within the spheres. The reflector was effectively infinite. The spherical containers were fabricated from aluminum to minimize the effect of the container wall. When these data are fitted by means of Equation 1.6 to bucklings calculated by the

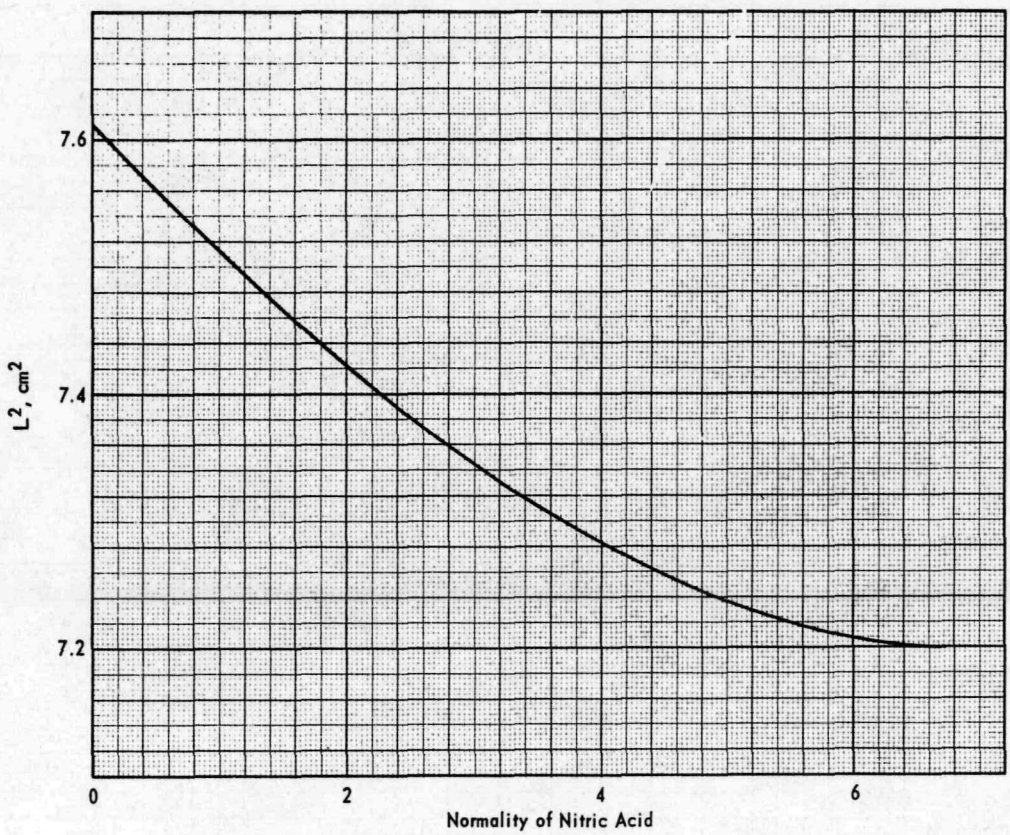

FIG. 4.1 L^2 FOR AQUEOUS SOLUTIONS OF NITRIC ACID

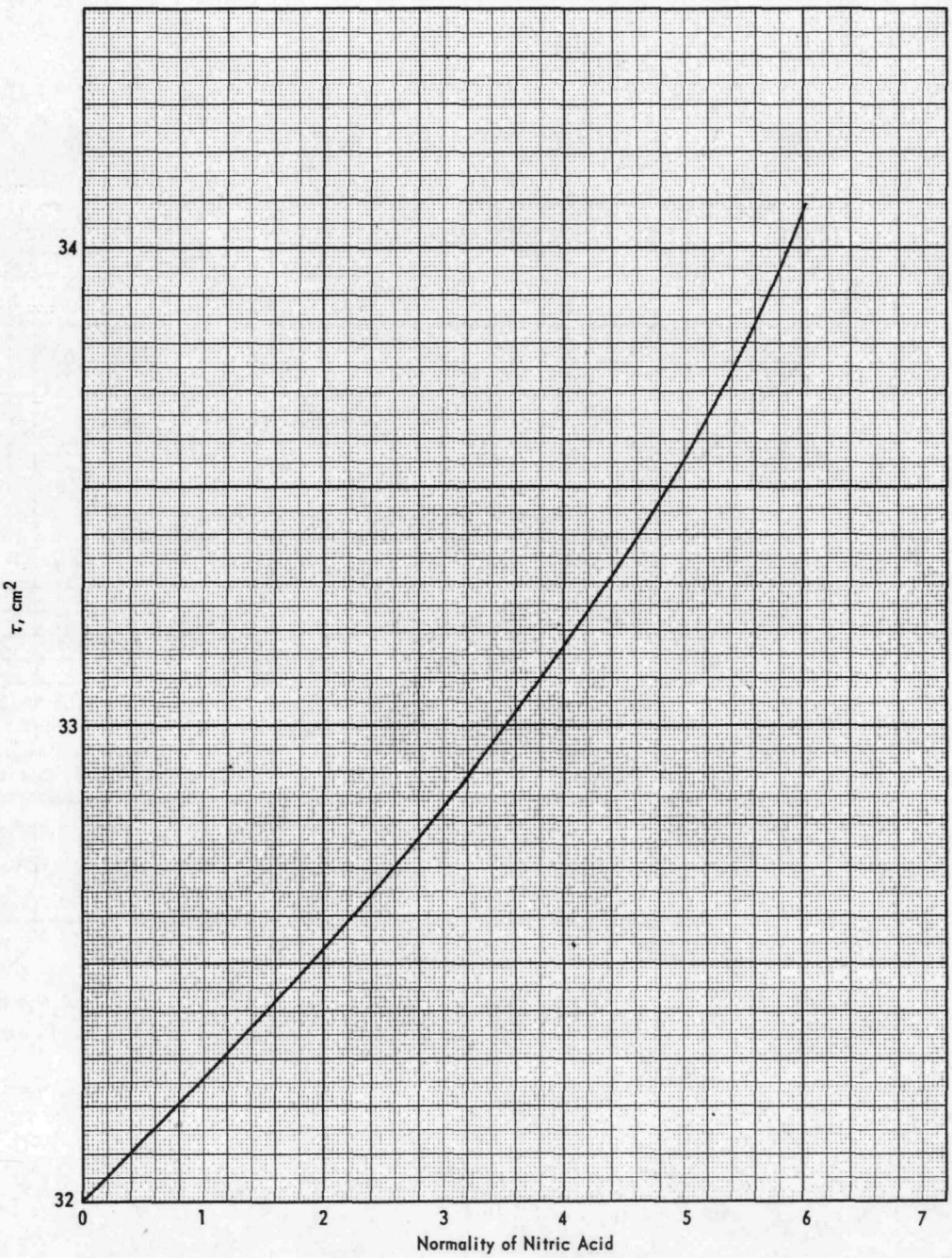

FIG. 4.2 τ FOR AQUEOUS SOLUTIONS OF NITRIC ACID

procedure just outlined, the reflector savings reported in Table IV.2 are obtained. These reflector savings are plotted against solution concentration in Figure 4.3 with the not unreasonable assumption being made that the bare and water-reflected curves are parallel. Use of values obtained from Figure 4.3 by interpolation leads to Figures 4.4 and 4.5 in which critical masses and radii of bare and water-reflected spheres are plotted against concentration. Also presented in these figures are safe masses and radii corresponding to k_{eff}'s of 0.98 and 0.95, determined from Equation 1.15. Since at a given buckling an increment in radius is the negative of an increment in reflector saving, Figure 4.5 also illustrates the margins in S that correspond to margins of 0.02 and 0.05 in k_{eff}. The data appear to be good enough that in the region of the minimum mass a k_{eff} of 0.98 allows an adequate margin of safety.

TABLE IV.2

Critical Mass Data Obtained with Spheres of UO_2F_2 Solution

(The data are expressed in terms of reflector savings. The uranium contains approximately 93.5% U^{235}.)

Conc., g U^{235}/liter	H/U^{235}	Reflector Saving(S), cm	
		Bare	Infinite H_2O Reflector
18.7	1393	4.15	
20.4	1270		7.37
23.4	1112	3.81	
49.4	524		6.65
95.1	268.8		6.57
125.2	203.5	3.16	
200	126.5		6.56
325	76.1		6.36
483	49.9		6.12
649	35.8		5.99

The data and the curves are, of course, for homogeneous solutions. A concentration gradient in the solution affects the results. Goertzel[4.8] has shown theoretically that in a reflected sphere in which the concentration decreases from the center toward the outer boundary in such a manner as to give a flat thermal flux in the solution, the critical mass is 30% lower than with a zero gradient. Morfitt[4.8] has confirmed this effect experimentally in cylinders containing a number of coaxial annular regions with successively lower concentrations, but he found the magnitude of the effect to be somewhat less than the calculated value. Conversely, a concentration gradient in the opposite direction would be expected to lead to a higher critical mass.

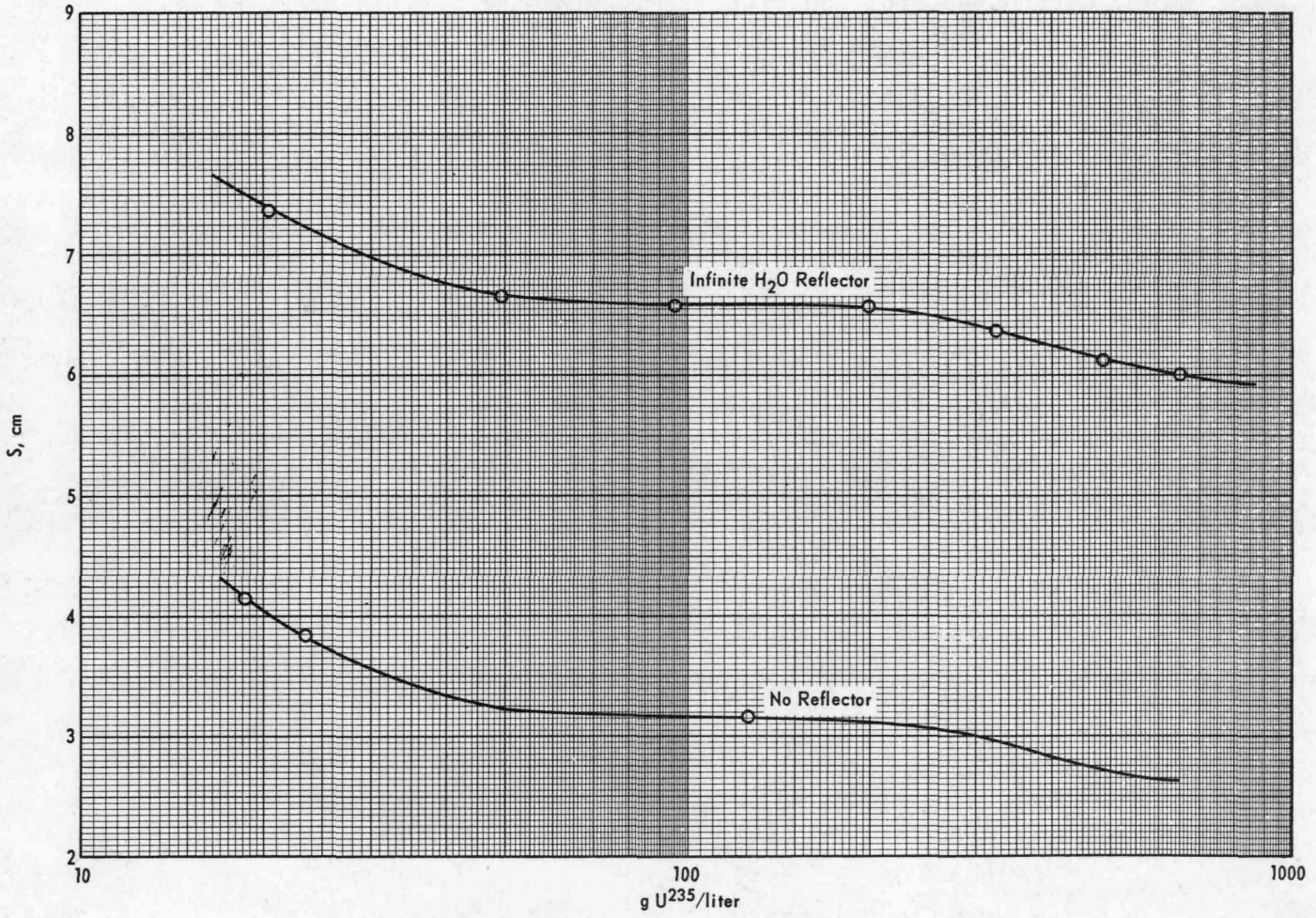

FIG. 4.3 S FOR SPHERES OF UO_2F_2 SOLUTION
(The reflector savings were obtained by equating the geometric bucklings to calculated material bucklings as a function of U^{235} concentration in the solution.)

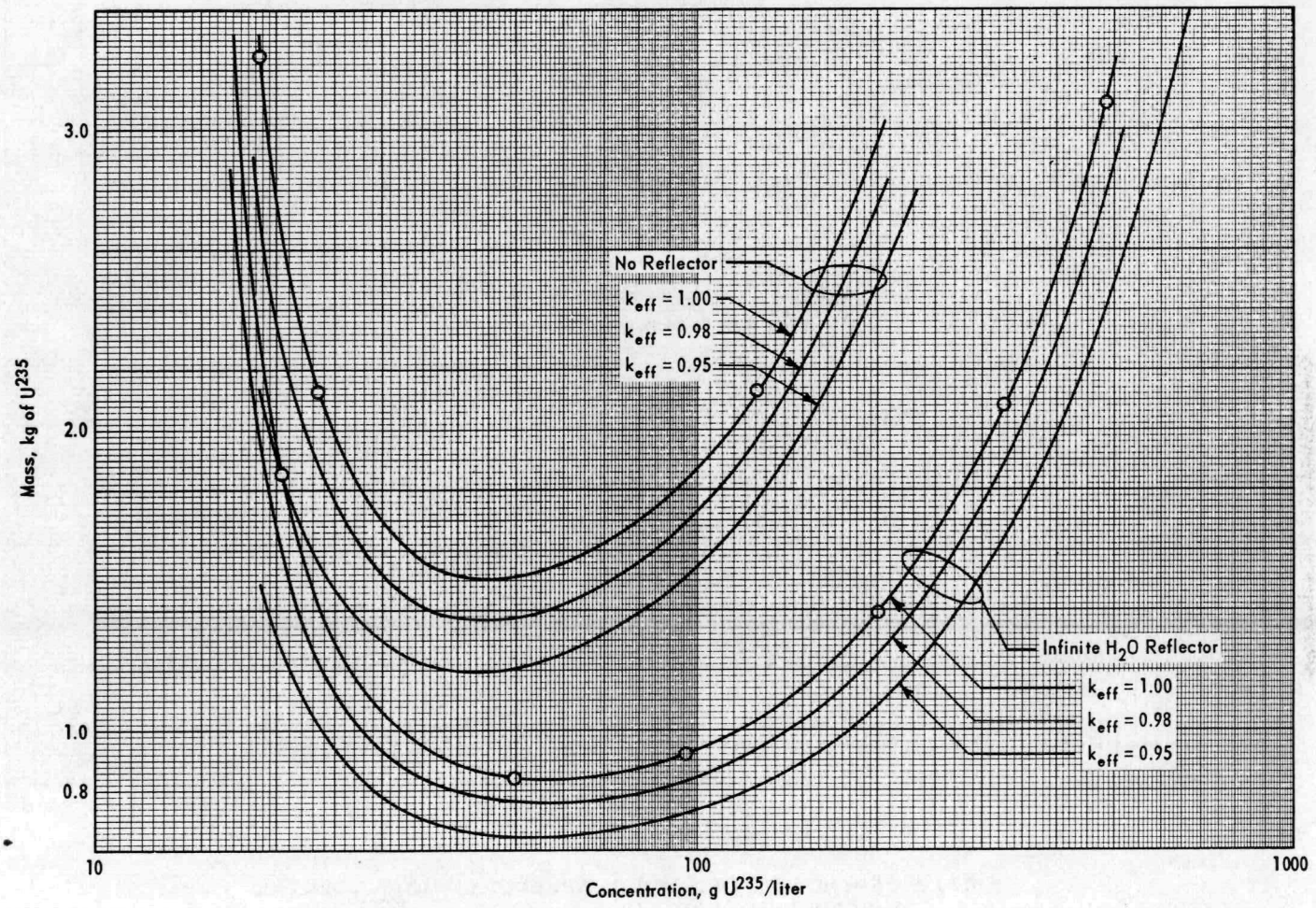

FIG. 4.4 DEPENDENCE OF MASSES OF U^{235} IN SPHERES OF UO_2F_2 SOLUTION ON CONCENTRATION AND k_{eff}

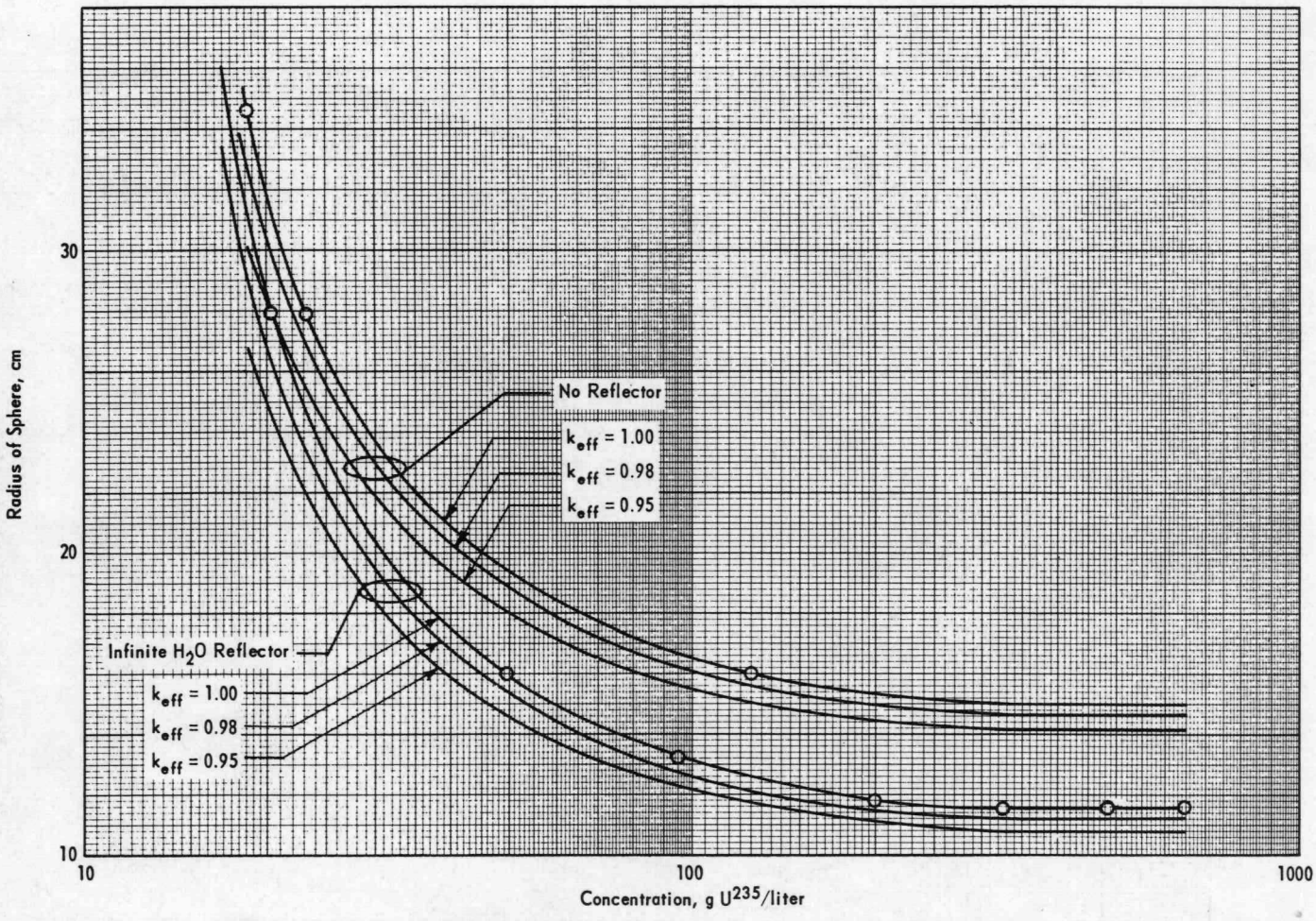

FIG. 4.5 DEPENDENCE OF RADII OF SPHERES OF UO_2F_2 SOLUTION ON CONCENTRATION AND k_{eff}

4.2.2.2 Cylinders

A large number of experiments[4.1-4.5,4.15] have been performed at the Oak Ridge National Laboratory in which the critical heights of bare and water-reflected cylinders of uranyl fluoride solution were measured as a function of cylinder diameter and of solution concentration. Both aluminum-walled and stainless-steel-walled vessels were employed, but almost all of the more recent data have been obtained with aluminum-walled vessels. For both materials the wall thickness was 1/16 inch. Fitting the data to calculated bucklings through the use of Equation 1.9 gives the reflector savings recorded in Tables IV.3 through IV.6. These values are generally smaller than values for spheres for the same concentration and reflector read from Figure 4.3. In determining critical and safe conditions for cylinders (and also for slabs), reflector savings from Figure 4.3 may therefore be used for situations for which fairly direct experimental data on cylinders and slabs may be lacking.

TABLE IV.3

Critical Mass Data Obtained with Bare, Aluminum-Walled Cylinders of UO_2F_2 Solution

(The data are expressed in terms of reflector savings.)

Conc., g U^{235}/liter	H/U^{233}	Reflector Saving(S) in cm for Cylinder Diameter in Inches of:						
		8.76	9.5	10	12	15	20	30
34.3	755					3.05		
52.2	499					3.45		
77.9	331			3.05	3.12	3.03		2.90
78.7	329					3.38		
78.5	328			3.06				
79.1	325						2.86	
151	169			2.97		3.09		
291	85.7			2.68				
300	83.1			2.70				
331	74.6					3.00		
337	73.4			2.67			2.63	
342	72.4							2.52
350	71.5	2.61		2.63				
373	66.1	2.58		2.58				
402	60.8	2.53		2.53	2.47		2.51	
437	55.4	2.49		2.47	2.43			
459	52.9			2.48				
470	51.5	2.48	2.46	2.51	2.42			2.71
480	50.1	2.43		2.39	2.41	2.40	2.39	2.45
532	44.7	2.41	2.36	2.35				
538	44.3	2.38	2.36	2.32	2.22	2.36	2.54	2.47
537	43.2			2.32				
829	27.1			1.91		2.01	2.07	

TABLE IV.4

Critical Mass Data Obtained with Water-Reflected, Aluminum-Walled Cylinders of UO_2F_2 Solution

(The data are expressed in terms of reflector savings.)

Conc., g U^{235}/liter	H/U^{235}	Reflector Saving(S) in cm for Cylinder Diameter in Inches of: 6	6.5	8	10	15	30
26.0	999					7.15	
34.3	755					6.49	
52.2	499				6.56	6.54	
78.7	329				6.45		
88.1	290			6.38			
116	221					6.24	
134	192			6.29			
199	127				6.39		
212	119		6.34				
254	99.5			6.11			
315	78.7		6.25	6.37			
342	72.4						6.6 ±0.5
415	58.8	6.26		6.02			
424	56.7		6.14			6.24	
459	52.9	6.22	6.14	6.12	6.05	6.47	
470	51.5				6.64(a)		
488	49.5			6.21	6.26		
538	44.3		6.09				6.8 ±0.5
537	43.2	6.15		6.18	6.24		
759	29.9			5.74			
829	27.1	5.93			6.14	6.39	6.6 ±0.5
827	26.2		5.78	5.60		~5.99(b)	

(a) This value is considered to be in error by the experimenters.[4.15]

(b) ~ is placed in front of values derived from estimates of critical conditions based on subcritical measurements.

TABLE IV.5

Critical Mass Data Obtained with Bare, Stainless-Steel-Walled Cylinders of UO_2F_2 Solution

(The data are expressed in terms of reflector savings.)

Conc., g U^{235}/liter	H/U^{235}	Reflector Saving (S) in cm for Cylinder Diameter in Inches of:				
		9	10	12	15	20
26.0	999					~4.55[a]
34.3	755				3.89	3.91
52.2	499			3.40	3.55	3.57
78.7	329					3.45
80.5	320			3.37		
114	226		3.21	3.18		
116	221				3.17	3.39
148	174		3.17	3.01		
205	123.2		3.05			
288	86.4		2.95			
331	74.6	2.81				
396	62.7		2.77			
394	62.6			~2.73[a]		
424	56.7				2.75	
538	43.9		2.55			

(a) ~ is placed in front of values derived from estimates of critical conditions based on subcritical measurements.

TABLE IV.6

Critical Mass Data Obtained with Water-Reflected, Stainless-Steel-Walled Cylinders of UO_2F_2 Solution

(The data are expressed in terms of reflector savings.)

Conc., g U^{235}/liter	H/U^{235}	Reflector Saving (S) in cm for Cylinder Diameter in Inches of: 6	6.5	7	8	9	10	12	15
26.0	999								~6.34(a)
34.3	755							6.36	6.10
52.2	499						~6.14(a)	5.86	5.53
80.5	320				6.05	6.00	5.94	5.82	
114	226				6.00	5.92	5.94	5.54	
116	221								5.56
134	192				6.18				
141	183			~6.07(a)					
148	174			6.09	5.96	5.89	5.88	5.59	
205	123.2		~6.07(a)	6.02	5.89	5.82	5.74		
254	99.5				5.88				
288	86.4		6.06	5.96	5.82	5.72	5.78		
396	62.7		5.98		5.73	5.66	5.64		
394	62.6							5.58	
394	61.1			5.93					
415	58.8				5.98				
424	56.7				5.76				5.56
538	44.3	5.97							
538	43.9		5.85	5.78	5.69	5.54	5.56		
724	31.6		5.72	5.61	5.50	5.38	5.36		
827	26.2					5.34			
869	24.4			5.48	5.34	5.26	5.30		

(a) ~ is placed in front of values derived from estimates of critical conditions based on subcritical measurements.

For bare cylinders, stainless steel walls are seen to give slightly greater reflector savings than aluminum walls, whereas for water-reflected cylinders the opposite is true. The reasons for this behavior are that (1) stainless steel has a higher scattering cross section than aluminum and hence reduces the leakage of fast neutrons, and (2) stainless steel also has a higher thermal absorption cross section and hence captures more of the thermal neutrons headed back to the solution from the reflector.

From close examination of these reflector savings one can gain some feeling for the uncertainty in the experimental data. Plotting the reflector savings against concentration or against cylinder diameter permits interpolations and extrapolations to be made and reveals data that should perhaps be regarded with suspicion. Estimates of reflector savings obtained from examining the values in Table IV.3 and IV.4 have been used to calculate the critical and safe (k_{eff} = 0.98 or 0.95) diameters of infinite aluminum-walled cylinders of UO_2F_2 solution, both bare and water-reflected, as functions of solution concentration. The results are plotted in Figure 4.6. As in the case of spheres, an increment in the critical or safe radius is the negative of the corresponding increment in reflector saving; hence the margin in S corresponding to a margin of 0.02 or of 0.05 in k_{eff} is readily apparent from Figure 4.6. From a comparison of these margins with the scatter in the values in Table IV.3 and IV.4 a margin of safety of 0.02 in k_{eff} appears adequate at concentrations where data are fairly extensive.

The curves of Figure 4.6 exhibit minima at concentrations in the neighborhood of 500 g of U^{235} per liter. Similar minima no doubt occur for spheres, but the data are not sufficiently extensive to show them. The minima may appear surprising since the critical diameters of bare and water-reflected cylinders of uranium (93.5% U^{235}) metal are only about 4.6 and 3.1 inches, respectively (see Figures 2.4 and 2.5), or much smaller than the minima shown in Figure 4.6; but it should be remembered that pure UO_2F_2 rather than pure metal is being approached as the concentration increases and that the dilution of uranium by oxygen and fluorine increases the critical size markedly.

In Figure 4.7 (H + 2S) and (D + 2S) are plotted against each other on reciprocal scales for a number of solution concentrations where H and D are the height and diameter of a cylinder. The concentrations are so chosen that the buckling at a particular concentration is equal to the geometric buckling corresponding to k_{eff} = 0.95 for the next lower concentration. The curves thus permit both critical and safe (k_{eff} = 0.95) cylinder sizes to be determined as functions of solution concentration when the appropriate values of S are employed. These values of S are determined from Tables IV.3 through IV.6, from data on the effect of reflector thickness and material, or from estimates of interaction. It should be noted that unless the values of S are the same, cylinder dimensions that are critical at one concentration do not correspond exactly to a k_{eff} of 0.95 at the next lower concentration.

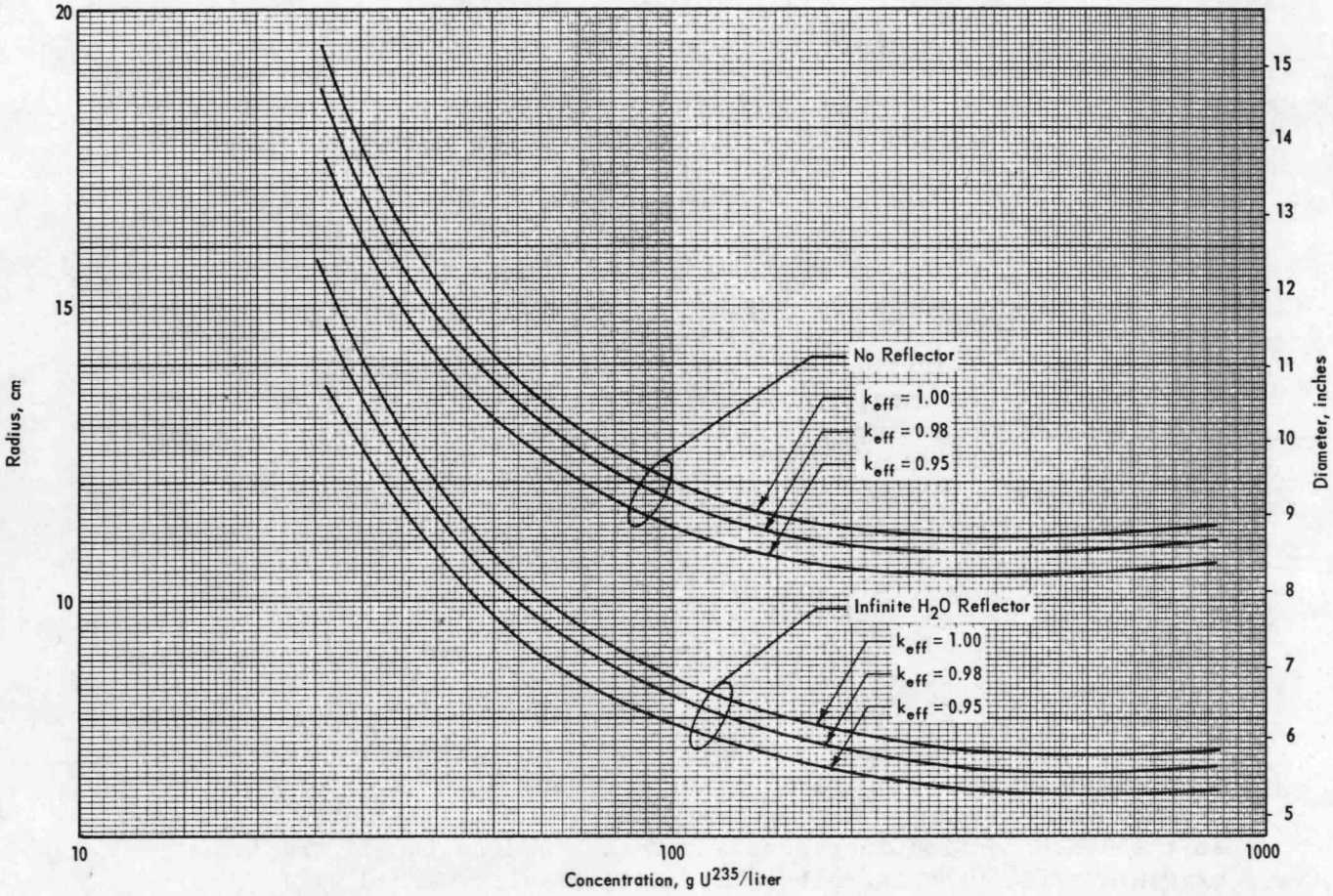

FIG. 4.6 DEPENDENCE OF DIAMETERS OF INFINITE CYLINDERS OF UO_2F_2 SOLUTION ON CONCENTRATION AND k_{eff}

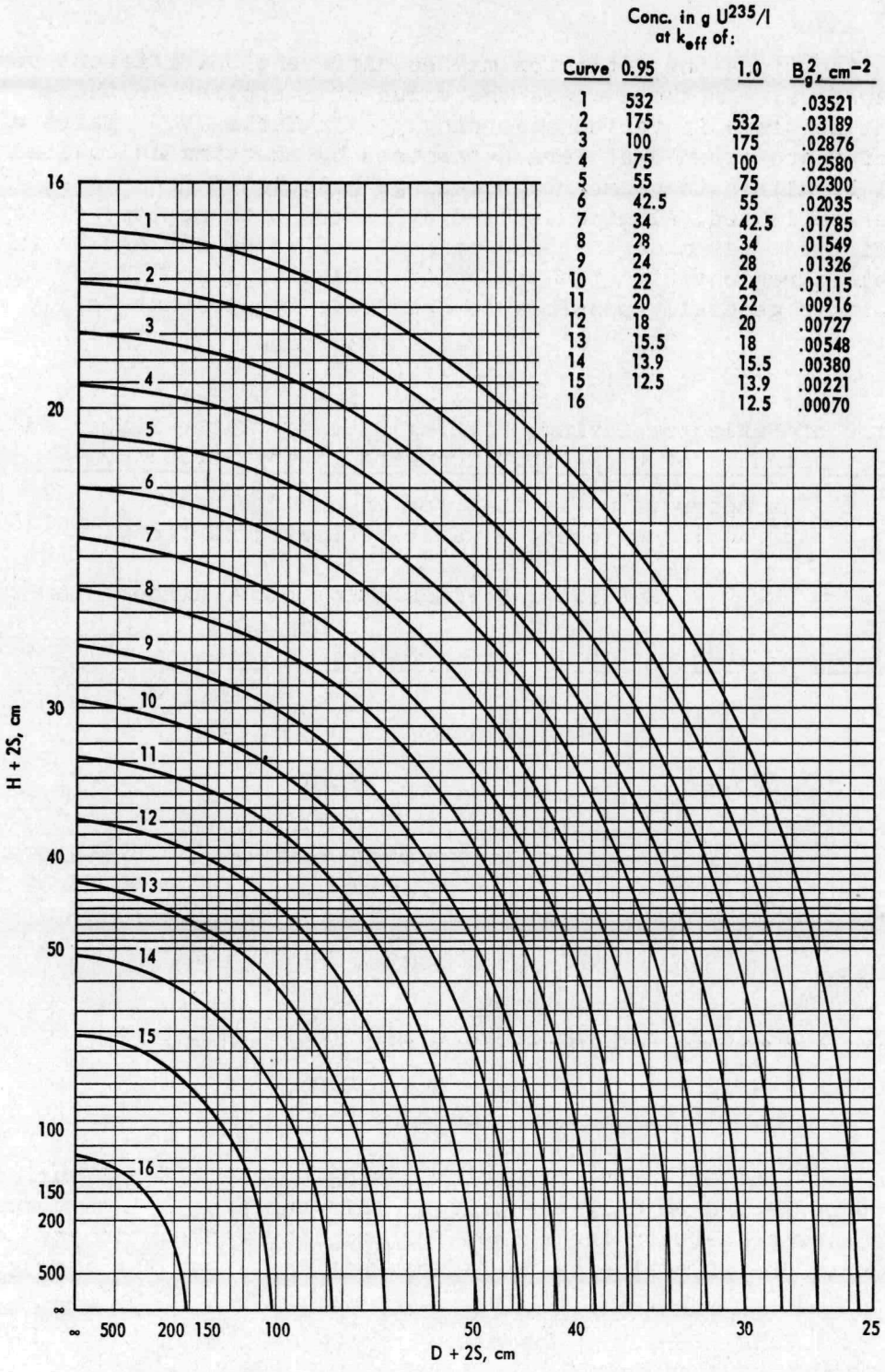

FIG. 4.7 DEPENDENCE OF SAFE (k_{eff} = 0.95) AND CRITICAL (k_{eff} = 1.0) DIMENSIONS OF CYLINDERS OF UO_2F_2 SOLUTION ON S AND CONCENTRATION

In some situations the reflector may be different on different portions of the surface. In these cases the value of S applied to these different portions is varied accordingly. In Table IV.7 pairs of values of S are given that were determined by equating calculated material bucklings to geometric bucklings calculated from data[4.2,4.3] for water-reflected, aluminum-walled cylinders with no top reflector. The requirement was made that the pair of reflector savings be in reasonable agreement with the values of Tables IV.3 and IV.4. As can be seen it is generally possible to meet this requirement fairly well.

TABLE IV.7

Pairs of Reflector Savings Fitting Data for Water-Reflected Cylinders of UO_2F_2 Solution with No Top Reflector

(The upper value is that for an unreflected surface; the lower, a water-reflected surface.)

Conc., g U^{235}/liter	H/U^{235}	Reflector Savings in cm for Cylinder Diameter in Inches of: 6	7.5	8	10	15	20	30
331	74.6					2.86		
						6.36		
337	73.4				2.67			
					6.28			
342	72.4			2.67	2.67		2.67	2.92
				6.25	6.31		6.48	6.62
470	51.5			2.32				
				6.01				
538	44.3	2.38	2.38	2.29				
		6.15	6.17	5.99				
537	43.2				2.08			
					5.98			

In Table IV.8 the effective reflector saving on the lateral surface of cylinders reflected on only one-half of this surface[4.3] is compared with the average between the values for complete reflection and no reflection. The effective value is somewhat less than the average value.

TABLE IV.8

Average Lateral Reflector Savings for Partially Reflected Cylinder

Conc., g U^{235}/liter	H/U^{235}	Cylinder Diameter, inches	Reflector	$\bar{S}$, cm	S_r, cm	S_o, cm	$\frac{S_r + S_o}{2}$
78.5	328	10	4-inch thickness of H_2O on bottom and on one-half (180°) of lateral surface	4.60	6.45	3.06	4.76
470	51.5	8	6-inch thickness of H_2O on entire lateral surface	6.48	-	2.48	-
470	51.5	8	6-inch thickness of H_2O on one-half (180°) of lateral surface	4.25	6.48	2.48	4.48

$\bar{S}$ is the average reflector saving, S_r is the value for infinite H_2O, and S_o is the bare extrapolation distance.

4.2.2.3 Rectangular Parallelepipeds

A few experiments[4.3] have been performed with rectangular parallelepipeds. In one set of experiments the heights of reflected slabs of solution were measured as functions of their thicknesses. The containing walls were constructed of "Lucite", and the thickness of slab was varied by inserting thin sheets of "Lucite" adjacent to one wall. Since "Lucite" appears to be a somewhat better reflector than water (see Table IV.12), the critical thicknesses of water-reflected slabs of the same height would have been somewhat greater. The slabs were surrounded by water on all surfaces except the top. The reflector saving for this surface was estimated from Table IV.3, but the reflector savings for the water-reflected surfaces that fit the data are fairly insensitive to the particular value of reflector saving used for the top surface.

These and other data obtained with rectangular parallelepipeds are presented in Table IV.9. The reflector savings of Table IV.9, or of Figure 4.3 at concentrations where data are lacking, may be used in conjunction with Figure 4.7 to determine the critical and safe thicknesses of infinite slabs.

By multiplication of the critical and safe thicknesses of infinite water-reflected slabs by the solution concentration, minimum critical and maximum safe masses of U^{235} per unit area can be determined. Such masses are useful in cases where precipitation or evaporation is possible. For U^{235} the minimum critical mass per unit area is 335 g/ft^2. The maximum safe mass at $k_{eff} = 0.95$ is 280 g/ft^2. The concentration at which the minimum mass occurs is 25 g U^{235}/liter.

TABLE IV.9

Critical Mass Data Obtained with Rectangular Parallelepipeds of UO_2F_2 Solution

(The data are expressed in terms of reflector savings.)

Conc., g U^{235}/liter	H/U^{235}	Length[a], inches	Width[a], inches	Reflector Saving (S), cm	
				No Reflector	H_2O Reflector
77.9	331	20	20	2.93	
		6	48	2.87	
87.8	293			2.92	6.23
342	72.4	20	20	2.83	6.6 ±0.5
469	51.5	2.06	58		6.40
		1.995	58		6.42
532	44.7	2.12	58		6.38
		2.06	58		6.38
		2.00	58		6.41
		1.995	58		6.40
538	44.3	20	20		7.35 ±0.5
829	27.1	20	20	2.2 ±0.5	6.3 ±0.5

(a) The height is the dimension varied to make the parallelepiped critical and hence is different for each case.

4.2.3 URANYL NITRATE SOLUTIONS

4.2.3.1 Spheres

Experiments have been performed[4.4] with bare spheres of $UO_2(NO_3)_2$ solution having diameters of 27.5 and 48 inches. The H/U^{235} ratios were respectively 1379 and 1849, and the concentrations were 18.75 and 14.11 g U^{235}/liter. The N/U^{235} ratio was 3.64 in the former case and presumably about the same in the latter. Expressing the data as reflector savings gives values of 4.32 and 5.05, respectively. The increase in S with H/U^{235} is probably partly the result of increased sensitivity to errors in buckling as the buckling decreases. These reflector savings are slightly larger than those obtained with spheres of UO_2F_2 solutions, but the bucklings of these nitrate solutions are enough lower than those of the fluoride solutions to make the critical masses slightly larger.

4.2.3.2 Cylinders

In Tables IV.10 and IV.11, reflector savings for $UO_2(NO_3)_2$ solutions are presented that were obtained by fitting data[4.5] to calculated bucklings. Except at high concentrations (low H/U^{235} ratios) the values are of the same order of magnitude as those for UO_2F_2 solutions. At high concentrations the nitrate values are lower, presumably because $UO_2(NO_3)_2$ displaces more solvent than UO_2F_2, and hence taking τ as small as it is in pure moderator is a poorer approximation.

TABLE IV.10

Critical Mass Data Obtained with Bare, Aluminum-Walled Cylinders of $UO_2(NO_3)_2$ Solution

(The data are expressed in terms of reflector savings.)

Conc., g U^{235}/liter	H/U^{235}	N/U^{235}	Reflector Saving (S) in cm for Cylinder Diameter in Inches of: 10	12	15
36	733	2.86			3.49
53	493	2.86		3.49	3.36
73	352	2.86		3.03	3.07
105	240	2.86	2.87	2.95	3.02
73	327	7.48		2.82	2.86
102	230	7.48		2.70	2.71
237	88	7.48		1.36	1.75

TABLE IV.11

Critical Mass Data Obtained with Water-Reflected Aluminum-Walled Cylinders of $UO_2(NO_3)_2$ Solution

(The data are expressed in terms of reflector savings.)

Conc., g U^{235}/liter	H/U^{235}	N/U^{235}	Reflector Saving (S) in cm for Cylinder Diameter in Inches of: 8	9	10	12	15
36	733	2.86				6.70	6.52
53	493	2.86			6.53	6.31	6.32
73	352	2.86		6.33	6.25	6.08	6.24
105	240	2.86	6.27	6.22	6.22	6.25	6.17
359	61.8	2.86	5.63	5.54	5.48		6.06
73	327	7.48			6.09	6.01	6.08
102	230	7.48			6.04	6.01	6.02
237	88	7.48		5.16	5.00	5.15	5.32

4.2.4 REFLECTOR MATERIAL AND THICKNESS

Experiments were performed with $UO_2(NO_3)_2$ solutions[4.5] in which the reflector thickness and material were varied on the lateral surfaces of 8- and 10-inch-diameter cylinders. The reflectors employed were water, stainless steel, and stainless steel surrounded by water. In the first two cases the top and bottom were bare and in the third case, water reflected. Reflector savings consistent with the values in Table IV.10 and IV.11 were assigned to these surfaces, and the reflector savings on the lateral surface were determined. In some cases small adjustments in the values of reflector saving used for the top and bottom were necessary to obtain a reflector saving for 3.5 or 4.5 inches of water on the lateral surface consistent with the fact that these thicknesses are nearly effectively infinite.

It is convenient to express these results in terms of the albedo of the particular thickness and material relative to that of an infinite water reflector where the albedo is the ratio of the neutron current returned by the reflector to that entering it. If the assumption is made that the reflector saving as a function of thickness is independent of vessel shape, the shape may be taken to be an infinite slab. In terms of the reflector savings and material buckling the albedo of the reflector is then given by

$$\beta_r = \frac{\sin B_m (S-S_o)}{\sin B_m (S+S_o)} \qquad (4.4)$$

where S_o is the bare extrapolation distance. In Figures 4.8 and 4.9, β_r/β_{H_2O} is plotted against reflector thickness for water and stainless steel reflectors where β_{H_2O} is the albedo of an infinitely thick water reflector. In Figure 4.10, β_r/β_{H_2O} is plotted against the thickness of stainless steel separating the uranium solution from an infinitely thick water reflector*. The curves are nearly independent of solution concentration and may be used not only for uranium solutions of other concentrations but also for plutonium and U^{233} solutions. In using

---

* If the data of Tables IV.3, IV.4, and IV.6 are used to obtain points on Figure 4.10 corresponding to a stainless steel thickness of 1/16 inch, a wide scatter in the data is observed. In particular, for a 15-inch-diameter cylinder at an H/U^{235} ratio of 499, $\beta_r/\beta_{H_2O} = 0.75$, and for an 8-inch cylinder at an H/U^{235} ratio of 58.8, $\beta_r/\beta_{H_2O} = 0.99$. Although the steel wall might be expected to be slightly more effective at high H/U^{235} values, a variation of this magnitude is too great, and leads one to suspect that there are inaccuracies in these data.

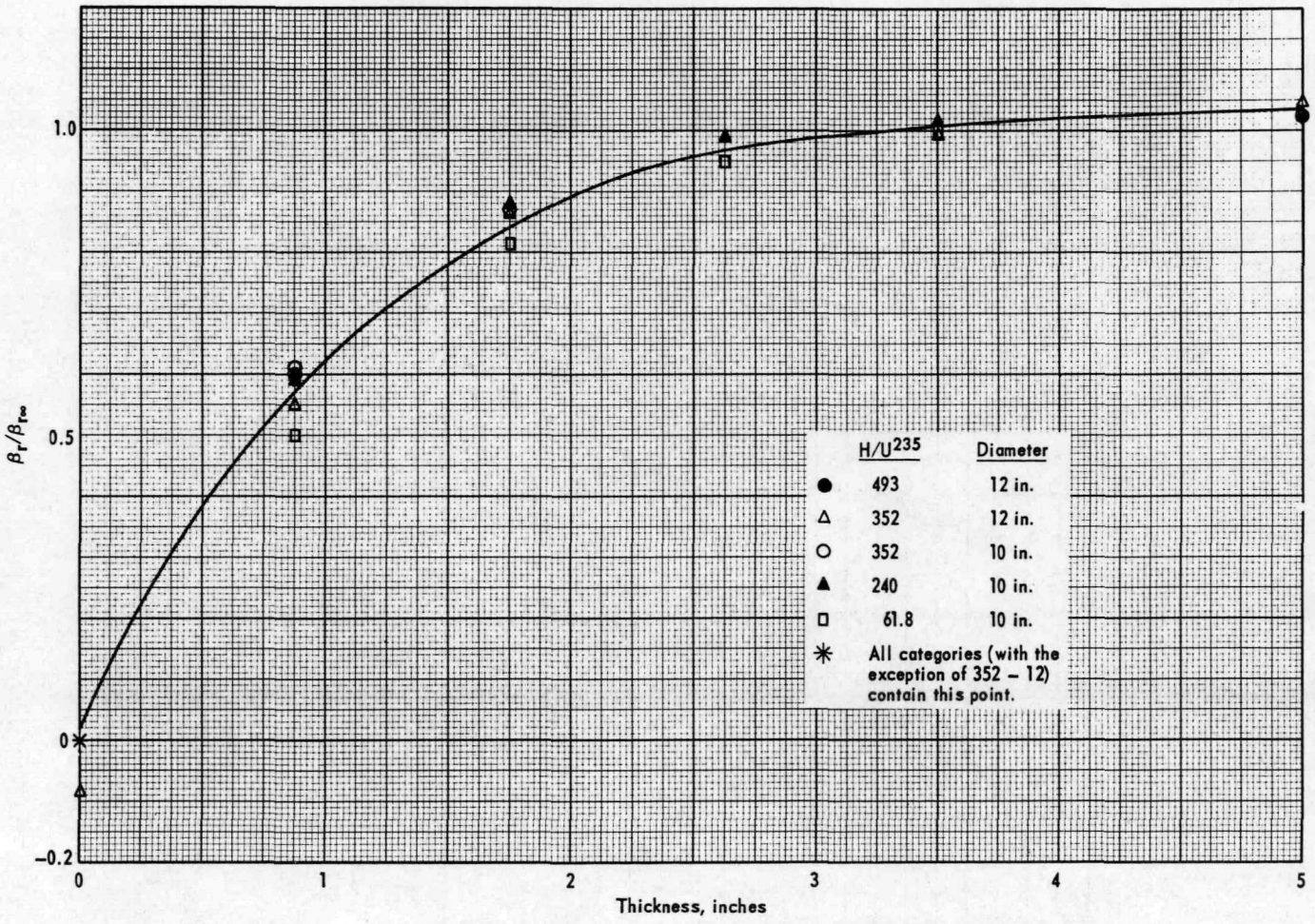

FIG. 4.8 ALBEDO OF VARIOUS THICKNESSES OF H_2O RELATIVE TO THAT OF AN INFINITELY THICK WATER REFLECTOR

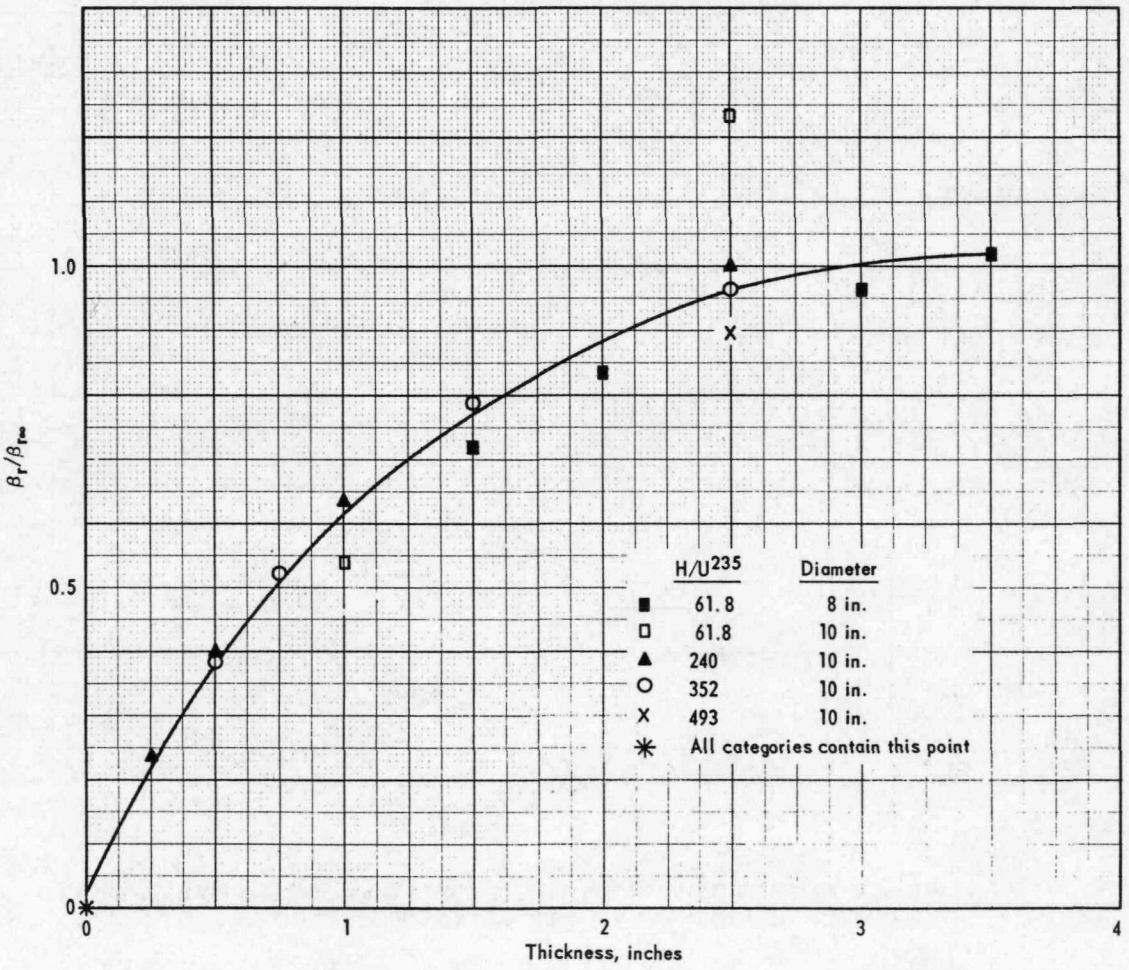

FIG. 4.9 ALBEDO OF VARIOUS THICKNESSES OF STAINLESS STEEL RELATIVE TO THAT OF AN INFINITE WATER REFLECTOR

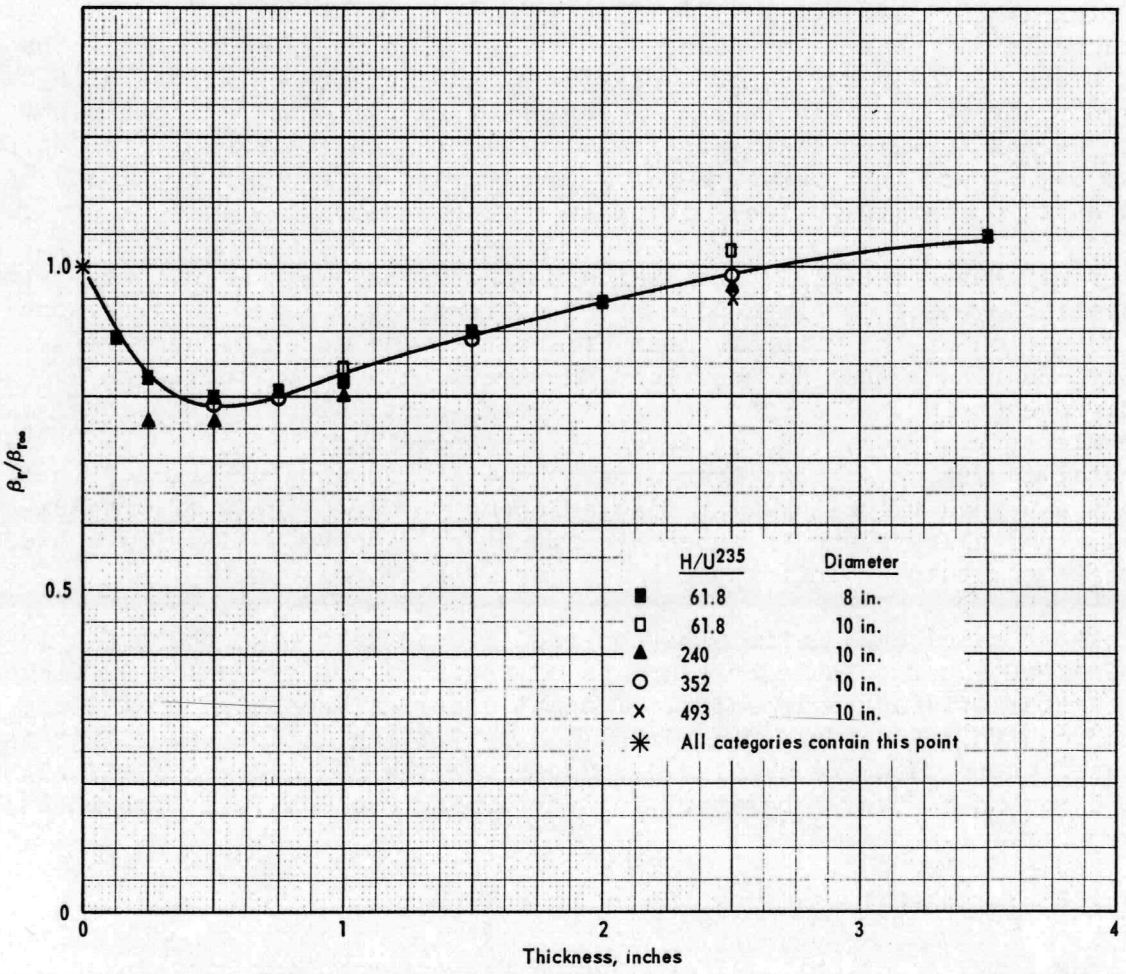

FIG. 4.10 ALBEDO OF VARIOUS THICKNESSES OF STAINLESS STEEL BACKED UP BY AN EFFECTIVELY INFINITE THICKNESS OF WATER RELATIVE TO THAT OF AN INFINITE WATER REFLECTOR

the curves to obtain the reflector saving for a particular case, it is convenient to express Equation 4.4 as

$$S = \frac{1}{B_m} \tan^{-1} \left[\frac{1+\beta_r}{1-\beta_r} \tan B_m S_o \right]. \qquad (4.5)$$

Other reflector materials have been studied. In one experiment[4.3] a pair of slabs of UO_2F_2 solution interacting in water was reflected on the outer surfaces by water and by a 1-inch-thick layer of "Plexiglas" surrounded by water. The water thicknesses were effectively infinite. "Plexiglas"[4.8], steel[4.8], carbon[4.2], fire brick[4.2], and magnesia[4.8] have also been investigated with UO_2F_2 solutions. The albedos of these reflectors relative to an infinite thickness of H_2O are recorded in Table IV.12. A series of experiments[4.1] has been performed in which stainless steel cylinders containing UO_2F_2 solutions were enclosed in 0.020-inch-thick cadmium and surrounded by water. Results are given in Table IV.13 as reflector savings.

For reflector materials, for which data obtained with solutions are not available, data obtained with metal systems may be used to give some indication of the effectiveness of a particular material as a reflector. Some caution should be exercised, however, because of the large difference in the neutron energy spectra, particularly in nonmoderating reflectors. Thus, lead as a reflector enclosing uranium (93.5% U^{235}) metal is less effective than water up to a thickness of about 7 inches, but a 4-inch-thick layer of lead adjacent to an assembly of uranium-aluminum alloy slugs in water was found[4.11] to be a slightly better reflector than an infinitely thick layer of water.

In some cases calculations may be required to determine the effectiveness of a reflector. Two energy groups of neutrons are generally sufficient to give satisfactory results. The calculations should be normalized to agree with reflector savings obtained by fitting data to bucklings in cases where data are available. Codes for the IBM 650 are available at the Savannah River Laboratory for performing such calculations in slab geometry.

4.2.5 INTERSECTIONS OF CYLINDERS

Investigations of critical conditions for intersecting pipes have been made[4.2] with UO_2F_2 solutions with concentrations (337-538 g U^{235}/l) corresponding to minimum volume. The pipes had 1/16-inch-thick-aluminum walls and had diameters of 4, 5, and 7.5 inches. The two types of intersection investigated were a 60° Y and a 90° cross. The four arms of the cross and the three arms of the Y were each at least 24 inches long, measured from the center of the intersection. The 5-inch cross and 5-inch Y, when reflected by an effectively infinite amount of water, became critical before they were completely filled with solution. A greater height of solution (measured from the

TABLE IV.12

Effectiveness of Various Reflectors Compared with an Infinite Thickness of Water

Reflector Material	H/U^{235}	Vessel	β/β_{H_2O}
1 inch of "Plexiglas" backed by water	337	6 x 48-inch-slab	1.06
1 inch of "Plexiglas"	337	6 x 48-inch-slab	0.70
1/2 inch of stainless steel	337	6 x 48-inch-slab	0.35
2 inches of magnesia (0.32 g/cc)	337	6 x 48-inch-slab	0.17
4 inches of magnesia (0.24 g/cc)	337	6 x 48-inch-slab	0.18
4 inches of magnesia at 0.24 g/cc backed by 2 inches of magnesia 0.32 g/cc	337	6 x 48-inch-slab	0.24
2 inches of magnesia at 0.32 g/cc backed by 4 inches of magnesia 0.24 g/cc	337	6 x 48-inch-slab	0.27
3 inches of "Styrofoam"	293	6 x 48-inch-slab	0.057
6 inches of "Styrofoam"	293	6 x 48-inch-slab	0.081
3 inches of "Styrofoam" backed by water	293	6 x 48-inch-slab	0.55
6 inches of "Styrofoam" backed by water	293	6 x 48-inch-slab	0.41
0.5 inch of fire brick	27.1	20-inch-dia. cyl. reflected on bottom	0.089
2.0 inches of fire brick	27.1	20-inch-dia. cyl. reflected on bottom	0.17
5.5 inches of fire brick	27.1	20-inch-dia. cyl. reflected on bottom	0.32
0.5 inch of carbon	27.1	20-inch-dia. cyl. reflected on bottom	0.25
1 inch of carbon	27.1	20-inch-dia. cyl. reflected on bottom	0.42
2 inches of carbon	27.1	20-inch-dia. cyl. reflected on bottom	0.69
3.5 inches of carbon	27.1	20-inch-dia. cyl. reflected on bottom	0.82
5.5 inches of carbon	27.1	20-inch-dia. cyl. reflected on bottom	0.95
1 inch of wet fire brick backed by water	27.1	20-inch-dia. cyl. reflected on bottom	0.95
2 inches of wet fire brick backed by water	27.1	20-inch-dia. cyl. reflected on bottom	0.93
2 inches of wet fire brick	27.1	20-inch-dia. cyl. reflected on bottom	0.69
3 inches of carbon backed by water	27.1	20-inch-dia. cyl. reflected on bottom	1.17
5.5 inches of carbon backed by water	27.1	20-inch-dia. cyl. reflected on bottom	1.26
5.5 inches of carbon backed by water with 0.25 inch of water between vessel and carbon	27.1	20-inch-dia. cyl. reflected on bottom	1.28
Same as above but, with 0.5 inch of water	27.1	20-inch-dia. cyl. reflected on bottom	1.30
Same, but with 0.75 inch of water	27.1	20-inch-dia. cyl. reflected on bottom	1.26
Same, but with 1.0 inch of water	27.1	20-inch-dia. cyl. reflected on bottom	1.24

TABLE IV.13

Critical Mass Data Obtained with Water-Enclosed, Cadmium-Wrapped, Stainless-Steel-Walled Cylinders of UO_2F_2 Solution

(The data are expressed in terms of reflector savings.)

Conc., g U^{235}/liter	H/U^{235}	Reflector Saving (S) in cm for Cylinder Diameter in Inches of: 8	9	10	12
52	499				4.84
114	226				4.34
116	221			4.49	
148	174		4.37		4.24
205	123.2		4.30		
288	86.4	4.17	4.24	4.31	
396	62.7	4.16	4.13	4.11	
424	56.7				4.36
538	43.9	3.93	3.92	4.06	
724	31.6		3.79	4.02	
827	26.2				~4.22
869	24.4			~3.53	

intersection of center lines) was required in the final arm being filled in the Y than in the cross. It was not possible to make the reflected 4-inch cross, or the unreflected 5-inch Y or 7.5-inch cross critical, and extrapolation of the reciprocal source-neutron multiplication curve indicated that filling the final arm to infinite height would still not make the system critical.

The minimum critical diameters of reflected and unreflected infinitely long cylinders are respectively 5.75 and 8.70 inches (see Figure 4.6). In the reflected case, the cross and Y intersections are thus equivalent to an increment of between 0.75 inches (5.75 - 5.0) and 1.75 inches (5.75 - 4.0) in diameter, or to an increase in reflector saving of more than 0.95 cm but less than 2.22 cm. In the unreflected case, the cross intersection is equivalent to an increase in reflector saving of less than 1.5 cm. Since a 7.5-inch Y was not investigated, the same statement cannot be made concerning it. Although in the reflected case the cross is closer to being critical than the Y, the same statement cannot be made for the unreflected case because of the interaction between the two arms at 60° to ea h other.

4.2.6 MINIMUM CRITICAL CONCENTRATION

At sufficiently high dilution, absorption of neutrons by hydrogen makes criticality impossible for solutions (or mixtures) of U^{235} in hydrogenous materials. The critical and safe concentrations are readily obtained from Equations 4.1 and 4.2. In the absence of nitrogen the minimum critical (k = 1) H/U^{235} ratio is 2185, and the corresponding concentration in aqueous solution is 11.94 g U^{235}/l. The minimum safe (k = 0.95) ratio is 2408, and the maximum safe concentration in aqueous solution is 10.83 g U^{235}/l. Experiments[4.15] performed with dilute uranyl nitrate solutions indicate that the minimum critical concentration is actually slightly higher than 11.94 g/l, namely 12.2 g U^{235}/l. In Table IV.14 the data obtained in these experiments, performed in unreflected stainless-steel-walled cylinders, are presented as reflector savings obtained by equating material and geometric bucklings. The negative values obtained at low concentrations indicate that the calculated material bucklings are too large; they also point to the desirability of using the second approach, Section 1.4 for fitting data when the buckling is small.

TABLE IV.14

Critical Mass Data Obtained with Dilute Solutions of $UO_2(NO_3)_3$

(The N/U ratio is about 3.8. The data are expressed as reflector savings.)

Conc., g U^{235}/liter	H/U^{235}	S, cm
25.9	1000	4.39
16.13	1604	4.29
14.22	1821	3.16
13.59	1905	0.82
13.24	1951	0.62
13.07	1981	- 1.42
12.92	2000	- 4.95
12.61	2052	-25.96

4.3 AQUEOUS SOLUTIONS OF URANIUM CONTAINING LESS THAN 93.5% U^{235}

Data for solutions of uranium (93.5% U^{235}) may be used as points of departure for calculating bucklings and hence critical and safe conditions for solutions of uranium containing lower concentrations of U^{235}. For a particular solution concentration (in moles/liter) the neutron spectrum may be assumed independent of the concentration of U^{235} in the uranium. All non-1/v events in U^{235} may then be assumed to be included in an effective value of η (identical with the thermal value), as is assumed when k is taken to be ηf for uranium (93.5% U^{235}) solutions. The non-1/v events in U^{238} consist of high energy fissions and resonance absorptions that may be allowed for by the factors ϵ and p in the four-factor formula for k. Since for simplicity the product of these two factors is assumed to be unity in calculations made for a concentration of 93.5% U^{235} the product must be normalized to unity at this concentration in extrapolating the data to lower concentrations. (For the highest concentration of UO_2F_2 solution for which data exist, 3.77 molar, ϵp is calculated to be 0.98 at a uranium composition of 93.5% U^{235}, 6.5% U^{238}. The product approaches unity as the solution concentration decreases.)

Calculations of k and B_m^2 for aqueous solutions of UO_2F_2 in which the uranium contains less than 93.5% U^{235} have been made for this Handbook by the procedure outlined above. The same approximations regarding f, η, L^2, and τ were made as for the uranium (93.5% U^{235}) solutions. The fast fission factor ϵ was obtained from a three-group calculation involving Hansen's[2.7] cross sections for U^{235} and U^{238} and removal cross sections for oxygen and hydrogen calculated from the neutron spectrum obtained in calculating τ for this Handbook. The removal cross sections of fluorine were assumed to equal those of oxygen. The resonance escape probability, p, was calculated from the resonance integral of U^{238}, which in turn was calculated as a function of scattering cross section per U^{238} atom from resonance parameters and from data giving the resonance integral both in pure U^{238} and at infinite dilution. The buckling was calculated as before from the one-group expression.

A code, which is available at the Savannah River Laboratory, was developed for the IBM 650 to perform these calculations. Values of B_m^2 and k calculated for selected concentrations and assays are given in Tables IV.15 and IV.16. These parameters may be used in conjunction with the reflector savings determined for uranium (93.5% U^{235}) solutions of the same uranium concentration (Figure 4.3 or Tables IV.2 through IV.9) to give critical and safe conditions for solutions in which the uranium contains lower concentrations of U^{235}.

TABLE IV.15

Dependence of B^2 on Solution Concentration and on Isotopic Composition of Uranium

Solution Conc., moles UO_2F_2/liter	B^2 (cm^{-2} x 10^4) for Isotopic Composition in % U^{235} of:									
	H/U	93.5	75	50	30	15	5	3	2	1
3.77	25.3	324.9	304.6	283.2	261.3	226.4	133.12	70.59	15.68	-76.65
2.45	41.4	319.1	301.2	280.1	254.6	208.9	92.37	22.84	-33.10	
2.14	48.2	316.6	299.8	278.2	250.9	201.4	77.76	6.90	-48.47	
1.83	56.8	313.5	297.2	274.8	245.3	191.0	59.97	-11.57		
1.59	66.9	310.0	293.9	270.6	238.5	179.3	41.43	-30.02		
1.37	77.7	306.2	290.2	265.7	231.1	166.8	23.59	-47.07		
1.16	93.0	301.0	284.9	258.7	220.4	150.21	1.63	-67.25		
0.933	115	293.6	277.1	248.4	205.4	127.94	-24.66			
0.610	180	273.3	254.8	219.4	165.4	74.50	-77.50			
0.358	308	236.8	214.3	168.8	101.97	22.07	-132.8			
0.238	467	198.1	171.6	118.50	45.37	-52.82				
0.156	706	150.16	120.01	61.63	-12.84					
0.118	934	113.04	81.20	21.47	-50.47					
0.0851	1300	65.71	33.08	-25.47						
0.0774	1430	51.62	19.02	-38.64						

TABLE IV.16

Dependence of k on Solution Concentration and on Isotopic Composition of Uranium

Solution Conc., moles UO_2F_2/liter		k for Isotopic Composition in % U^{235} of:								
	H/U	93.5	75	50	30	15	5	3	2	1
3.77	25.3	2.0429	1.9786	1.9115	1.8440	1.7373	1.4448	1.2402	1.0542	0.7274
2.45	41.4	2.0261	1.9699	1.9044	1.8267	1.6870	1.3147	1.0795	0.8826	
2.14	48.2	2.0191	1.9662	1.8996	1.8164	1.6648	1.2667	1.0242	0.8267	
1.83	56.8	2.0102	1.9590	1.8904	1.8006	1.6333	1.2073	0.9590		
1.59	66.9	2.0000	1.9497	1.8784	1.7809	1.5975	1.1444	0.8928		
1.37	77.7	1.9891	1.9393	1.8646	1.7589	1.5589	1.0829	0.8305		
1.16	93.0	1.9737	1.9240	1.8442	1.7272	1.5067	1.0058	0.7556		
0.933	115	1.9522	1.9014	1.8140	1.6817	1.4354	0.9115			
0.610	180	1.8922	1.8356	1.7267	1.5574	1.2589	0.7156			
0.358	308	1.7827	1.7128	1.5696	1.3519	1.0079	0.5006			
0.238	467	1.6635	1.5796	1.4073	1.1600	0.8070				
0.156	706	1.5113	1.4128	1.2163	0.9537					
0.118	934	1.3900	1.2832	1.0765	0.8154					
0.0851	1300	1.2306	1.1174	0.9077						
0.0774	1430	1.1820	1.0678	0.8593						

The code may also be used to determine the minimum concentration of U^{235} in uranium for which k can be made unity in homogeneous aqueous UO_2F_2 systems. Since an extrapolation of bucklings is not being made, the normalization of ϵp to unity at a concentration of 93.5% is not made here. The minimum concentrations for which the maximum values of k are 0.95, 0.98, and 1.00 are calculated to be respectively 0.916, 0.990, and 1.042% U^{235} by weight. The hydrogen-to-uranium ratios corresponding to maximum k is approximately 5. These results are in excellent agreement with experimental results[4.12], which give 1.02 ±0.02 wt % U^{235} as the minimum concentration for which the maximum value of k is unity in homogeneous mixtures of UO_3 and H_2O. The experimental H/U ratio for which k is maximum is about 5.

4.4 PLUTONIUM SOLUTIONS

4.4.1 THEORY

There are apparently a number of compensating effects that make it possible to represent the buckling of uranium (~93.5% U^{235}) solutions adequately by the simple relation

$$B_m^2 = \frac{\eta f - 1}{\tau + L_o^2(1-f)}$$

where η is a constant and f is the ratio of thermal cross sections, with a small 1/v correction (determined for a Maxwellian distribution of neutrons) applied to the U^{235} cross section. It appears unlikely, however, that such a simple representation would be adequate for plutonium solutions. Plutonium-239 has a large resonance peak at 0.3 ev at the upper end of the thermal region in which the ratio of absorptions to fissions is considerably smaller than at energies on either side. Both η and f are therefore strongly dependent on the neutron energy spectrum, which is in turn dependent on the plutonium concentration. In addition, plutonium-240 has a very large absorption resonance at 1 ev, which must be treated properly.

As a compromise between a multigroup calculation of buckling and the simple expression used for U^{235} solutions, the one-group model is used for the buckling with k being the sum of contributions from four energy regions. The highest energy region extends from 0.1 Mev to ∞. In this region Pu^{240} is assumed equivalent to Pu^{239}, and Hansen's cross sections[2.7] for Pu^{239} and removal cross sections calculated for H, O, and N are employed. The next region extends from 6.25 ev to 0.1 Mev. Capture in Pu^{240} is considered insignificant, and capture in Pu^{239} is calculated from the resonance integral, which in turn is calculated as a function of the scattering cross section per Pu^{239} atom. The neutron spectrum is assumed to vary as 1/E. In this region η is calculated from resonance parameters to be 1.61. The third region extends from 0.625 to 6.25 ev. The neutron spectrum is assumed here also to vary as 1/E. Absorptions in the Pu^{240} resonance at 1 ev are calculated from the resonance integral, which is a function of the scattering cross section per Pu^{240} atom. Allowance is made for 1/v absorptions. The absorption cross section of Pu^{239} in this region is determined from cross section curves and the 1/E spectrum. The value calculated for η is 2.15. In the fourth or thermal region lying below 0.625, Amster's[4.13] cross sections for Pu^{239} and for 1/v absorbers are used. The 1/v absorbers considered are Pu^{240} (295 b), H, N, and Fe (present as an impurity in the Hanford experiments). The diffusion area, L^2, is computed from the cross sections in this region as $\frac{D}{\Sigma a}$. The computation of k by this procedure and of B^2 as $\frac{k-1}{L^2+\tau}$, where τ is given in Figure 4.2, has been coded for the IBM 650, and the code is

available at the Savannah River Laboratory. Since Amster's cross sections are for Pu^{239} ratios greater than or equal to 100, the code is not valid for lower ratios.

4.4.2 PLUTONIUM NITRATE SOLUTIONS

Critical experiments[4.14] have been performed at Hanford with 9-, 10-, 11-, and 12-inch diameter stainless-steel-walled cylinders and with 11-, 12-, 13-, 14-, and 15-inch-diameter stainless-steel-walled spheres containing plutonium nitrate solutions and surrounded by an effectively infinite thickness of water. The thickness of the stainless steel wall was 0.050 inch for the spheres and 0.062 inch for the cylinders. The parameters that were varied in the experiments were the nitrate ion concentration, the acid normality, the concentration of Pu^{240} in the plutonium, and the plutonium concentration. Reflector savings determined by fitting the data to bucklings calculated by the procedure outlined in the preceding section are recorded in Table IV.17. All the data for plutonium nitrate solutions are presented including, in a number of cases, duplicate runs to illustrate the order of magnitude of the experimental error. As can be seen from the table the bulk of the experiments were performed at plutonium concentrations between 25 and 60 grams per liter. The total spread in S is 0.75 cm.

Extrapolation outside the range of the experiments could be performed by means of calculated bucklings and an average value of S. It is desirable, however, to make use of any trends in S that may be observed. If for the critical spheres the acid normality is plotted against the H/Pu^{239} ratio, it is apparently possible (see Figure 4.11) to represent the data within experimental error by parallel straight lines. If the data are interpolated and extrapolated on these straight lines to give values at acid normalities of 0, 2, 4, and 6 and if three nitrate ions are assumed per plutonium atom (the data show considerable variation in this figure), reflector savings determined from the sphere dimensions and from bucklings calculated for these points bear out trends exhibited by the values of Table IV.17. Plotting values for the same acid normality against plutonium concentration shows a trend toward higher reflector savings as the plutonium concentration increases. This same trend is exhibited by the data obtained with cylinders. There appears to be no appreciable trend in reflector saving with Pu^{240} concentration in the plutonium.

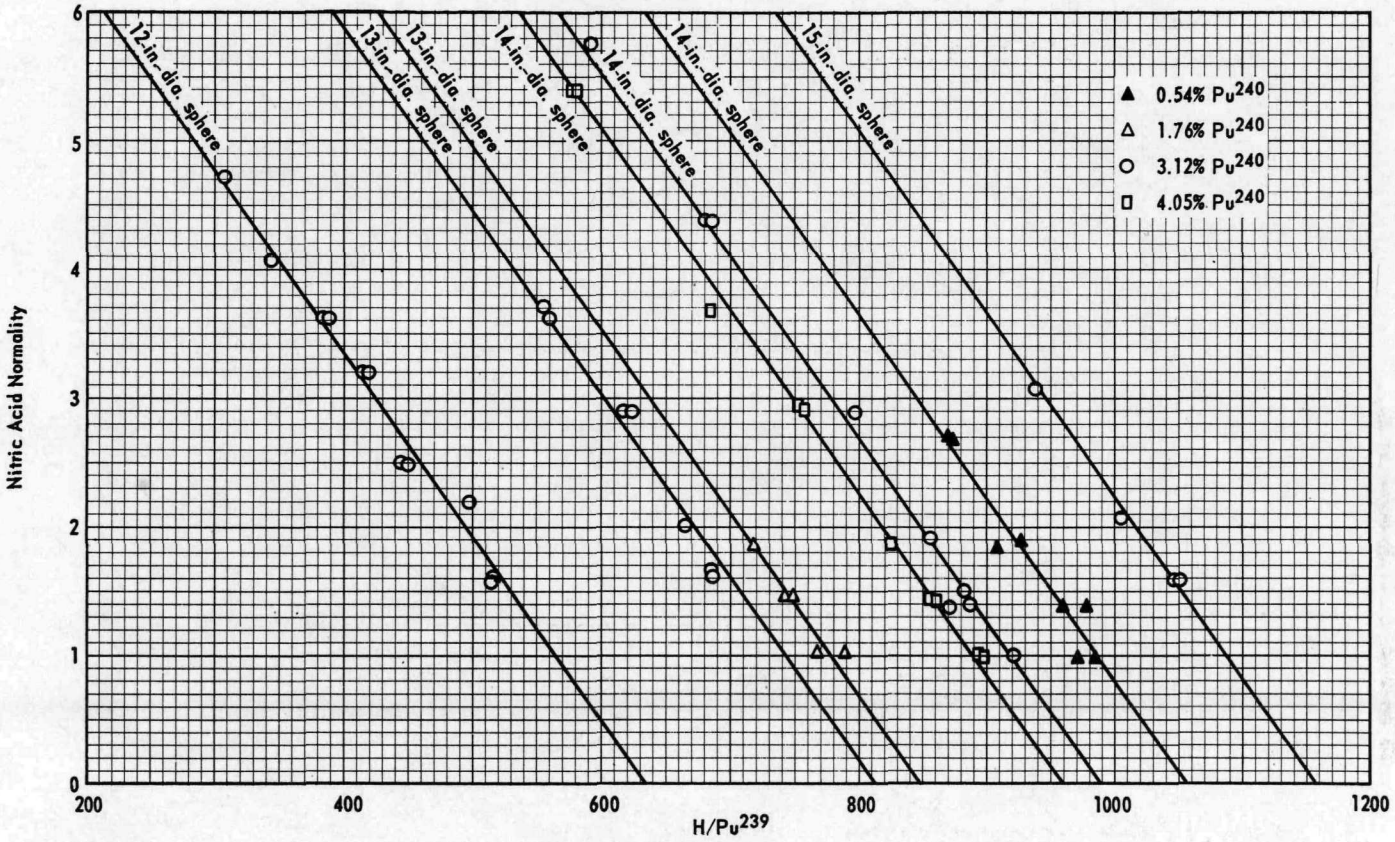

FIG. 4.11 DATA OBTAINED WITH WATER-REFLECTED SPHERES OF PLUTONIUM NITRATE SOLUTION

TABLE IV.17

Critical Mass Data Obtained with Water-Reflected, Stainless-Steel-Walled Spheres and Cylinders of Plutonium Solutions

(The data are expressed in terms of reflector savings.)

Conc., g Pu/liter	H/Pu^{239}	% Pu^{240}	g NO_3/liter	Acid Normality	Vessel	S, cm
25.02	1049	3.12	116	1.60	15-inch-dia. sphere	7.09
25.10	1046	3.12	116	1.60	15-inch-dia. sphere	7.06
25.83	1005	3.12	147	2.08	15-inch-dia. sphere	6.97
26.23	978	0.54	107	1.41	14-inch-dia. sphere	7.14
26.33	984	0.54	77.3	0.99	14-inch-dia. sphere	6.96
26.45	976	2.90	134	1.09	12-inch-dia. cylinder	6.59
26.69	971	0.54	78.3	0.97	14-inch-dia. sphere	6.86
26.77	958	0.54	107	1.42	14-inch-dia. sphere	6.98
27.05	937	3.12	212	3.07	15-inch-dia. sphere	6.93
27.39	927	0.54	137	1.90	14-inch-dia. sphere	6.95
27.91	908	0.54	138	1.85	14-inch-dia. sphere	6.81
27.92	928	1.76	110	1.42	14-inch-dia. sphere	6.99
27.95	928	1.76	109	1.44	14-inch-dia. sphere	6.99
28.50	875	0.54	187	2.70	14-inch-dia. sphere	6.90
28.63	871	0.54	188	2.72	14-inch-dia. sphere	6.88
28.78	920	3.12	87.4	1.02	14-inch-dia. sphere	7.01
29.61	887	3.12	110	1.40	14-inch-dia. sphere	6.93
29.74	882	3.12	115	1.51	14-inch-dia. sphere	6.93
29.82	896	4.05	87.5	1.01	14-inch-dia. sphere	7.01
29.94	893	4.05	87.5	1.01	14-inch-dia. sphere	6.98
30.15	871	3.12	109	1.39	14-inch-dia. sphere	6.80
30.33	857	3.12	143	1.92	14-inch-dia. sphere	6.94
30.75	859	4.05	119.3	1.44	14-inch-dia. sphere	6.94
30.79	858	4.05	119.3	1.44	14-inch-dia. sphere	6.93
30.79	860	4.40	126	1.63	14-inch-dia. sphere	7.07
30.81	843	2.85	136	1.78	11-inch-dia. cylinder	6.57
31.04	853	4.40	127	1.71	14-inch-dia. sphere	7.03
31.14	840	2.90	114	1.44	12-inch-dia. cylinder	6.61
31.72	825	4.05	147	1.88	14-inch-dia. sphere	6.87
31.79	798	3.12	208	2.90	14-inch-dia. sphere	6.93
32.41	809	4.40	158	2.22	14-inch-dia. sphere	6.91
33.17	788	1.76	86.2	1.02	13-inch-dia. sphere	7.03
33.54	773	2.85	137	1.76	11-inch-dia. cylinder	6.64
33.81	756	4.05	211	2.92	14-inch-dia. sphere	6.79
34.06	767	1.76	87.1	1.04	13-inch-dia. sphere	6.89
34.07	750	4.05	211	2.92	14-inch-dia. sphere	6.75
34.59	747	1.76	117	1.44	13-inch-dia. sphere	6.92
34.81	742	1.76	116	1.46	13-inch-dia. sphere	6.89
35.53	686	3.12	311	4.32	14-inch-dia. sphere	6.73
35.65	717	1.76	145	1.88	13-inch-dia. sphere	6.88
35.82	682	3.12	308	4.39	14-inch-dia. sphere	6.69

TABLE IV.17 (Continued)

Conc., g Pu/liter	H/Pu^{239}	$\% Pu^{240}$	g NO_3/liter	Acid Normality	Vessel	S, cm
36.38	686	4.05	272	3.69	14-inch-dia. sphere	6.65
36.52	719	2.90	107	1.39	12-inch-dia. cylinder	6.51
36.90	666	2.83	300	4.28	11-inch-dia. cylinder	6.59
37.84	649	4.05	334	5.46	14-inch-dia. sphere	6.90
37.99	686	3.12	132	1.64	13-inch-dia. sphere	6.86
38.11	686	3.12	128	1.67	13-inch-dia. sphere	6.84
38.74	635	4.05	335	5.46	14-inch-dia. sphere	6.79
38.83	665	3.12	156	2.01	13-inch-dia. sphere	6.86
39.10	663	2.85	138	1.70	10-inch-dia. cylinder	6.87
39.10	663	2.85	138	1.70	11-inch-dia. cylinder	6.82
39.62	592	3.12	408	5.75	14-inch-dia. sphere	6.65
40.69	624	3.12	205	2.90	13-inch-dia. sphere	6.87
41.10	618	3.12	205	2.90	13-inch-dia. sphere	6.83
41.12	581	4.05	385	5.40	14-inch-dia. sphere	6.59
41.19	580	4.05	385	5.40	14-inch-dia. sphere	6.58
41.73	603	2.83	215	2.77	11-inch-dia. cylinder	6.65
42.29	615	2.90	127	1.36	12-inch-dia. cylinder	6.55
44.12	561	3.12	270	3.63	13-inch-dia. sphere	6.78
44.64	555	3.12	269	3.71	13-inch-dia. sphere	6.75
47.21	553	2.83	117	1.38	11-inch-dia. cylinder	6.69
48.75	535	2.90	116	1.27	12-inch-dia. cylinder	6.70
48.98	527	2.90	139	1.38	11-inch-dia. cylinder	6.83
49.26	524	2.85	142	1.63	10-inch-dia. cylinder	6.89
49.26	524	2.85	142	1.63	10-inch-dia. cylinder	6.90
50.25	5.17	3.12	139	1.61	12-inch-dia. sphere	7.05
50-39	515	3.12	138	1.57	12-inch-dia. sphere	7.04
51.80	498	3.12	163	2.20	12-inch-dia. sphere	7.08
54.53	478	2.83	120	1.36	9-inch-dia. cylinder	6.85
56.20	450	3.12	207	2.49	12-inch-dia. sphere	7.01
56.75	445	3.12	207	2.49	12-inch-dia. sphere	6.98
59.93	418	3.12	237	3.20	12-inch-dia. sphere	7.00
60.35	415	3.12	237	3.20	12-inch-dia. sphere	6.99
61.49	421	2.83	134	1.34	9-inch-dia. cylinder	6.90
62.47	412	2.85	146	1.52	10-inch-dia. cylinder	7.06
63.75	388	3.12	270	3.62	12-inch-dia. sphere	7.01
63.99	407	2.90	121	1.17	11-inch-dia. cylinder	6.84
64.16	386	3.12	270	3.62	12-inch-dia. sphere	7.00
70.22	344	3.12	322	4.07	12-inch-dia. sphere	6.99
73.92	353	2.83	126	1.78	9-inch-dia. cylinder	7.02
76.93	334	2.85	146	1.52	10-inch-dia. cylinder	7.17
77.22	309	3.12	359	4.72	12-inch-dia. sphere	6.99
77.40	332	2.85	152	1.41	10-inch-dia. cylinder	7.10
85.14	304	2.83	151	1.29	9-inch-dia. cylinder	7.13
99.09	261	2.83	137	1.37	9-inch-dia. cylinder	7.17
109.16	234	2.83	166	1.68	9-inch-dia. cylinder	7.26
109.16	234	2.83	166	1.68	12-inch-dia. cylinder	7.08
135.8	183	3.12	229	1.81	11-inch-dia. sphere[a]	<7.56

(a) The sphere was subcritical by an unknown amount and the reciprocal neutron multiplication curve was concave as the concentration was increased.

Two experiments[4.14] were performed with 13-inch-diameter, 20-gage aluminum-walled spheres containing plutonium nitrate solution and surrounded by an infinite water reflector. The data are expressed as reflector savings in Table IV.18. Comparison of these reflector savings with values for stainless-steel-walled spheres at the same acid normality, Pu^{240} concentration, and plutonium concentration, obtained by interpolation, shows that the reflector saving with stainless steel walls is about 0.25 cm smaller, which is in agreement with similar results obtained with uranium solutions. The ratio of the albedos for the water-reflected stainless steel and aluminum spheres is 0.935, in excellent agreement with Figure 4.10.

TABLE IV.18

Critical Mass Data Obtained with Water-Reflected, Aluminum-Walled Spheres of Plutonium Solution

(The data are expressed in terms of reflector savings.)

Conc., g Pu/liter	H/Pu^{239}	% Pu^{240}	g NO_3/liter	Acid Normality	Vessel	S, cm
36.27	729	3.12	93.1	1.15	13-inch-dia. sphere	7.20
37.11	705	3.12	125	1.66	13-inch-dia. sphere	7.22

Five experiments[4.14] were performed in a bare 16-inch-diameter stainless-steel-walled sphere. The results, expressed as reflector savings, are given in Table IV.19. Comparison of these reflector savings with corresponding values for reflected stainless steel spheres, obtained by interpolation, gives an average ratio of unreflected to reflected of 0.54 and an average difference between reflected and unreflected of 3.14 cm.

TABLE IV.19

Critical Mass Data Obtained with Bare, Stainless-Steel-Walled Spheres of Plutonium Solution

(The data are expressed in terms of reflector savings.)

Conc., g Pu/liter	H/Pu^{239}	% Pu^{240}	g NO_3/liter	Acid Normality	Vessel	S, cm
34.80	763	4.15	104	1.12	16-inch-dia. sphere	3.82
36.22	733	4.15	109	1.31	16-inch-dia. sphere	3.65
38.31	691	4.15	163	2.79	16-inch-dia. sphere	3.72
38.15	679	4.15	180	2.58	16-inch-dia. sphere	3.72
43.20	578	4.15	282	4.18	16-inch-dia. sphere	3.63

4.4.3 EXTRAPOLATIONS OF DATA

Because of the large number of variables involved with plutonium solutions, graphical representation of critical and safe conditions is not feasible unless restrictions are placed on these variables. In this Handbook tabular presentation is employed so that anyone using the Handbook can make the plots he considers most useful, if he considers such plots necessary to interpolate between tabulated values. For the tabular presentation, concentrations of 5, 10, 15, 20, 30, 40, 50, 70, 90, 120, 150, and 200 g of plutonium per liter, nitric acid normalities of 0, 2, 4, and 6, and plutonium-240 concentrations in the plutonium of 0, 2, and 4% are chosen. The plutonium is assumed to be present as $Pu(NO_3)_3$. The hydrogen concentration is calculated from the Hanford formula[4.14]: hydrogen concentration = 111.8 - hydrogen ion concentration - 0.0535 x nitrate ion concentration where all concentrations are in g/l. Critical bucklings for these conditions are presented in Table IV.20. The corresponding values of k are given in Table IV.21 and the H/Pu^{239} ratios in Table IV.22.

TABLE IV.20

Material Bucklings of Aqueous Solutions of $Pu(NO_3)_3$

B_m^2, cm^{-2}

HNO_3 Normality	0			2			4			6		
% Pu^{240}	0	2	4	0	2	4	0	2	4	0	2	4
Conc., g Pu/liter												
200	.02445	.02232	.02102	.02390	.02176	.02045	.02329	.02114	.01984	.02250	.02037	.01909
150	.02439	.02257	.02136	.02380	.02197	.02075	.02316	.02132	.02011	.02236	.02053	.01933
120	.02418	.02258	.02145	.02357	.02195	.02082	.02291	.02130	.02017	.02209	.02048	.01936
90	.02366	.02231	.02129	.02300	.02164	.02062	.02231	.02095	.01992	.02146	.02011	.01910
70	.02298	.02183	.02090	.02227	.02111	.02018	.02153	.02036	.01943	.02065	.01949	.01857
50	.02168	.02072	.01990	.02090	.01995	.01913	.02009	.01914	.01833	.01917	.01822	.01742
40	.02032	.01947	.01870	.01952	.01867	.01791	.01870	.01785	.01709	.01778	.01694	.01619
30	.01797	.01723	.01653	.01715	.01641	.01571	.01632	.01558	.01490	.01541	.01468	.01401
20	.01359	.01296	.01236	.01273	.01211	.01151	.01189	.01128	.01069	.01102	.01042	.00984
15	.00991	.00936	.00881	.00904	.00850	.00796	.00822	.00768	.00715	.00739	.00686	.00635
10	.00424	.00377	.00330	.00341	.00295	.00248	.00264	.00219	.00174	.00193	.00149	.00105

TABLE IV.21

Multiplication Constants of Aqueous Solutions of $Pu(NO_3)_3$

	k											
HNO_3 Normality	0			2			4			6		
% Pu^{240}	0	2	4	0	2	4	0	2	4	0	2	4
Conc., g Pu/liter												
200	1.7916	1.7227	1.6805	1.7867	1.7164	1.6734	1.7816	1.7098	1.6663	1.7761	1.7028	1.6589
150	1.7913	1.7324	1.6932	1.7852	1.7250	1.6851	1.7792	1.7175	1.6770	1.7733	1.7101	1.6689
120	1.7862	1.7345	1.6980	1.7796	1.7262	1.6888	1.7727	1.7184	1.6805	1.7657	1.7100	1.6715
90	1.7724	1.7287	1.6954	1.7637	1.7188	1.6850	1.7554	1.7095	1.6749	1.7470	1.7000	1.6649
70	1.7534	1.7159	1.6856	1.7424	1.7040	1.6733	1.7320	1.6926	1.6611	1.7215	1.6813	1.6494
50	1.7159	1.6847	1.6577	1.7021	1.6703	1.6429	1.6883	1.6560	1.6283	1.6747	1.6418	1.6137
40	1.6750	1.6470	1.6219	1.6594	1.6310	1.6056	1.6444	1.6154	1.5895	1.6297	1.6001	1.5739
30	1.6026	1.5779	1.5548	1.5847	1.5597	1.5363	1.5673	1.5420	1.5184	1.5503	1.5246	1.5009
20	1.4626	1.4415	1.4211	1.4406	1.4194	1.3989	1.4197	1.3983	1.3776	1.3996	1.3780	1.3571
15	1.3417	1.3227	1.3041	1.3169	1.2979	1.2792	1.2935	1.2743	1.2556	1.2712	1.2520	1.2331
10	1.1489	1.1325	1.1160	1.1217	1.1052	1.0888	1.0960	1.0796	1.0633	1.0719	1.0556	1.0393
5	.8006	.7881	.7755	.7740	.7617	.7493	.7494	.7373	.7252	.7266	.7148	.7029

TABLE IV.22

H/Pu^{239} Ratio for Aqueous Solutions of $Pu(NO_3)_3$

	H/Pu^{239}											
HNO_3 Normality	0			2			4			6		
% Pu^{240}	0	2	4	0	2	4	0	2	4	0	2	4
Conc., g Pu/liter												
250	96.2	98.2	100	91.8	93.7	95.6	87.4	89.2	91.1	83.1	84.8	86.5
200	123	125	128	117	120	122	112	114	116	106	109	111
150	167	170	174	160	163	166	152	155	159	145	148	151
120	211	216	220	202	206	210	193	197	201	184	188	191
90	285	291	297	273	278	284	260	266	271	248	253	259
70	369	377	384	353	361	368	338	345	352	322	329	336
50	521	531	542	499	509	519	477	487	497	455	464	474
40	653	667	680	626	639	652	598	611	623	571	583	595
30	874	892	911	838	855	873	801	817	835	765	780	796
20	1316	1343	1371	1261	1287	1314	1207	1231	1257	1152	1175	1200
15	1758	1794	1831	1685	1720	1755	1612	1645	1679	1539	1571	1603
10	2642	2696	2753	2533	2585	2638	2423	2473	2524	2314	2361	2410
5	5294	5402	5515	5075	5179	5287	4856	4955	5058	4637	4731	4830

Reflector savings for an infinite water reflector, obtained by adding 0.25 cm to the values for stainless-steel-walled spheres surrounded by water, are presented in Table IV.23. In making the extrapolations outside the range of the data, the procedures previously outlined, based on Figure 4.11, were followed, and consideration was given to the subcriticality of the 11-inch sphere (see Table IV.17). These reflector savings, calculated from the data obtained with spheres, are greater than the corresponding values for cylinders and in most cases are considerably greater than for spheres of U^{235} solutions at the same concentrations (see Figure 4.3); hence the bucklings with which they are associated are probably too small. As the discussion in Chapter I indicates, applying these reflector savings to cylinders and slabs will result in underestimates of the critical dimensions and thus be conservative from the point of view of nuclear safety.

The reflector savings, S_o, for bare systems are obtained from the values of Table IV.23 by subtracting 3.39 cm (3.14 + 0.25), since the U^{235} solution data indicate that a constant difference rather than a constant ratio is the better approximation. The values of S_o are required in determining the effect of reflectors other than infinitely thick water.

TABLE IV.23

S for Water-Reflected Spheres of $Pu(NO_3)_3$ Solution

	S, cm											
HNO_3 Normality	0			2			4			6		
% Pu^{240}	0	2	4	0	2	4	0	2	4	0	2	4
Conc., g Pu/liter												
200	7.75	7.75	7.75	7.60	7.60	7.60	7.45	7.45	7.45	7.25	7.25	7.25
150	7.75	7.75	7.75	7.60	7.60	7.60	7.45	7.45	7.45	7.25	7.25	7.25
120	7.75	7.75	7.75	7.60	7.60	7.60	7.45	7.45	7.45	7.25	7.25	7.25
90	7.70	7.70	7.70	7.55	7.55	7.55	7.40	7.40	7.40	7.20	7.20	7.20
70	7.65	7.65	7.65	7.45	7.45	7.45	7.24	7.24	7.24	7.00	7.00	7.00
50	7.52	7.52	7.52	7.29	7.29	7.29	6.97	6.97	6.97	6.75	6.75	6.75
40	7.42	7.42	7.42	7.15	7.15	7.15	6.90	6.90	6.90	6.75	6.75	6.75
30	7.30	7.30	7.30	7.15	7.15	7.15	7.06	7.06	7.06	7.00	7.00	7.00
20	7.45	7.45	7.45	7.45	7.45	7.45	7.45	7.45	7.45	7.45	7.45	7.45
15	7.65	7.65	7.65	7.65	7.65	7.65	7.65	7.65	7.65	7.65	7.65	7.65
10	7.85	7.85	7.85	7.85	7.85	7.85	7.85	7.85	7.85	7.85	7.85	7.85

4.4.4 CRITICAL AND SAFE CONDITIONS

Safe bucklings, determined from the relation $B_s^2 = \frac{\frac{k}{0.95} - 1}{k - 1} B_m^2$, are given in Table IV.24. In Tables IV.25 and IV.26 critical and safe masses of plutonium (as $Pu(NO_3)_3$) in water-reflected spheres are given. In Tables IV.27 and IV.28 critical and safe water reflected infinite cylinder diameters are given. In Tables IV.29 and IV.30 critical and safe water-reflected infinite slab thicknesses are given. For finite slabs and finite cylinders, the critical and safe dimensions can be obtained from Equation 1.9 or 1.10 and the proper choice of buckling and reflector saving or from Figure 4.7 if attention is given to the buckling labels for the curves rather than the concentration labels.

TABLE IV.24

Safe Bucklings (k_{eff} = 0.95) for Aqueous Solutions of $Pu(NO_3)_3$

	Safe Buckling (k_{eff} = 0.95), cm^{-2}											
HNO_3 Normality	0			2			4			6		
% Pu^{240}	0	2	4	0	2	4	0	2	4	0	2	4
Conc., g Pu/liter												
200	.02722	.02498	.02362	.02661	.02437	.02299	.02594	.02369	.02232	.02507	.02284	.02149
150	.02715	.02524	.02397	.02651	.02458	.02330	.02580	.02387	.02260	.02492	.02300	.02174
120	.02693	.02525	.02406	.02626	.02456	.02337	.02554	.02385	.02266	.02464	.02295	.02177
90	.02637	.02496	.02389	.02566	.02423	.02316	.02490	.02347	.02239	.02397	.02255	.02149
70	.02565	.02445	.02347	.02488	.02366	.02269	.02408	.02285	.02187	.02311	.02189	.02093
50	.02428	.02327	.02241	.02343	.02244	.02157	.02255	.02156	.02071	.02155	.02055	.01971
40	.02284	.02195	.02114	.02198	.02108	.02028	.02109	.02019	.01939	.02008	.01920	.01841
30	.02036	.01958	.01885	.01947	.01870	.01796	.01857	.01780	.01708	.01758	.01681	.01611
20	.01574	.01508	.01444	.01481	.01416	.01353	.01390	.01326	.01264	.01295	.01232	.01171
15	.01186	.01128	.01070	.01092	.01035	.00978	.01003	.00946	.00891	.00912	.00856	.00803
10	.00588	.00538	.00489	.00498	.00450	.00400	.00415	.00368	.00320	.00337	.00290	.00244

TABLE IV.25

Critical Masses of Pu in Water-Reflected Spheres of $Pu(NO_3)_3$ Solution

HNO_3 Normality	Critical Mass of Pu, kg											
	0			2			4			6		
% Pu^{240}	0	2	4	0	2	4	0	2	4	0	2	4
Conc., g Pu/liter												
200	1.57	1.96	2.26	1.72	2.15	2.49	1.90	2.38	2.74	2.15	2.70	3.11
150	1.19	1.44	1.63	1.31	1.58	1.81	1.44	1.75	2.00	1.64	1.98	2.27
120	.970	1.14	1.29	1.07	1.26	1.43	1.18	1.40	1.59	1.35	1.60	1.81
90	.778	.893	.997	.859	.993	1.11	.955	1.10	1.24	1.09	1.26	1.41
70	.655	.741	.818	.739	.834	.924	.836	.947	1.05	.962	1.09	1.21
50	.553	.614	.672	.631	.701	.769	.736	.818	.895	.848	.944	1.04
40	.525	.577	.631	.605	.667	.730	.697	.768	.844	.797	.880	.969
30	.527	.578	.632	.599	.659	.723	.678	.746	.818	.773	.851	.936
20	.620	.686	.754	.711	.788	.872	.818	.908	1.01	.950	1.06	1.19
15	.859	.961	1.08	1.03	1.16	1.32	1.24	1.41	1.61	1.52	1.74	2.02
10	2.76	3.41	4.30	4.06	5.24	7.06	6.34	8.73	12.87	10.81	16.66	29.64

TABLE IV.26

Sare Masses (k_{eff} = 0.95) of Pu in Water-Reflected Spheres of $Pu(NO_3)_3$ Solution

HNO_3 Normality	Safe Mass (k_{eff} = 0.95) of Pu, kg											
	0			2			4			6		
% Pu^{240}	0	2	4	0	2	4	0	2	4	0	2	4
Conc., g Pu/liter												
200	1.21	1.49	1.71	1.33	1.65	1.89	1.47	1.82	2.10	1.68	2.08	2.39
150	.909	1.09	1.24	1.01	1.21	1.37	1.12	1.34	1.53	1.27	1.53	1.75
120	.743	.873	.984	.824	.970	1.09	.915	1.08	1.21	1.04	1.23	1.39
90	.595	.681	.758	.661	.760	.846	.738	.849	.948	.845	.974	1.09
70	.502	.564	.624	.569	.641	.707	.644	.728	.805	.749	.845	.933
50	.423	.469	.512	.485	.536	.587	.569	.629	.687	.659	.731	.800
40	.400	.438	.479	.463	.510	.555	.537	.590	.645	.614	.676	.739
30	.401	.438	.475	.456	.497	.543	.514	.563	.615	.584	.642	.704
20	.455	.499	.547	.518	.570	.627	.593	.652	.722	.686	.759	.843
15	.599	.663	.738	.707	.789	.882	.840	.940	1.06	1.01	1.14	1.29
10	1.52	1.80	2.14	2.06	2.48	3.07	2.87	3.55	4.53	4.16	5.38	7.26

TABLE IV.27

Critical Diameters of Infinite, Water-Reflected Cylinders of $Pu(NO_3)_3$ Solution

HNO_3 Normality	Critical Cylinder Diameter, inches											
	0			2			4			6		
% Pu^{240}	0	2	4	0	2	4	0	2	4	0	2	4
Conc., g Pu/liter												
200	6.01	6.57	6.96	6.26	6.85	7.26	6.54	7.16	7.57	6.92	7.56	7.99
150	6.02	6.51	6.85	6.29	6.79	7.17	6.58	7.10	7.49	6.96	7.51	7.92
120	6.07	6.50	6.82	6.35	6.79	7.14	6.64	7.11	7.47	7.03	7.52	7.91
90	6.25	6.61	6.92	6.54	6.93	7.24	6.85	7.26	7.59	7.26	7.69	8.03
70	6.47	6.80	7.07	6.83	7.17	7.46	7.21	7.57	7.88	7.67	8.05	8.38
50	6.94	7.24	7.50	7.36	7.67	7.95	7.88	8.20	8.50	8.36	8.71	9.03
40	7.45	7.73	8.01	7.93	8.23	8.52	8.42	8.74	9.06	8.89	9.23	9.57
30	8.37	8.67	8.98	8.83	9.15	9.48	9.27	9.61	9.95	9.75	10.11	10.48
20	10.37	10.77	11.16	10.92	11.35	11.78	11.51	11.97	12.45	12.17	12.68	13.22
15	13.00	13.55	14.15	13.90	14.52	15.20	14.86	15.58	16.37	16.00	16.84	17.74
10	22.90	24.66	26.78	26.25	28.69	31.85	30.68	34.28	39.22	36.93	42.88	52.27

TABLE IV.28

Safe Diameters of Infinite, Water-Reflected Cylinders of $Pu(NO_3)_3$ Solution

HNO_3 Normality	Safe (k_{eff} = 0.95) Cylinder Diameter, inches											
	0			2			4			6		
% Pu^{240}	0	2	4	0	2	4	0	2	4	0	2	4
Conc., g Pu/liter												
200	5.37	5.88	6.22	5.63	6.15	6.51	5.89	6.44	6.81	6.25	6.82	7.21
150	5.39	5.82	6.13	5.65	6.09	6.42	5.93	6.39	6.73	6.28	6.77	7.14
120	5.44	5.82	6.11	5.71	6.10	6.40	5.98	6.40	6.72	6.35	6.79	7.13
90	5.60	5.92	6.19	5.88	6.22	6.50	6.17	6.53	6.83	6.56	6.94	7.25
70	5.80	6.08	6.34	6.14	6.45	6.71	6.50	6.82	7.10	6.95	7.28	7.58
50	6.23	6.50	6.73	6.63	6.90	7.15	7.12	7.41	7.67	7.59	7.89	8.17
40	6.69	6.94	7.18	7.14	7.41	7.67	7.61	7.89	8.17	8.05	8.35	8.64
30	7.52	7.79	8.04	7.94	8.21	8.50	8.33	8.64	8.93	8.77	9.09	9.41
20	9.22	9.55	9.89	9.69	10.05	10.42	10.20	10.57	10.98	10.77	11.19	11.64
15	11.37	11.81	12.29	12.10	12.60	13.12	12.89	13.44	14.04	13.81	14.45	15.11
10	18.51	19.65	20.91	20.64	22.04	23.78	23.22	25.02	27.28	26.47	28.95	32.15

TABLE IV.29

Critical Thicknesses of Infinite, Water-Reflected Slabs of $Pu(NO_3)_3$ Solution

HNO_3 Normality	Critical Slab Thickness, inches											
	0			2			4			6		
% Pu^{240}	0	2	4	0	2	4	0	2	4	0	2	4
Conc., g Pu/liter												
200	1.81	2.18	2.43	2.02	2.40	2.67	2.24	2.64	2.91	2.54	2.96	3.24
150	1.81	2.13	2.36	2.03	2.36	2.61	2.26	2.61	2.86	2.56	2.92	3.19
120	1.85	2.13	2.34	2.07	2.36	2.59	2.30	2.61	2.84	2.61	2.93	3.19
90	1.98	2.22	2.41	2.21	2.46	2.67	2.45	2.72	2.94	2.77	3.06	3.28
70	2.13	2.35	2.53	2.43	2.65	2.84	2.73	2.97	3.17	3.09	3.35	3.56
50	2.48	2.67	2.85	2.81	3.02	3.20	3.24	3.46	3.65	3.62	3.85	4.06
40	2.84	3.02	3.20	3.22	3.43	3.61	3.61	3.82	4.03	3.96	4.19	4.41
30	3.48	3.67	3.87	3.81	4.02	4.24	4.13	4.35	4.57	4.46	4.69	4.93
20	4.74	5.00	5.26	5.10	5.38	5.66	5.48	5.78	6.09	5.91	6.25	6.60
15	6.40	6.76	7.15	6.99	7.39	7.84	7.62	8.09	8.60	8.36	8.91	9.50
10	12.81	13.96	15.35	15.00	16.59	18.65	17.89	20.25	23.47	21.97	25.86	31.99

TABLE IV.30

Safe (k_{eff} = 0.95) Thicknesses of Infinite, Water-Reflected Slabs of $Pu(NO_3)_3$ Solution

HNO_3 Normality	Safe Slab Thickness, inches											
	0			2			4			6		
% Pu^{240}	0	2	4	0	2	4	0	2	4	0	2	4
Conc., g Pu/liter												
200	1.39	1.72	1.94	1.60	1.94	2.17	1.81	2.17	2.41	2.11	2.48	2.73
150	1.40	1.68	1.89	1.61	1.91	2.11	1.83	2.14	2.36	2.13	2.44	2.68
120	1.43	1.68	1.87	1.65	1.91	2.11	1.87	2.15	2.35	2.17	2.46	2.68
90	1.55	1.76	1.94	1.78	2.00	2.18	2.01	2.25	2.44	2.32	2.57	2.77
70	1.70	1.89	2.05	1.98	2.18	2.35	2.27	2.48	2.66	2.63	2.85	3.04
50	2.02	2.19	2.34	2.34	2.52	2.68	2.75	2.94	3.11	3.11	3.31	3.50
40	2.34	2.50	2.67	2.71	2.89	3.06	3.09	3.27	3.45	3.41	3.61	3.80
30	2.92	3.09	3.26	3.24	3.41	3.60	3.52	3.71	3.91	3.81	4.02	4.24
20	3.99	4.20	4.43	4.30	4.53	4.77	4.63	4.87	5.14	5.00	5.28	5.57
15	5.33	5.62	5.94	5.81	6.14	6.48	6.33	6.69	7.08	6.93	7.35	7.78
10	9.94	10.69	11.51	11.34	12.25	13.39	13.02	14.20	15.67	15.15	16.77	18.86

In the Hanford presentation of the critical mass data[4.14] the logarithm of the critical mass was found to vary approximately linearly with the nitrate ion concentration. From extrapolations of such linear plots and from calculations of bucklings with nitrate absent, reflector savings for solutions containing no nitrate are obtained. These values, together with the corresponding critical and safe bucklings are given in Table IV.31. The critical and safe masses of water-reflected spheres with no nitrate present are given in Table IV.32, the critical and safe infinite cylinder diameters in Table IV.33, and the critical and safe infinite slab thicknesses in Table IV.34.

TABLE IV.31

S, B_m^2, and B_s^2 ($k_{eff} = 0.95$) for
Plutonium Solutions Containing No Nitrate Ion

	S, cm			B_m^2, cm^{-2}			B_s^2 ($k_{eff} = 0.95$), cm^{-2}		
% Pu^{240}	0	2	4	0	2	4	0	2	4
Conc., g Pu/liter									
200	8.33	8.23	8.40	.02468	.02263	.02136	.02746	.02531	.02397
150	8.10	8.16	8.13	.02458	.02281	.02162	.02735	.02549	.02424
120	8.04	8.06	8.05	.02435	.02280	.02168	.02711	.02548	.02430
90	7.87	7.95	7.93	.02381	.02248	.02147	.02653	.02514	.02408
70	7.82	7.82	7.78	.02312	.02200	.02108	.02580	.02463	.02366
50	7.65	7.63	7.63	.02179	.02085	.02003	.02439	.02341	.02255
40	7.50	7.57	7.53	.02042	.01957	.01881	.02295	.02205	.02125
30	7.39	7.41	7.35	.01805	.01731	.01661	.02044	.01967	.01893
20	7.52	7.49	7.44	.01365	.01302	.01242	.01580	.01514	.01451
15	7.84	7.75	7.66	.00996	.00941	.00886	.01191	.01133	.01075
10	8.02	8.13	7.99	.00427	.00380	.00333	.00590	.00541	.00492

TABLE IV.32

Critical and Safe (k_{eff} = 0.95) Masses of Water-Reflected Spheres of Plutonium Solution Containing No Nitrate Ion

% Pu^{240}	Critical Mass, kg			Safe (k_{eff} = 0.95) Mass, kg		
	0	2	4	0	2	4
Conc., g Pu/liter						
200	1.33	1.70	1.88	1.01	1.28	1.41
150	1.07	1.27	1.46	.811	.958	1.10
120	.89	1.04	1.18	.675	.789	.890
90	.735	.83	.93	.561	.629	.703
70	.62	.70	.78	.474	.532	.594
50	.531	.59	.648	.405	.450	.492
40	.509	.553	.610	.389	.421	.462
30	.513	.561	.620	.389	.424	.466
20	.61	.675	.750	.447	.493	.542
15	.83	.94	1.07	.579	.649	.729
10	2.7	3.3	4.2	1.49	1.73	2.09

TABLE IV.33

Critical and Safe (k_{eff} = 0.95) Diameters of Infinite, Water-Reflected Cylinders of Plutonium Solution Containing No Nitrate Ion

% Pu^{240}	Critical Cylinder Diameter, inches			Safe Cylinder Diameter, inches		
	0	2	4	0	2	4
Conc., g Pu/liter						
200	5.49	6.11	6.34	4.87	5.42	5.62
150	5.70	6.12	6.48	5.07	5.43	5.76
120	5.81	6.19	6.52	5.17	5.52	5.81
90	6.08	6.37	6.68	5.43	5.68	5.95
70	6.29	6.61	6.91	5.63	5.91	6.19
50	6.81	7.10	7.37	6.10	6.37	6.60
40	7.35	7.58	7.88	6.59	6.79	7.06
30	8.27	8.56	8.91	7.42	7.67	7.98
20	10.30	10.70	11.14	9.15	9.50	9.86
15	12.80	13.42	14.09	11.18	11.70	12.23
10	22.69	24.34	26.53	18.35	19.33	20.72

TABLE IV.34

Critical and Safe (k_{eff} = 0.95) Thicknesses of Infinite, Water-Reflected Slabs of Plutonium Solution Containing No Nitrate Ion

% Pu^{240}	Critical Slab Thickness, inches			Safe Slab Thickness, inches		
	0	2	4	0	2	4
Conc., g Pu/liter						
200	1.31	1.74	1.85	.906	1.30	1.37
150	1.51	1.77	2.01	1.10	1.32	1.54
120	1.60	1.84	2.06	1.18	1.40	1.59
90	1.82	1.99	2.20	1.40	1.54	1.72
70	1.98	2.18	2.39	1.54	1.72	1.92
50	2.36	2.56	2.73	1.89	2.07	2.23
40	2.75	2.88	3.09	2.26	2.37	2.56
30	3.38	3.57	3.81	2.83	2.99	3.20
20	4.67	4.94	5.25	3.92	4.16	4.41
15	6.22	6.65	7.11	5.17	5.52	5.90
10	12.63	13.67	15.14	9.79	10.40	11.35

By multiplying the slab thicknesses obtained from Tables IV.33 and IV.34 by the concentration and plotting the resulting product against the concentration, a minimum mass per unit area is determined. These minima can be used to provide safe mass limits when precipitation is a possibility. The critical and safe values expressed as grams of plutonium per square foot of horizontal surface are given in Table IV.35 as a function of plutonium-240 concentration. The minima in the curves of mass per unit area occur at a concentration of about 17 g Pu/liter.

TABLE IV.35

Minimum Critical and Maximum Safe (k_{eff} = 0.95) Concentration of Plutonium Per Unit Area in Solutions Containing No Nitrate Ion

% Pu^{240}	Minimum Critical Mass, g/ft^2	Maximum Safe Mass, g/ft^2
0	217	182
2	233	194
4	246	207

Critical and safe concentrations of plutonium can be calculated for unlimited amounts of solutions; these concentrations correspond respectively to k = 1 and k = 0.95. They are useful in cases where concentration control alone is relied on to ensure safety. In Table IV.36, the critical and safe concentrations of plutonium in unlimited amounts of solution are tabulated as a function of nitric acid normality and Pu^{240} concentration. Values are also given for the case of no nitrate in the event the plutonium is present as some other compound. The results are expressed both in terms of concentration and of H/Pu^{239} ratio since the solvent may be a hydrocarbon rather than water.

TABLE IV.36

Critical and Safe (k_{eff} = 0.95) Concentrations of Plutonium in Infinite Amounts of Solution

			Critical Conc.,		Safe (k_{eff} = 0.95) Conc.,	
Pu Compound	HNO_3 Normality	% Pu^{240}	g/liter	H/Pu^{239}	g/liter	H/Pu^{239}
No Nitrate Ion	0	0	7.42	3570	6.73	3940
	0	2	7.66	3535	6.94	3905
	0	4	7.88	3500	7.14	3875
$Pu(NO_3)_3$	0	0	7.44	3535	6.75	3900
	0	2	7.68	3515	6.95	3880
	0	4	7.90	3490	7.16	3855
	2	0	7.85	3215	7.15	3550
	2	2	8.10	3185	7.34	3525
	2	4	8.34	3160	7.55	3490
	4	0	8.27	2930	7.49	3225
	4	2	8.53	2900	7.73	3200
	4	4	8.80	2870	7.95	3170
	6	0	8.68	2665	7.86	2935
	6	2	8.95	2640	8.10	2915
	6	4	9.24	2615	8.36	2890

4.4.5 NATURE OF SOLVENT

The critical and safe conditions given in Tables IV.25 through IV.35 and the bucklings given in Table IV.20 apply to aqueous solutions or slurries. If the solvent is organic or if the plutonium is held in an ion exchange resin, k will be essentially the same as in an aqueous solution at the same H/Pu^{239} ratio (and at the same N/Pu^{239} ratio if nitrate is present). If the hydrogen density in the solvent is less than in water (or in nitric acid), the buckling is less, due to a greater migration area. In this case it is conservative to use the safe and critical conditions for aqueous solutions with the same H/Pu^{239} ratio. If the hydrogen density is greater in the solvent, allowance must be made for this fact. The proper procedure is to calculate τ as was done for this Handbook for nitric acid solutions. A code for the IBM 650 is available at the Savannah River Laboratory for performing such a calculation. In the absence of such a calculation, M^2 may be assumed to vary approximately inversely as the hydrogen density in the solvent, and adequate margins of safety should be employed to compensate for errors introduced by this approximation.

REFERENCES

4.1 Beck, C. K., et al. Critical Mass Studies. Part III. Union Carbide and Carbon Chemicals Corp. K-25 Plant, Oak Ridge, Tenn. AEC Research and Development Report K-343, 77 pp. (April 1949).

4.2 Fox, J. K., et al. Critical Mass Studies. Part IX. Aqueous U^{235} Solutions. Oak Ridge National Laboratory, Tenn. AEC Research and Development Report ORNL-2367, 57 pp. (March 1958).

4.3 Fox, J. K. and L. W. Gilley. "Critical Parameters of Aqueous Solutions of U^{235}", pp. 71-83; "Critical Parameters of a Proton-Moderated and Proton-Reflected Slab of U^{235}", pp. 87-88. Applied Nuclear Physics Division Annual Progress Report for Period Ending September 1, 1957. Oak Ridge National Laboratory, Tenn. AEC Research and Development Report ORNL-2389, 283 pp. (November 1957).

4.4 Fox, J. K. and L. W. Gilley. "Some Studies of Water, Styrofoam, and Plexiglas Reflectors", pp. 38-99; Fox, J. K., et al., "Critical Parameters of Uranium Solutions in Simple Geometry", p. 42. Neutron Physics Division Annual Progress Report for Period Ending September 1, 1958.

4.5 Callihan, D., et al. Critical Mass Studies. Part V. Union Carbide and Carbon Chemicals Corp. K-25 Plant, Oak Ridge, Tenn. AEC Research and Development Report K-643 57 pp. (June 1950).

4.6 Thomas, J. T., et al. A Direct Comparison of Some Nuclear Properties of U^{233} and U^{235}. Oak Ridge National Laboratory, Tenn. AEC Research and Development Report ORNL-1992, 25 pp. (December 1955).

4.7 Thomas, J. T. Parameters for Two Group Analysis of Critical Experiments with Water Reflected Spheres of UO_2F_2 Aqueous Solutions. Oak Ridge National Laboratory, Tenn. AEC Research and Development Report ORNL-CF-56-8-201, 14 pp. (August 1956).

4.8 Goertzel, G. "Minimum Critical Mass and Flat Flux". J. Nuclear Energy, 2, 193-201 (1956).

4.9 Morfitt, J. W. "Minimum Critical Mass and Uniform Thermal-Neutron Core Flux in an Experimental Reactor". Nuclear Science and Technology, 4, 107-25. Union Carbide and Carbon Chemicals Corp. Y-12 Plant, Oak Ridge, Tenn. AEC Research and Development Report TID-2505, 210 pp. (March - December 1954).

4.10 Fox, J. K. and L. W. Gilley. Preliminary Report of Critical Experiments in Slab Geometry. Oak Ridge National Laboratory, Tenn. AEC Research and Development Report ORNL-CF-56-7-148, 15 pp. (July 1956).

4.11 Callihan, D., et al. Critical Mass Studies. Part VI. Oak Ridge National Laboratory, Tenn. AEC Research and Development Report Y-801, 34 pp. (August 1951)(Confidential).

4.12 Handler, H. E. "Measurements of k_∞ for Homogeneous Mixtures of Enriched Uranyl Oxide and Water". Nuclear Physics Research Quarterly Report - October, November, December 1957. General Electric Co., Hanford Atomic Products Operation, Richland, Wash. AEC Research and Development Report HW-54591, 85 pp. (March 1958). pp. 41-42.

4.13 Amster, H. J. A Compendium of Thermal Neutron Cross Section Averaged Over the Spectra of Wigner and Wilkins. Westinghouse Electric Corp., Bettis Plant Pittsburgh, Penn. AEC Research and Development Report. WAPD-185, 157 pp. (January 1958).

4.14 Kruesi, F. E., et al. Critical Mass Studies of Plutonium Solutions. General Electric Co., Hanford Atomic Products Operation, Richland, Wash. AEC Research and Development Report HW-24514, 85 pp. (May 1952).

4.15 Fox, J. K., et al. "Critical Parameters of U^{235} and U^{233} Solutions in Simple Geometry". Neutron Physics Division Annual Progress Report for Period Ending September 1, 1959. Oak Ridge National Laboratory, Tenn. AEC Research and Development Report ORNL-2842, 244 pp. (November 1959). pp. 76-77.

CHAPTER V - INTERACTION

5.1 INTRODUCTION

One of the more difficult problems encountered in nuclear safety is that of determining interactions between units which if individually isolated would be subcritical, but which if brought close together could constitute a critical assembly. Since complete isolation of units from reflectors or from other units is often impractical, it is important to have some means of calculating the reduction in size that must be made to permit a certain minimum separation between units or between a unit and a reflector. A large amount of experimental data exists[5.1-5.8] against which methods of calculation may be checked; but, except where a specific situation happens to duplicate one studied experimentally, direct reference to such data may not be very helpful. A generally conservative method has been developed[5.9] for computing interactions between units in air. In water, interactions can be computed satisfactorily by two-group methods. In the present chapter methods of calculating interaction in air are described first.

5.2 INTERACTIONS IN AIR

5.2.1 INTERACTIONS BETWEEN FISSIONABLE UNITS

Consider two interacting surfaces (see Figure 5.1). The total* neutron current out of the surroundings that enters surface No. 1 is some fraction ρ_{12} of the total neutron current into the surroundings from Surface No. 2 and vice versa. If J_{out} represents the total current out of the surroundings and J_{in} represents the total current into the surroundings, the following equations must be satisfied:

$$J_{1\ out} = \rho_{12} J_{2\ in}$$

and

$$J_{2\ out} = \rho_{21} J_{1\ in}.$$

The albedo of the surroundings is equal to J_{out} divided by J_{in}. Thus the equations may be written as

$$\beta_1 J_{1\ in} - \rho_{12} J_{2\ in} = 0$$

and

$$-\rho_{21} J_{1\ in} + \beta_2 J_{2\ in} = 0$$

where β is the albedo. They are satisfied only if $\beta_1\beta_2 = \rho_{12}\rho_{21}$, which becomes $\beta = \rho$ if the two interacting units are identical.

*The total current is the current in neutrons of all energies per cm^2 per second integrated over the entire surface under consideration.

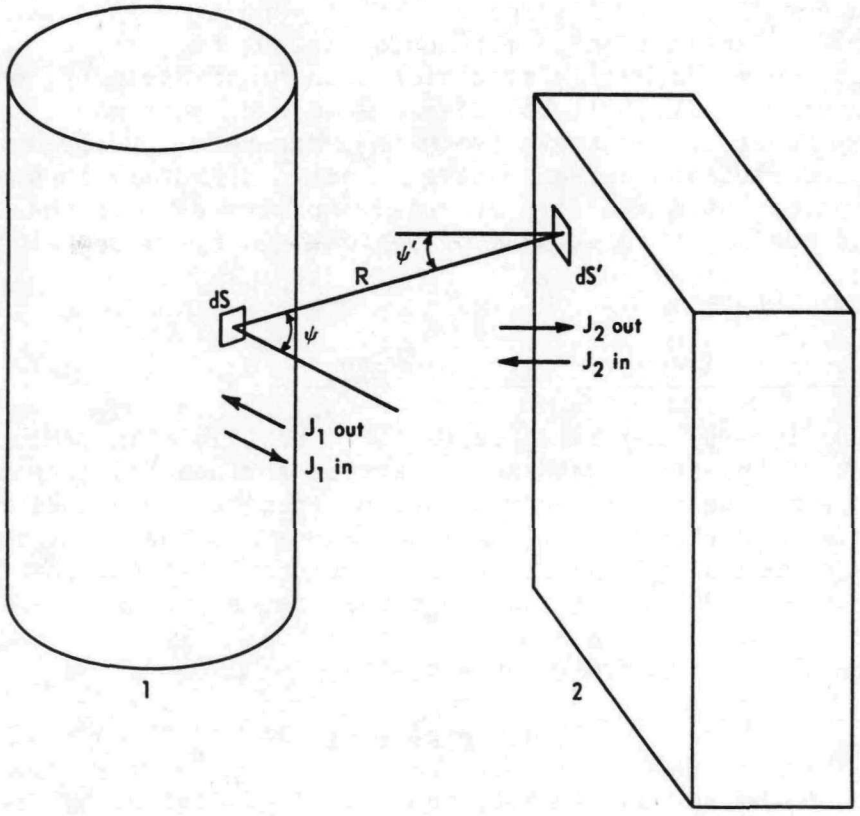

FIG. 5.1 INTERACTING SLAB AND CYLINDER

5.2.2 CALCULATION OF ρ

Simplifying assumptions are made so that ρ can be calculated solely from the geometry of the system. In particular, the directions of travel of the neutrons issuing from a surface are assumed to have a cosine distribution and the neutron current is assumed to be independent of position on the surface. The latter assumption is good if the two surfaces are of equal size and shape, but as will be shown later, can be poor if they are not. The resulting equation for ρ is

$$\rho = \frac{\int_{S'}\int_{S} \frac{\cos\psi \cos\psi'}{\pi R^2} \, dS dS'}{\int dS} \qquad (5.1)$$

where S and S' denote the two surfaces (e.g., a cylinder and a slab as in Figure 5.1), R denotes the distance from an element of surface on one to an element of surface on the other, and ψ and ψ' denote the angles R makes with normals to the elements of surface. This integration is not readily performed for curved surfaces, and they are approximated by flat surfaces, i.e., a circular cylinder is replaced by a square cylinder with a base of equal area and a sphere by a cube of equal volume, axis-to-axis or center-to-center distances remaining the same.

The basic equation for ρ is derived for two rectangular surfaces at right angles to each other since the integral in Equation 5.1 cannot be evaluated easily for parallel surfaces except for circular discs, rectangles with one infinite dimension, or finite rectangles at a large separation compared to the dimensions of the rectangles. Results for parallel surfaces are obtained by subtracting from unity the contributions reaching slabs perpendicular to the parallel slabs. For example, the fraction of the neutrons from a rectangle (see Figure 5.2) in the (X,Z) plane at Y = 0 with vertices at (0,0,0), (2,0,0), (2,0,1), and (0,0,1) reaching a parallel plane at Y = 1 with vertices at (0,1,0), (3,1,0), (3,1,2), and (0,1,2) is obtained by subtracting from unity the fractions that reach perpendicular rectangles with vertices at:

(0,0,0), (0,0,2), (0,1,2), and (0,1,0)
(3,0,0), (3,0,2), (3,1,2), and (3,1,0)
(0,0,0), (0,1,0), (3,1,0), and (3,0,0)
(0,0,2), (0,1,2), (3,1,2), and (3,0,2)

The fraction in the reverse direction (i.e., those from the larger rectangle reaching the smaller) is readily obtained by noting that the integral in the numerator of Equation 5.1 is the same whichever rectangle is considered as the emitter, and hence that the fraction from the larger reaching the smaller is obtained by multiplying the fraction from the smaller reaching the larger by the ratio of the

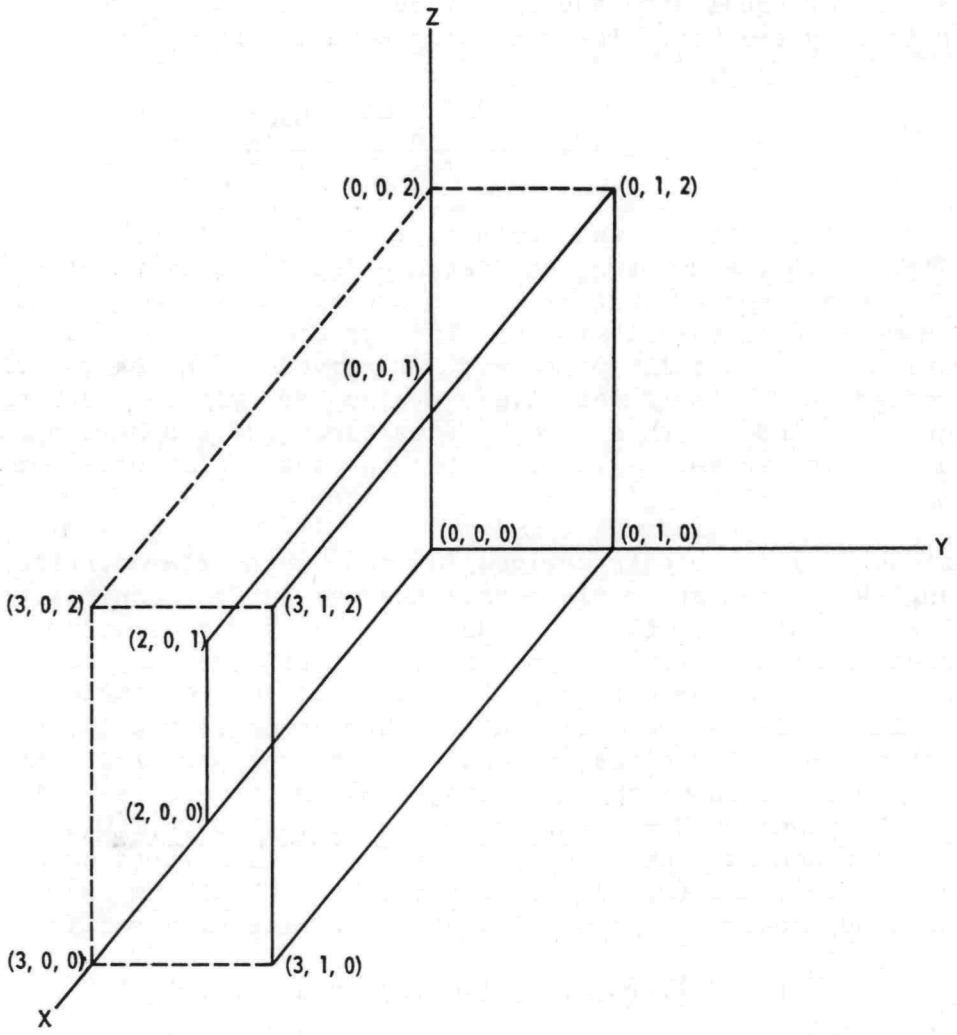

FIG. 5.2 INTERACTION BETWEEN TWO PARALLEL PLANES

smaller to the larger surface area. The general case is not as simple as pictured in the example, but the same procedures apply.

The fraction of the neutrons from a rectangle with dimensions 2a x 2h reaching a perpendicular rectangle with dimensions 2d x 2g with the rectangles arranged as shown in Figure 5.3 is

$$\rho' = \frac{1}{8\pi ah}\sum\left[(Z+f-Z')\sqrt{(Y'+a+b)^2+(X+e)^2}\,\sin\frac{(Z+f-Z')}{\sqrt{(Y'+a+b)^2+(X+e)^2+(Z+f-Z')^2}}\right.$$

$$+\frac{(Z+f-Z')^2}{4}\log\left(1+\frac{(Y'+a+b)^2+(X+e)^2}{(Z+f-Z')^2}\right)$$

$$\left.+\frac{(Y'+a+b)^2+(X+e)^2}{4}\log\frac{(Y'+a+b)^2+(X+e)^2}{(Y'+a+b)^2+(X+e)^2+(Z+f-Z')^2}\right] \quad (5.2)$$

where Y' and Z' are measured along the 2a and 2h edges of the vertical plane and X and Z along the 2d and 2g edges of the horizontal plane, and where the summation is made over the 16 terms resulting from setting Y' equal to -a and a, X equal to -e (or -d if $e > d$) and d, Z equal to -g and g, and Z' equal to -h and h. The separation between the nearer edge of rectangular surface 4ah and the plane of surface 4dg is b. The separation between centers of the rectangles in the direction that the 2h and 2g edges have in common is f. The separation between the trace of rectangle 4ah obtained by projection onto the plane of 4dg and a line through the center of 4dg parallel to the 2g edge is e. Where $e < d$, ρ includes only contributions from the front face of 4ah. An IBM 650 code, which is available at the Savannah River Laboratory, has been prepared for evaluating Equation 5.2.

By subtracting contributions calculated from Equation 5.2 with b = o, f = o, e = d, and g = h from unity, ρ has been calculated for equal, parallel rectangles as a function of α and σ where α is the separation between surfaces divided by the smaller dimension of the surface and σ is the smaller dimension divided by the larger dimension. The results are plotted in Figure 5.4 against α and against $1/\alpha$ for $\alpha > 1$. In Figure 5.5 the region of small $1/\alpha$ is blown up for greater accuracy in reading the graph. This region is of importance when large numbers of units interact.

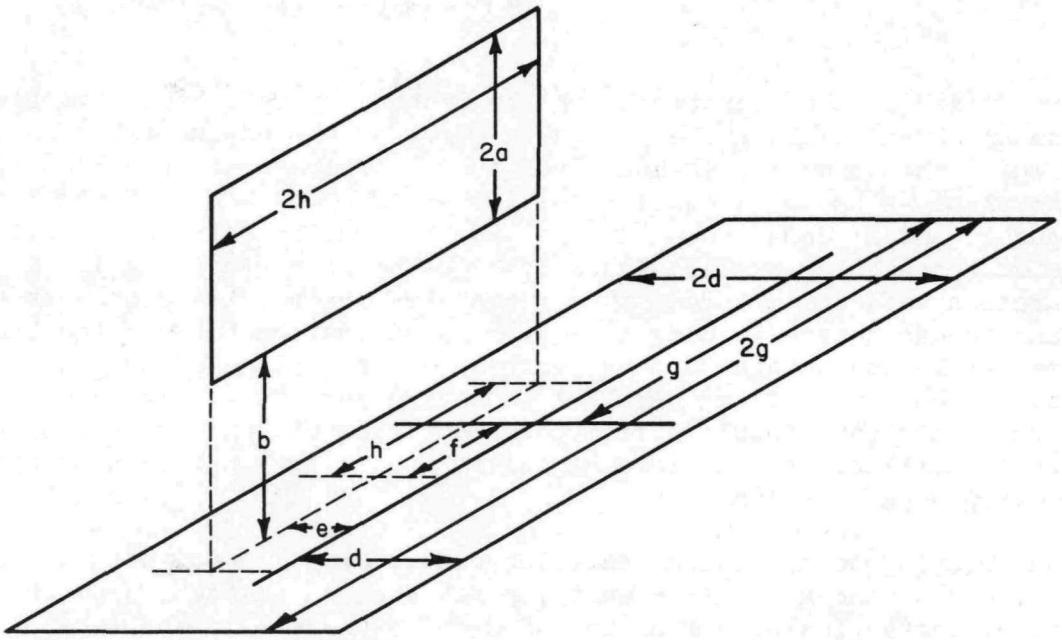

FIG. 5.3 INTERACTION BETWEEN PERPENDICULAR RECTANGLES
(The 2g and 2h edges are parallel)

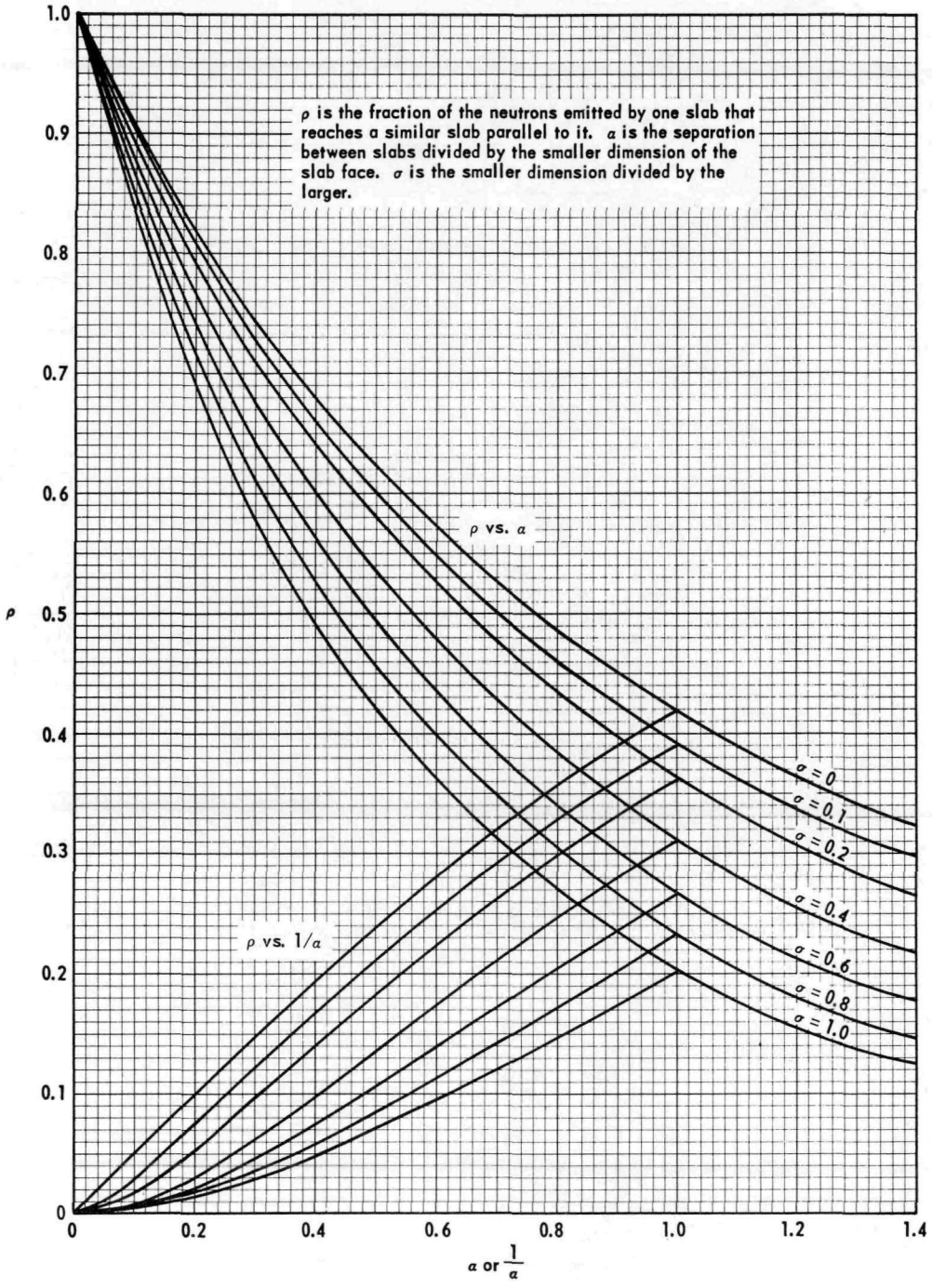

FIG. 5.4 ρ FOR PARALLEL RECTANGULAR SLABS

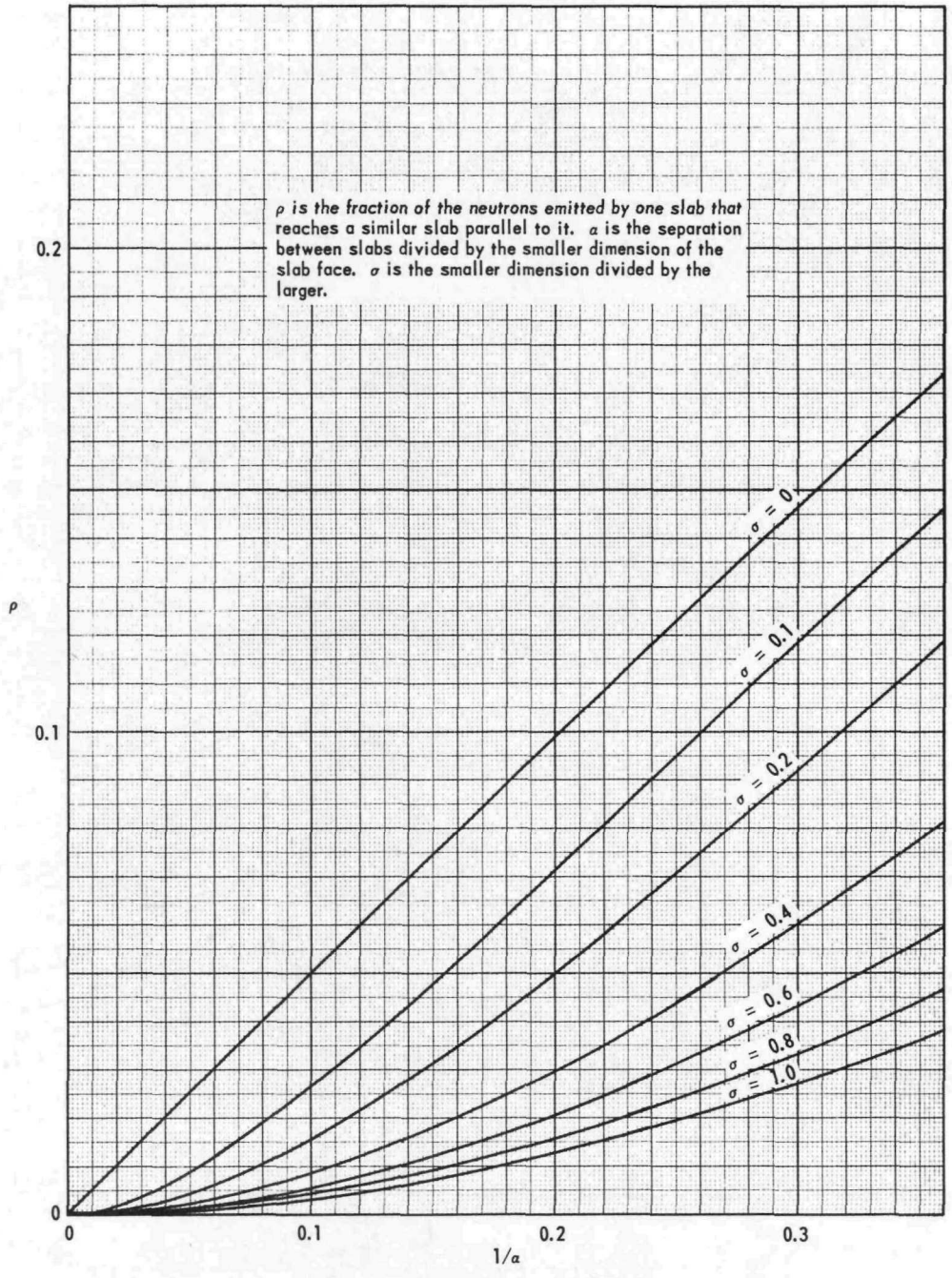

FIG. 5.5 ρ FOR PARALLEL RECTANGULAR SLABS, $1/\alpha \leq 0.36$

5.2.3 ALBEDO EXPRESSION

For a slab the albedo at the surface is given by

$$\beta = \frac{\sin B(S-S_o)}{\sin B(S+S_o)} = \frac{\tan BS - \tan BS_o}{\tan BS + \tan BS_o} \tag{5.3}$$

where B is the square root of the buckling in the direction normal to the surface, S is the effective reflector saving provided by the surroundings, and S_o is the bare extrapolation distance determined by fitting data for unreflected vessels to calculated bucklings, as described in Chapters II and III. In some applications it is desirable to work with the total albedo defined as

$$\beta_T = \frac{J_{L\ out} + J_{R\ out}}{J_{L\ in} + J_{R\ in}}$$

where L and R denote the left- and right-hand surfaces of the slab. The expression for β_T is

$$\beta_T = \frac{\sin B(\bar{S}-S_o)}{\sin B(\bar{S}+S_o)} \tag{5.4}$$

where $2\bar{S} = S_R + S_L$.

For an infinite cylinder the expression for β_T is

$$\beta_T = \frac{\dfrac{J_o(2.405-B\bar{S})}{J_1(2.405-B\bar{S})} - \dfrac{J_o(2.405-BS_o)}{J_1(2.405-BS_o)}}{\dfrac{J_o(2.405-B\bar{S})}{J_1(2.405-B\bar{S})} + \dfrac{J_o(2.405-BS_o)}{J_1(2.405-BS_o)}}. \tag{5.5}$$

For a sphere the expression is

$$\beta_T = \frac{\dfrac{\pi-B\bar{S}}{1+(\pi-B\bar{S})\cot B\bar{S}} - \dfrac{\pi-BS_o}{1+(\pi-BS_o)\cot BS_o}}{\dfrac{\pi-B\bar{S}}{1+(\pi-B\bar{S})\cot B\bar{S}} + \dfrac{\pi-BS_o}{1+(\pi-BS_o)\cot BS_o}}. \tag{5.6}$$

For the cylinder and sphere $\bar{S}$ is the effective reflector saving of the surroundings averaged over the entire surface of the cylinder or sphere.

5.2.4 CALCULATION OF THE INTERACTION

The interaction problem can be stated in several ways. Thus in the case of two parallel identical slabs, B^2, S_o, the dimensions of the interacting surfaces, and the separation between the surfaces may be given, and the safe slab thickness may be required. Solution of the equation $\beta = \rho$ with ρ read from Figure 5.4 or 5.5 gives the critical value of $\bar{S}$ and the critical thickness as $\pi/B - 2\bar{S}$. The safe thickness corresponding to a choice of k_{eff} is then readily calculated as:

$$T_{safe} = \frac{\pi}{B_m}\sqrt{\frac{k-1}{k-k_{eff}}\,k_{eff}} - 2\bar{S}.$$

Conversely, the surface dimensions and thickness of the slabs and the buckling may be given, and the safe separation may be required. In this case, the safe buckling and hence a safe value of $\bar{S}$ are used in the equation $\beta = \rho$ and the solution gives the safe value of ρ from which the safe separation can be determined. For a safe separation to exist, the safe $\bar{S}$ must be greater than S_o. In some cases the surface dimensions, the thickness, the separation, and the buckling may all be given. Solution of $\beta = \rho$ then gives $\bar{S}$ from which the geometric buckling can be calculated as $\frac{\pi^2}{(T+2\bar{S})^2}$, and hence k_{eff} and the multiplication can be determined.

For square cylinder and cube approximations to circular cylinders and spheres, it is necessary to assume that J_{in} is independent of the emitting face as well as of position on the face if β_T, as expressed by Equations 5.5 and 5.6, is to be employed in the calculation. This approximation is nonconservative, but it tends to compensate for conservatism in some of the other approximations and to yield fairly good results when compared with experiment. It is poorest when the separation between units and the number of units are small, sometimes giving nonconservative results (see Reference 5.9).

In the case of slabs the above approximation is convenient, but permitting the currents at the left and right surfaces to have different values does not greatly complicate the calculation. For n parallel slabs the equations are:

$$J_{1R\ out} = \rho_{1R,2L} J_{2L\ in}$$

$$\rho_{2L,1R} J_{1R\ in} = J_{2L\ out}$$

$$\cdots$$

$$J_{(n-1)R\ out} = \rho_{(n-1)R,nL} J_{nL\ in}$$

$$\rho_{nL,(n-1)R} J_{(n-1)R\ in} = J_{nL\ out}$$

For equally spaced, identical slabs the ρ's and the slab thicknesses are all equal, and the following matrix equation can be derived:

$$\begin{bmatrix} 0 & 1 \end{bmatrix} \; M \; P \; M \; P \; \ldots \; PM \begin{bmatrix} 0 \\ 1 \end{bmatrix} = 0,$$

where

$$M = \begin{bmatrix} -\sin 2B(\bar{S}+S_o) & \sin 2B\bar{S} \\ -\sin 2B\bar{S} & \sin 2B(\bar{S}-S_o) \end{bmatrix}$$

and

$$P = \begin{bmatrix} \rho & 0 \\ 0 & 1/\rho \end{bmatrix}.$$

There are n M matrices and (n-1) P matrices in the product. For two slabs the result is

$$\rho = \frac{\sin 2B(\bar{S}-S_o)}{\sin 2B\bar{S}} = \beta = \beta_T \left(1 + \frac{\sin 2BS_o}{\sin 2B\bar{S}}\right)$$

since in this case $2\bar{S} = S + S_o$. For three slabs the result is

$$\rho = \beta_T \left(1 + \frac{\sin 2BS_o}{\sin 2B\bar{S}}\right)^{\frac{1}{2}}$$

For an infinite number of slabs, the result is $\rho = \beta_T$. With small numbers of closely spaced slabs these or other equations derived on the same basis should be employed.

Where the currents may be assumed independent of the face, equations may be written in terms of the total albedo as

$$\left.\begin{aligned} -\beta_{T_1} J_{1\,in} + \rho_{12} J_{2\,in} + \ldots + \rho_{1n} J_{n\,in} &= 0 \\ \cdots & \\ \rho_{n_1} J_{1\,in} + \rho_{n2} J_{2\,in} + \ldots - \beta_{Tn} J_{n\,in} &= 0 \end{aligned}\right\} . \qquad (5.7)$$

If the units are identical, the β_T's are all equal and β_T is determined as the appropriate eigenvalue of the matrix of coefficients of the J_{in}'s. The expressions obtained for two, three, and an infinite number of equally spaced identical slabs in this approximation are respectively $\rho = 2\beta_T$, $\rho = \sqrt{2}\,\beta_T$, and $\rho = \beta_T$. If the units are not identical, all β_T's except one can be specified or relations between the β_T's may be found. For example, with two slabs of unequal thickness either the

thickness of one can be specified and the equation solved to give the critical thickness of the other, or the ratio of the two thicknesses can be specified and the equation solved for one or the other of the thicknesses.

The ρ_{ij} required in Equation 5.7 are simple modifications of values calculated from Equation 5.2 or read from Figures 5.4 or 5.5. For parallel slabs ρ_{ij} is 1/2 the value read from Figures 5.4 or 5.5 since only 1/2 the total interacting surface of one slab sees an adjacent slab. For cylinders in the square cylinder approximation the factor is 1/4 and for spheres it is 1/6.

Shielding of one unit by another results in a reduction in the ρ_{ij} for some situations. For parallel identical slabs numbered consecutively, $\rho_{ij} = 0$ for $|i - j| > 1$. For spheres in a regular array, contributions from nearest neighbors, next nearest, etc., are calculated with the array considered infinite in all directions. Contributions, from neighbors sufficiently far away that $\sum_j \rho_{ij}$ would become greater than unity as a result of their contributions, are multiplied by a factor chosen to make the sum exactly unity. More distant neighbors are assumed to be completely shielded by the intervening spheres. In the actual finite array this same factor is employed, and the same neighbors are included. A similar procedure is employed for regular arrays of cylinders. The cylinders are considered infinite in length and the array infinite in extent for the purpose of determining the factor to be applied to contributions from the most distant neighbor included. For some types of finite arrays of both spheres and cylinders, this procedure may require modification, since units on the boundary may not be shielded from each other to the same extent as in an infinite array.

As pointed out earlier, the assumption that the current is independent of position on the interacting surface may be poor if surfaces are not congruent; for example, if a very large slab (1) and a small slab (2) are parallel to each other, $\rho_{12} \rightarrow 1$ and $\rho_{21} \rightarrow 0$ if calculations are made on the basis that the current is independent of position. If both slabs have the same thickness, and if the small slab is large enough that $\beta_1 \cong \beta_2$, the equation $\beta_1\beta_2 = \rho_1\rho_2$ leads to the result $\beta \cong 0$, which is clearly wrong. This difficulty may be avoided by considering the larger slab to be made up of a number of small slabs in edge-to-edge contact.

In interaction problems involving unequal slabs or cylinders, or slabs at right angles to each other, perpendicular faces of a particular unit may be involved so that more than one buckling component is required. For example, both the end and large side surfaces of slabs may be involved in the interaction; hence, the albedos at both the end and side surfaces will enter into the calculations. The equations for the currents at the surfaces have to be solved subject to the condition that in each slab the sum of the buckling components equals the material

buckling. In such situations, the calculation is considerably simplified if contributions to and from the smaller surfaces are considered as entering or leaving the larger surfaces so that only the albedos at the large surfaces need be considered. Since the numerator of Equation 5.1 represents the number of neutrons reaching one surface from another, and the denominator represents the area of the emitting surface, all neutrons can be treated as coming from the large surface by always making the denominator the area of the large surface.

When regular arrays are being investigated, Equation 5.7 may be greatly simplified if the currents for equivalent units are lumped together. If, for example, three identical units are equally spaced in a line, the two outer units are equivalent. If the outer units are designated 1 and the center unit 2, the equations become:

$$- \beta J_{1\ in} + \rho_{12} J_{2\ in} = 0$$

and

$$2\rho_{21} J_{1\ in} - \beta J_{2\ in} = 0.$$

In an infinite regular array all units are equivalent; hence there is only a single equation.

5.2.5 INTERACTIONS WITH REFLECTORS

The interaction between a unit and a reflector is calculated in a manner similar to that employed for the interaction between fissionable units. If the current emitted by the reflecting surface may be assumed independent of position,

$$\beta_u J_{u\ in} = J_{u\ out} = \rho_{ur} J_{r\ out} = \rho_{ur} \beta_r J_{r\ in} = \rho_{ur}\ \beta_r \rho_{ru} J_{u\ in}$$

where u denotes the fissionable unit and r the reflector, and where β_r is the albedo of the reflector. Thus $\beta_u = \rho_{ur}\rho_{ru}\beta_r$.

Situations in which the current from the reflector may be considered independent of position are; (1) ones in which a surface of a fissionable unit faces a reflecting surface of equal size and shape, and (2) ones in which symmetry requires that the current distribution be uniform, as for example, a spherical unit surrounded by a concentric reflecting spherical shell. In other situations the reflector can be broken up into a number of surfaces equal in size to the surface of the fissionable unit, and the current distribution can be assumed uniform in each of these subdivisions. In all these situations it is apparent from Equation 5.1 that

$$\rho_{ur} = \frac{\text{Interacting area of fissionable unit}}{\text{Interacting area of reflector}}\ \rho_{ru} \qquad (5.8)$$

where ρ_{ur} is the fraction of the neutrons emitted by the reflector that reaches the fissionable unit and ρ_{ru} is the fraction of the neutrons emitted by the fissionable unit that reaches the reflector.

For the particular case of a slab parallel to an infinite plane reflector, the fraction (ρ_{ur}) of the neutrons that is returned from the reflector can be calculated by integrating the contributions to the slab from elements of surface of the plane reflector over the entire surface of the reflector. Results of this integration for an infinite plane reflector parallel to a circular disc and to an infinite slab of finite height are presented in Figure 5.6 as functions of disc radius or slab height and of separation from the reflector. Other shapes may be approximated by a disc of equal area or by an infinite slab of equal smaller dimension, whichever approximation gives the smaller ρ_{ur}. Since the reflector is infinite, ρ_{ru} is unity.

Although the albedo of the reflector can be calculated from its properties, it is much better to determine it from experimental results such as those given in Chapter IV, so that the correct result will be ensured in the limit of zero separation. When the reflector is in contact with the fissionable unit,

$$\beta = \frac{\sin B(S-S_o)}{\sin B(S+S_o)} = \beta_r$$

with $S = S_r$, the reflector savings of the reflector when in contact. Hence β_r is determined by the buckling and the reflector saving. For curved surfaces, such as a spherical shell surrounding a sphere, the effect of the radius of curvature on β_r must be taken into account. This can be done by eliminating the properties of the reflector from the equation $\beta_r = \frac{J_{r\ out}}{J_{r\ in}}$ by the use of albedos obtained with the reflector in contact with the curved surface and with the reflector in contact with a flat surface of the same fissionable material. In the case of a sphere of radius R_o, β_r for a reflector of radius R is given by

$$\beta_r = \frac{\beta_\infty - \left(\frac{R_o}{R}\right)\left(\frac{\beta_\infty - \beta_o}{1+\beta_o}\right)}{1 + \left(\frac{R_o}{R}\right)\left(\frac{\beta_\infty - \beta_o}{1+\beta_o}\right)} \qquad (5.9)$$

where β_o is the albedo with the reflector in contact with the sphere and β_∞ is the albedo with the reflector in contact with a slab of the same material. For cylinders, β_r as a function of radius can also be found in terms of β_o and β_∞, but an analytical expression cannot be written.

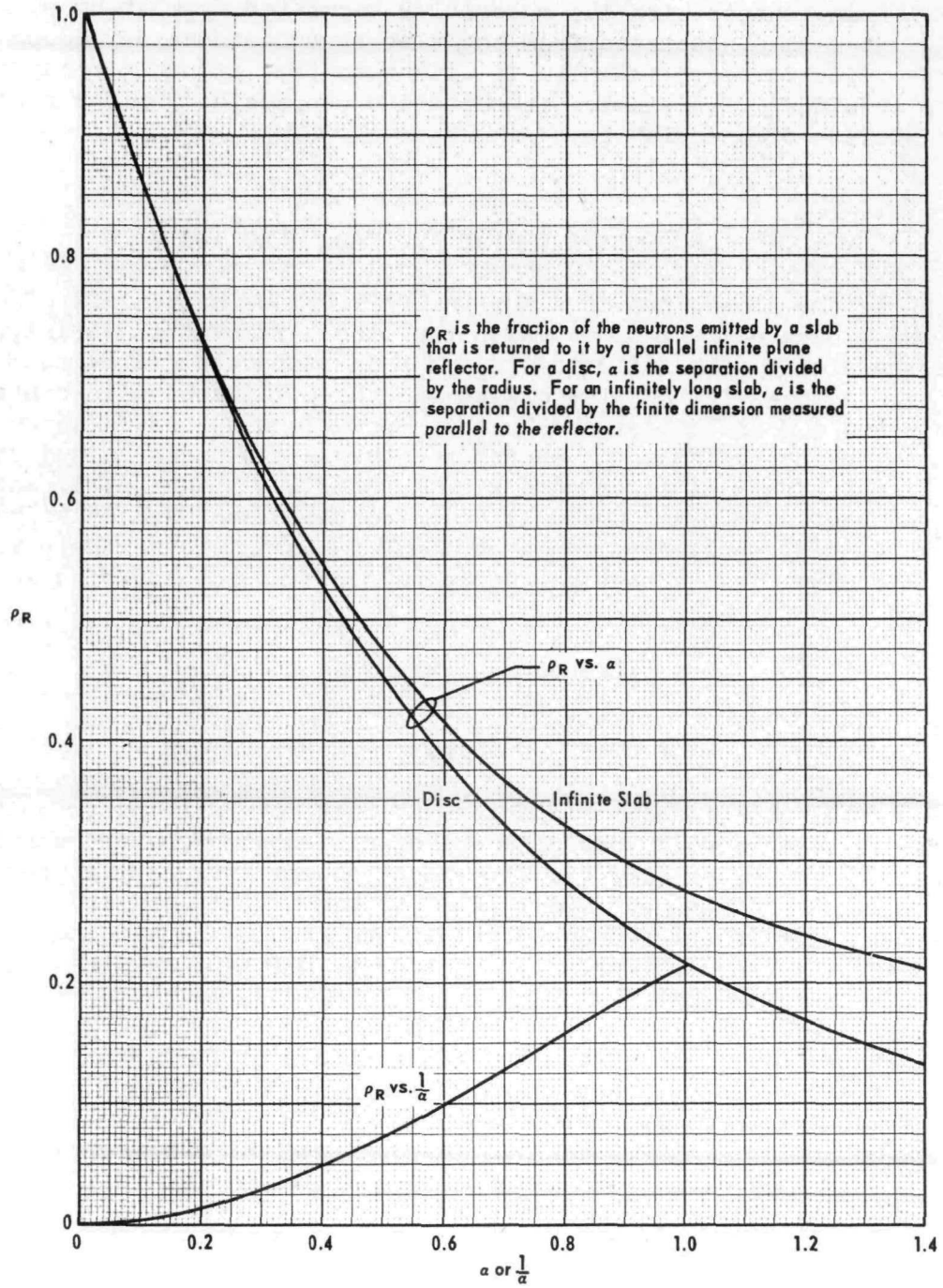

FIG. 5.6 ρ_R FOR AN INFINITE PLANE REFLECTOR

Occasionally, the components of a multicomponent reflector may be separated from each other as well as being separated from the surface of the fissionable unit. For example, consider a slab reflected by material A in contact with it, material B separated from it by a distance d_B, and material C separated from the slab by a distance d_C. Suppose that the reflectors are infinite in extent so that Figure 5.6 may be used to obtain ρ_{ur}. A simple, conservative expression for the albedo at the surface of the slab is

$$\beta_u = (1-\rho_{uB})\beta_A + (\rho_{uB}-\rho_{uC})\beta_{AB} + \rho_{uC}\beta_{ABC}$$

where β_u is the albedo provided for the unit by the system of reflectors, β_A is the albedo of reflector A with the others removed to infinity, β_{AB} is the albedo with reflectors A and B in contact and C removed to infinity, and β_{ABC} is the albedo with all three reflectors in contact. Both ρ_{uB} and ρ_{uC} are determined by the separations d_B and d_C between the unit and the reflector in question with the distances so adjusted that $\rho_{uB} = 1$ when B is in contact with A and $\rho_{uC} = 1$ when A, B, and C are in contact. If B and C should be in contact with each other but not with A, they would form a new medium B'. In this case there would be no third material so that ρ_{uC} would be zero and the equation would reduce to

$$\beta_u = (1-\rho_{uB'})\beta_A + \rho_{uB'}\beta_{AB'}.$$

5.2.6 INTERACTIONS WITH OTHER UNITS AND WITH REFLECTORS

In the general case fissionable units interact both with other units and with reflectors. If the units are of different sizes and shapes and of different materials, the situation becomes very complicated, and it is difficult to give any handy rules of thumb. In such situations generous margins of safety should be allowed in the assumptions made to simplify the calculations, e.g., all units may be taken to have the size of the largest unit.

Given a number of fissionable units and a number of reflecting surfaces on which the current may be assumed independent of position, equations of the following form may be written.

$$(-\beta_{u1}+\rho_{u1,u1})J_{u1\ in} + \rho_{u1,u2}J_{u2\ in} + \ldots + \rho_{u1,r1}\beta_{r1}J_{r1\ in} + \ldots = 0$$

$$\ldots$$

$$(1-\rho_{r1,r1}\beta_{r1})J_{r1\ in} = \rho_{r1,r2}\beta_{r2}J_{r2\ in} + \ldots + \rho_{r1,u1}J_{u1\ in} + \ldots \quad (5.10)$$

The $\rho_{u1,u1}$ and $\rho_{r1,r1}$ terms are required since some of the neutrons entering a unit may be emitted by an equivalent unit and some of the neutrons emitted by a reflector may re-enter it. The $J_{r\ in}$ terms can be eliminated from these equations and a homogeneous set of linear equations in $J_{u\ in}$ can be obtained. For a solution to exist the determinant of the coefficients must be zero, and the set of β_u's that gives this result can be found, provided the relations between the β_u's are known. Since it is clear that the albedos at the surface of the fissionable units are total albedos, the subscript T has been dropped. Equation 5.10 takes its simplest form when all the units are identical so that $\beta_{u1} = \beta_{u2} = \beta_{u3}$ etc., and when the current distribution may be considered uniform over the entire surface of the reflector so that only one reflecting surface is required. When the reflector entirely surrounds the units, the fraction of the neutrons reaching the reflector from a particular unit is obtained by subtracting from unity the fractions that reach all other units. It seems reasonable to assume that the fraction of the neutrons reaching this same unit from the reflector is given by Equation 5.8.

5.2.6.1 Sample Calculations

To illustrate the methods of calculation presented in this chapter, the various steps involved in calculating the interactions in a 3 by 3 by 3 cubic array of 20-kg spheres of uranium (93.5% U^{235}) with a lattice spacing of 11 inches are given for an unreflected array and for an array enclosed inside a reflecting cube measuring 3 feet on a side. This particular example was chosen because it has been studied experimentally.[5.8] Since the dimensions and spacings of the units are specified, the calculation yields the albedo β_T from which the reflector saving $\overline{S}$ is calculated and hence the k_{eff} of the system.

The 27 units can be divided into four groups within each of which all units occupy equivalent positions. Thus there are 1 central, 6 face centered, 12 edge centered, and 8 corner units. If the groups are numbered in this order, Equation 5.10 becomes:

$$-\beta_T J_{1\ in} + 6\rho_{12} J_{2\ in} + 12\rho_{13} J_{3\ in} + 8\rho_{14} J_{4\ in} + \rho_{1r}\beta_r J_{r\ in} = 0,$$

$$\rho_{21} J_{1\ in} + (4\rho_{22} - \beta_T) J_{2\ in} + (4\rho_{23} + 4\rho'_{23} + 4\rho''_{23}) J_{3\ in}$$

$$+ (4\rho_{24} + 4\rho'_{24}) J_{4\ in} + \rho_{2r}\beta_r J_{r\ in} = 0,$$

$$\rho_{31} J_{1\ in} + (2\rho_{32} + 2\rho'_{32} + 2\rho''_{32}) J_{2\ in} + (4\rho_{33} + 4\rho'_{33} - \beta_T) J_{3\ in}$$

$$+ (2\rho_{34} + 4\rho'_{34} + 2\rho''_{34}) J_{4\ in} + \rho_{3r}\beta_r J_{r\ in} = 0,$$

$$\rho_{41} J_{1\ in} + (3\rho_{42} + 3\rho'_{42}) J_{2\ in} + (3\rho_{43} + 6\rho'_{43} + 3\rho''_{43}) J_{3\ in}$$

$$- \beta_T J_{4\ in} + \rho_{4r} \beta_r J_{r\ in} = 0, \text{ and}$$

$$J_{r\ in} = \rho_{r1} J_{1\ in} + 6\rho_{r2} J_{2\ in} + 12\rho_{r3} J_{3\ in} + 8\rho_{r4} J_{4\ in} + \rho_{rr} \beta_r J_{r\ in}.$$

In the absence of the reflector $\beta_r = 0$ and the fifth equation is not required. In the presence of the reflector the fifth equation is used to eliminate $J_{r\ in}$ from the other four equations so that again four homogeneous equations in $J_{1\ in}$, $J_{2\ in}$, $J_{3\ in}$, and $J_{4\ in}$ are obtained. The various ρ's in the above equations are calculated for pairs of individual units. The primes are used to denote ρ's corresponding to greater separations between units of the same type. Thus, for example, a face-centered unit interacts with four edge-centered units (ρ_{23}) separated from it by one lattice spacing, s, with four (ρ'_{23}) separated from it by $\sqrt{2}$ s, and with four (ρ''_{23}) separated from it by $\sqrt{5}$ s.

In order to calculate the values of ρ, the uranium spheres are considered to be cubes of the same volume $\frac{20{,}000}{18.8} = 1064\ \text{cm}^3 = (4.02\ \text{in.}^3)$. The face-to-face separation is therefore obtained by subtracting 4.02 in. from the center-to-center separation in inches. Values of ρ are then obtained by multiplying values read from Figure 5.5 with $\frac{1}{\alpha} = \frac{4.02}{\text{center-to-center separation} - 4.02}$ and $\sigma = 1$ by 1/6. The center-to-center separation involved, the various ρ's that correspond to these separations, and the values of ρ are given in the following table.

Center-to-Center Separation, inches	ρ_{ij}	Value
11	ρ_{12}, ρ_{21}, ρ_{23}, ρ_{32}, ρ_{34}, ρ_{43}	0.01465
$11\sqrt{2}$	ρ_{13}, ρ_{31}, ρ_{22}, ρ_{24}, ρ_{42}, ρ_{33}	0.00600
$11\sqrt{3}$	ρ_{14}, ρ_{41}, ρ'_{23}, ρ'_{32}	0.00362
$11\sqrt{5}$	ρ''_{23}, ρ''_{32}, ρ'_{34}, ρ'_{43}	0.00200
$11\sqrt{6}$	ρ'_{24}, ρ'_{42}, ρ'_{33}	0.00165
11 x 3	ρ''_{34}, ρ''_{43}	0.00100

Shielding of one unit by another makes some values of ρ zero. Thus $\rho_{44} = 0$ since intervening central, edge-centered, or face-centered

units prevent a corner unit from "seeing" any of the other 7 corner units. To determine whether any other shielding is present, consider the neighbors at separations up to and including 3s that a unit would have in an infinite lattice and sum its contributions to these neighbors. This sum is performed in the following table and is well below unity; hence aside from units in a direct line, there is no shielding of units by intermediate units.

Center-to-Center Separation, inches	No. of Neighbors	Fraction Reaching These Neighbors
11	6	0.08790
11 x $\sqrt{2}$	12	0.07200
11 x $\sqrt{3}$	8	0.02896
11 x $\sqrt{5}$	24	0.04800
11 x $\sqrt{6}$	24	0.03960
11 x 3	24	0.02400
		0.30046

In the reflector the current is assumed to be independent of position. The reflector area of a cube (six sides, 36 inches on a side) is 6 sides x 36 in. x 36 in. = 7776 in.^{2}; the unit area is 6 sides x 4.02 in. x 4.02 in. = 96.96 in.^{2}. Thus ρ_{1r}, ρ_{2r}, ρ_{3r}, and ρ_{4r} are obtained by multiplying ρ_{r1}, ρ_{r2}, ρ_{r3}, and ρ_{r4} by $\frac{96.96}{7776}$

where

$$\rho_{r1} = 1 - 6\rho_{21} - 12\rho_{31} - 8\rho_{41},$$

$$\rho_{r2} = 1 - \rho_{12} - 4\rho_{22} - 4\rho_{32} - 4\rho'_{32} - 4\rho''_{32} - 4\rho_{42} - 4\rho'_{42},$$

$$\rho_{r3} = 1 - \rho_{13} - 2\rho_{23} - 2\rho'_{23} - 2\rho''_{23} - 4\rho_{33} - 4\rho'_{33} - 2\rho_{43}$$

$$- 4\rho'_{43} - 2\rho''_{43}, \text{ and}$$

$$\rho_{r4} = 1 - \rho_{14} - 3\rho_{24} - 3\rho'_{24} - 3\rho_{34} - 6\rho'_{34} - 3\rho''_{34}.$$

The fraction of the neutrons emitted by the reflector that re-enters it is given by $\rho_{rr} = 1 - \rho_{1r} - 6\rho_{2r} - 12\rho_{3r} - 8\rho_{4r}$.

In the experiment[5.8] the reflector was concrete. Let this be approximated by infinitely thick water; then a good value for the

reflector saving, whether for a sphere of uranium or for a slab, is 4.1 cm (see Section 2.2.1). The bare extrapolation distance is taken to be 2.15 cm in both cases. Then with the reflector in contact with a uranium sphere with a material buckling of 0.0837 cm^{-2} (Section 2.2.1) and a radius R_o = 6.76 cm, β_o = 0.32334 (from Equation 5.6); and with the reflector in contact with a uranium slab β_∞ = 0.55017 (from Equation 5.3). The actual reflector may be assumed to have an equivalent radius of $\frac{36 \times 2.54}{\sqrt[3]{\frac{4\pi}{3}}}$ = 56.7 cm. Applying Equation 5.9 then leads to a value of 0.51913 for β_r.

The matrices whose eigenvalues are to be determined in the unreflected and reflected cases are respectively,

$$\begin{bmatrix} 0 & 0.0879 & 0.0720 & 0.02896 \\ 0.01465 & 0.02400 & 0.08108 & 0.03060 \\ 0.00600 & 0.04054 & 0.03060 & 0.03930 \\ 0.00362 & 0.02295 & 0.05895 & 0 \end{bmatrix}$$

and

$$\begin{bmatrix} 0.0067058 & 0.130046 & 0.159654 & 0.089441 \\ 0.021674 & 0.068147 & 0.172896 & 0.093953 \\ 0.013305 & 0.086449 & 0.12608 & 0.10518 \\ 0.011180 & 0.070465 & 0.157771 & 0.0681858 \end{bmatrix}$$

An IBM 650 code, obtained by the Savannah River Laboratory from International Business Machines, was used to obtain the four eigenvalues for each matrix. In each case only one eigenvalue corresponds to the value of β_T desired. This value can be chosen from an inspection of the four values obtained for each matrix since two can be rejected immediately because they are negative and a third can be rejected because it is smaller than that corresponding to the interaction of two units. The results obtained were

$$\beta_T = 0.1235 \qquad \text{unreflected}$$

and

$$\beta_T = 0.3331 \qquad \text{reflected.}$$

From these albedos, $\overline{S}$ can be obtained from Equation 5.6 and k_{eff} can be calculated as $k_{eff} = \frac{k}{1 + \frac{k-1}{B_m^2} \frac{\pi^2}{(R+\overline{S})^2}}$ where, (see Section 2.2.1) for uranium (93.5% U^{235}), k = 2.3 and B_m^2 = 0.0837 cm^{-2} and where R, the radius of the 20-kg sphere, is 6.335 cm. The results may be compared with the multiplications observed[5.8] with an essentially unreflected array and with the reflected array. For the unreflected array the calculations give $\overline{S}$ = 2.77 cm, k_{eff} = 0.807, and a reciprocal over-all neutron multiplication of $\frac{1}{M_o} = \frac{1}{\frac{1}{1 - k_{eff}}} = 1 - k_{eff} = 0.193$. For the

reflected array the calculations give $\overline{S} = 4.18$, $k_{eff} = 0.964$. The experiments indicate multiplications of 0.195 and 0.031 respectively for the bare and reflected arrays, but they were not performed with uranium spheres but with composite units equivalent in reactivity (when isolated) to 20 kg of uranium (93.5% U^{235}). When this difference in the units is taken into consideration it appears that for this situation the calculation may underestimate k_{eff} by as much as 5%.

For situations of this sort, the maximum safe k_{eff} should be taken to be 0.90 to allow for possible nonconservatism in the calculation. The calculations thus show that it is unsafe to have twenty-seven 20-kg spheres of uranium (93.5% U^{235}) in the reflected cubic array for which the calculations were made. A safe array of these units can be achieved by increasing their spacing, by decreasing the amount of reflection, or by changing the shape of the array.

5.3 INTERACTIONS IN WATER

Water, in sufficient thickness effectively isolates fissionable units from each other through the absorption of neutrons by hydrogen. In principle, then, an infinite subcritical array is possible in water whereas it is impossible in air. For certain groupings the critical and safe sizes are actually larger when water is present between the units than when it is not, despite the reflection introduced by water. In some cases, as for example in the storage of spent enriched fuel elements, storage and handling in water is necessary. Thus, there are circumstances when it may be desirable or necessary to have fissionable units interacting with each other in water.

For separations between units of > 8 inches of water the effect of the interaction on k_{eff} is negligible when compared with margins of safety ordinarily allowed for reflected units. In some applications smaller separations may be desirable at the price of smaller unit sizes. In other cases the unit size may be restricted to discrete dimensions, i.e., the width of one element in parallel rows of fuel elements. In these circumstances methods of calculating the thickness of water required between units to provide an adequate margin of safety are necessary. A two-group model provides sufficient accuracy, and codes are available at the Savannah River Laboratory for performing such calculations on the IBM 650.

REFERENCES

5.1 Callihan, D., et al. Critical Mass Studies. Part IV. Union Carbide and Carbon Chemicals Corp., K-25 Plant, Oak Ridge, Tenn. AEC Research and Development Report K-406, 34 pp. (November 1949).

5.2 Callihan, D., et al. Critical Mass Studies. Part V. Carbide and Carbon Chemicals Division, Union Carbide and Carbon Corporation, Oak Ridge, Tenn. AEC Research and Develpment Report K-643, 57 pp. (June 1950).

5.3 Gilley, L. W., et al. "Critical Parameters of U^{235}-Enriched Solutions in Cylindrical Annular Geometry". pp. 4-6, Physics Division Semiannual Progress Report For Period Ending March 10, 1955. Oak Ridge National Laboratory, Tenn. AEC Research and Development Report ORNL-1926, 13 pp. (September 1955).

5.4 Fox, J. K. and L. W. Gilley. "Critical Experiments with Aqueous Solutions of U^{235}". pp 61-68, Applied Nuclear Physics Division Annual Report For Period Ending September 10, 1956. Oak Ridge National Laboratory, Tenn. AEC Research and Development Report ORNL-2081, 279 pp. (November 1956).

5.5 Fox, J. K., L. W. Gilley, and D. Callihan. "Critical Parameters of Aqueous Solutions of U^{235}". pp. 71-83, Applied Nuclear Physics Annual Progress Report for Period Ending September 1, 1957. Oak Ridge National Laboratory, Tenn. AEC Research and Development Report ORNL-2389, 283 pp. (November 1957).

5.6 Fox, J. K., et al. Critical Mass Studies, Part IX. Aqueous U^{235} Solutions. Oak Ridge National Laboratory, Tenn. AEC Research and Development Report ORNL-2367, 55 pp. (March 1958).

5.7 Fox, J. K. and L. W. Gilley. "Critical Parameters of Unreflected Arrays". pp. 82-84, Neutron Physics Division Annual Progress Report for Period Ending September 1, 1959. Oak Ridge National Laboratory, Tenn. AEC Research and Development Report ORNL-2842, 238 pp. (November 1959).

5.8 Mallary, E. C., et al. Safety Tests For The Storage of Fissile Units. Los Alamos Scientific Laboratory, New Mexico, AEC Research and Development Report LA-1875, 39 pp. (February 1955). (Secret).

5.9 Clark, H. K. Interaction of Subcritical Components. E. I. du Pont de Nemours & Co., Savannah River Laboratory, Aiken, S. C. AEC Research and Development Report DP-312, 48 pp. (November 1958).